İSTANBUL TECHNICAL UNIVERSITY ★ INSTITUTE OF SCIENCE AND TECHNOLOGY

THE EFFECTS OF THE POLYMERIC SIDE CHAINS ON THE STRUCTURAL AND PYHSICOMECHANICAL PROPERTIES OF POLY(P-PHENYLENE)S

M.Sc. Thesis by

Barış GÜNDOĞDU

Department : Polymer Science and Technology

Programme : Polymer Science and Technology

JUNE 2007

İSTANBUL TECHNICAL UNIVERSITY ★ INSTITUTE OF SCIENCE AND TECHNOLOGY

THE EFFECTS OF THE POLYMERIC SIDE CHAINS ON THE STRUCTURAL AND PYHSICOMECHANICAL PROPERTIES OF POLY(P-PHENYLENE)S

M. Sc. Thesis by

Barış GÜNDOĞDU

(515041029)

Date of submission : 7 May 2007

Date of defence examination: 13 June 2007

Supervisor (Chairman): Prof. Dr. Mine YURTSEVER

Members of the Examining Committee Prof. Dr. Nurseli UYANIK

Assist. Prof. Dr. Nurcan TÜZÜN

JUNE 2007

İSTANBUL TEKNİK ÜNİVERSİTESİ ★ FEN BİLİMLERİ ENSTİTÜSÜ

POLİ(P-FENİLEN)'İN YAPISAL VE FİZİKOMEKANİK ÖZELLİKLERİ ÜZERİNDE POLİMERİK YAN ZİNCİRLERİN ETKİSİ

YÜKSEK LİSANS TEZİ

Barış GÜNDOĞDU
(515041029)

Tezin Enstitüye Verildiği Tarih : 7 Mayıs 2007
Tezin Savunulduğu Tarih : 13 Haziran 2007

Tez Danışmanı : Prof. Dr. Mine YURTSEVER
Diğer Jüri Üyeleri Prof. Dr. Nurseli UYANIK
Yrd. Doç. Dr. Nurcan TÜZÜN

HAZİRAN 2007

ACKNOWLEDGEMENTS

I wish to thank at first place to my supervisor Prof. Dr. Mine YURTSEVER for her expert guidance, motivation and support at all levels of study. It was great pleasure for me to conduct this thesis under her supervision and to know her personally.

I would express my heartfelt thanks to all members of polymer science and technology programme and chemistry department, especially Prof. Dr. Nurseli UYANIK, Yrd. Doç. Dr. Nurcan TÜZÜN and Erol YILDIRIM.

I am forever indept to the love and caring of my family, Rıza and Leman GÜNDOĞDU and to H. Yeliz GÜLENER. They have always been a source of constant support and love.

Wishes to be scientific and technological leader of the world.

Barış GÜNDOĞDU

June, 2007

CONTENTS

ABBREVIATIONS……vi

LIST OF TABLES……vii

LIST OF FIGURES……**viii**

LIST OF SYMBOLS……....**ix**

ÖZET……...**x**

SUMMARY……...**xii**

1. INTRODUCTION……..**1**
1.1. Conjugated Polymers…….1
1.2. Studies On Poly(p-Phenylene)s……5
1.2.1. Experimental Studies……...5
1.2.2. Theoretical Studies……14

2. METHOD……..**17**
2.1.Quantum Mechanical Methods……17
2.1.1. Molecular Mechanics……17
2.1.2. Semi Emprical Methods……18
2.1.3. Ab-Initio Methods…...……...18
2.1.4. Density Functional Theory……19
2.2. Statistical Mechanical Methods……...19
2.2.1. Molecular Dynamics Simulation……...20
2.2.1.1. Minimization…….……...21
2.2.1.2. Dynamics…….……22
2.2.1.3. Forcefield…….……24
2.2.2. Dissipative Partical Dynamics……...26
2.2.2.1 Calculation of χ Parameter……28

3. ANALYSES……...……**32**
3.1. System Description...……...32
3.2. The Methods Used In Quantitative Structure-Property Relationship (QSPR) Calculations……..33

4. RESULTS AND DISCUSSIONS.....**40**
4.1. QSPR Results.....41
4.1.1. Glass Transition Temperature.....43
4.1.2. Molar Volume.....44
4.1.3. Cohesive Energy.....45
4.1.4. Solubility Parameter.....47
4.1.5. Thermal Conductivity.....48
4.1.6. Dielectric Constant.....49
4.1.7. Volume Resistivity.....50
4.1.8. Bulk Modulus.....50
4.1.9. Young's Modulus.....51
4.1.10. Permeability of Oxygen.....52
4.2. MD Results.....52
4.3. DPD Results.....56

5. CONCLUSION.....**60**

REFERENCES.....**61**

APPENDIX.....**68**

BIOGRAPHY.....**85**

ABBREVIATIONS

AM1	**:** Austin Model 1
BFGS	**:** Broyden, Fletcher, Goldfarb and Shannon Algorithm
B3LYP	**:** Becke Style Three Parameter Functonal in Combination with the Lee-Yang Parr Correlation Functional
COMPASS	**:** Condensed-phased Optimized Molecular Potential for Atomistic Simulation Studies
DFP	**:** Davidon, Fletcher and Powell Algorithm
DFT	**:** Density Functional Theory
DPD	**:** Dissipative Particle Dynamics
E	**:** Energy
HF	**:** Hartree - Fock
HOMO	**:** Highest Occupied Molecular Orbital
LUMO	**:** Lowest Unoccupied Molecular Orbital
MC	**:** Monte Carlo Method
MD	**:** Molecular Dynamics
MINDO	**:** Modified Intermediate Neglect of Differential Overlap
MM	**:** Molecular Mechanics
MO	**:** Molecular Orbital
MP2	**:** Moller-Plesset Second Perturbation
PCL	**:** Poly(ε-caprolactone)
PM3	**:** Parametic Method Number 3
PPP	**:** Polyparaphenylene
PPV	**:** Polyphenylenevinylene
PSt	**:** Polystyrene
STP	**:** Standart Temperature and Pressure
QM	**:** Quantum Mechanics
QSAR	**:** Quantitative Structure Activity Relationships
QSPR	**:** Quantitative Structure Property Relationships

LIST OF TABLES

Page No

Table 1.1 : Conductivities (in $S.cm^{-1}$) of Several Materials…..……....…….. 4
Table 1.2 : Conductivities (in $S.cm^{-1}$) of Several Conducting Polymers ….. 5
Table 1.3 : PPP Properties with Different Types of Pendant Side Groups..… 8
Table 2.1 : χ Interaction Parameters That are Calculated by Different Methods…….. 29
Table 2.2 : Calculated Repulsion Parameters of the Structures for DPD…… 30
Table 3.1 : Experimental Data……...……... 39
Table 4.1 : The QSPR Results..……...…… 41
Table 4.2 : The QSPR Results (Continued)……. 42
Table A.1 : The Optimized Structures of Single Chain PPPs With Alternating PSt and PCL Side Blocks After MD Simulations of 600 ps at 298K…… 68
Table A.2 : The Optimized Structures of Two PPP Chains With Alternating PSt and PCL Side Blocks After MD Simulations of 600 ps at 298K……... 77

LIST OF FIGURES

Page No

Figure 1.1 : Conductivity of The Molecules …… 3
Figure 1.2 : Mechanisms of PPP With Alternating Side Chains ……. 7
Figure 1.3 : PPP With Both PSt and PCL Side Chains ……... 11
Figure 1.4 : Three-dimensional Ball and Stick Models of PPPs ……. 12
Figure 1.5 : General Presentation of Grafting Process by Diels-Alder ……... 13
Figure 3.1 : The Macromonomer Modelled In This Study …….. 33
Figure 4.1 : The Poly(p-phenylene) Chain……... 40
Figure 4.2 : The Polystyrene Chain……..... 40
Figure 4.3 : The Poly (ε- caprolactone) Chain ……. 40
Figure 4.4 : The Effects of Side Chains on T_g…….. 43
Figure 4.5 : The Effects of Side Chains on Molar Volume…….. 44
Figure 4.6 : The Effects of Side Chains on Cohesive Energy (Fedors)……..... 45
Figure 4.7 : The Effects of Side Chains on Cohesive Energy (Van Kreven)... 46
Figure 4.8 : Comparison of the Cohesive energy of PPPs Containing One-type of Side Group In Terms of Two Different Methods…… 46
Figure 4.9 : The Effect of Side Chains on Solubility Parameter(Fedors)……. 47
Figure 4.10 : The Effect of Side Chains on Solubility Parameter (van Kreven) 48
Figure 4.11 : The Effect of Side Chains on Thermal Conductivity…… 48
Figure 4.12 : The Effect of Side Chains on Dielectric Constant…… 49
Figure 4.13 : The Effect of Side Chains on Volume Resistivity…… 50
Figure 4.14 : The Effect of Side Chains on Bulk Modulus...……. 50
Figure 4.15 : The Effect of Side Chains on Young Modulus ……...……. 51
Figure 4.16 : The Effect of Side Chains on Permeability of Oxygen …… 52
Figure 4.17 : Single Chain of PPP Backbone…….…… 53
Figure 4.18 : Single PPP Chain Substituted With PSt (n_{St}=16) and PCL (n_{CL})=4 Side Groups…….. 55
Figure 4.19 : Two PPP Chains Substituted With PSt (n_{St}=16) and PCL (n_{CL})=4 Side Chains …….. 55
Figure 4.20 : The Top Views From the Cell. Morphology of the Materials Formed By Varied Side-Chain Lenghts (a) (n_{St}=10; n_{CL}=10), (b) (n_{St}=20; n_{CL}=20), (c) (n_{St}=30; n_{CL}=30), (d) (n_{St}=40; n_{CL}=40). 58
Figure 4.21 : AFM Picture Showing the Layered Morphology of A 40 nm Thick Film of The PSt and PCL Substituted PPP Oligomers On The Glass Surface…….. 59

LIST OF SYMBOLS

Π	**:** Electron Bonding at Conjugated Polymers
Π*	**:** Electron Antibonding at Conjugated Polymers
Ψ	**:** Wavefunction
Å	**:** Dimension Unit
$\mathbf{C_n}$	**:** The Characteristic Ratio of the Polymer
$\mathbf{E_J}$	**:** Coulomb Energy
$\mathbf{E_T}$	**:** Kinetic Energy
$\mathbf{E_V}$	**:** Potential Energy
$\mathbf{E_{XC}}$	**:** Exchange Correlation Energy
fs	**:** Femtosecond
°K	**:** Kelvin
$\mathbf{M_m}$	**:** Molar Mass of a Repeat Unit
$\mathbf{M_p}$	**:** Molar Mass of the Polymer
N	**:** Number of Monomers per Polymer
n	**:** Repulsion Parameter
ps	**:** Molecular Orbital
S	**:** Conductivity
T	**:** Temperature
χ	**:** Flory – Huggins Interaction Parameter
ρ	**:** Density

POLİ(P-FENİLEN)'İN YAPISAL VE FİZİKOMEKANİK ÖZELLİKLERİ ÜZERİNDE POLİMERİK YAN ZİNCİRLERİN ETKİSİ

ÖZET

Konjuge polimerlerin kullanımı bütün uygulama alanlarında büyük orada artmaktadır. Poli(p-fenilen)(PPF)ler en popüler konjuge polimerlerden biridir ve çeşitli yollarla modifiye edilebilirler. Polimer ekleme, modifikasyon olarak kullanılabilir. Polisitren(PSt); rijit, ucuz ve izolasyon malzemesi olarak kullanılabilir. Diğer taraftan, poli(ε-kaprolakton)(PKL) esnek bir yapıya sahiptir. Bu çalışmada iletken malzeme PPF yapısının, rijit ve esnek PSt ve PKL ile modifiye edilmesi teorik metotlarla araştırıldı. Bu araştırmalar 'Materials Studio 4.1' kullanılarak gerçekleştirildi. Her şeyden önce, genel yapıyı temsil etmesi için, bir makromonomer oluşturuldu ve çoğaltıldı.

İlk araştırma metotu olarak QSPR kullanıldı. Optimize edilmeden ana zincire lineer olarak eklenip uzatılan monomerlerle elde edilen makromonomerler 'Synthia' modülü ile çalıştırıldı. Elde edilen sonuçlar şunu gösterdi ki; yapısal ve fizikomekaniksel özellikler direkt olarak yan zincir tiplerinin miktarı ve karakteristik özellikleri ile ilgilidir. Dolayısı ile nanokompozitlerde yan zincirlerin farklı varyasyonu ile gereken özellikler oluşturulabilir.

İkinci adım Moleküler Dinamik idi. Bu kısımda amaç; çoğaltılan makromonomerlerin simülasyon sonucunda elde edilen yapılarının incelemekti. Discover MD sonuçlarına göre; tek zincirlerde, dengeye gelmiş yapılara ait PKL yan zincirleri katlanmakta, ana zincirlerden çok uzaklaşmamakta veya birbirlerine paralel pozisyonda durmakta ya da birbirlerine düşük oranda sarılmaktadırlar. PSt ler ise; ana zincire yaklaşmakta, komşu PSt ile yumaklaşmaktadır. PSt ve PKL yan zincirler bağlı ikili PPF anazincirlerde ise, PPF zincirleri birbirlerine paralel olarak durmasına rağmen, yan zincir yönlenmesi daha baskın olmaktadır. Ana zincirlerin hareketi tamamıyla yan zincirlerin etkisi altındadır.

Son araştırma adımı Dağınık Partikül Dinamiği idi. Bir hücre içerisinde, PKL (10, 20, 30, 40 monomer sayısı ile) ve PSt 10, 20, 30, 40 monomer sayısı ile) yan zincirler ihtiva eden PPF zinciri oluşturuldu. Faz ayrımlı morfoloji sonuçları gösterdi ki; gerekli simulasyondan sonra son yapılar, mezoboyuttaki nanokompozitler hakkında fikir edinmeyi sağlar.

THE EFFECTS OF THE POLYMERIC SIDE CHAINS ON THE STRUCTURALS AND PHYSICOMECHANICAL PROPERTIES OF POLY(P-PHENYLENE)S

SUMMARY

Using of conjugated polymers are increasing widely at all fields of applications. Poly(p-pheylene)s are the one of the most popular conjugated polymers and are modified by different ways. Substitution with polymers can be used as modification. Polystyrene is a rigid, cheap and usable as insulation material. On the other hand, poly(ε – caprolactone) has a flexible structure. In this study, conducting material PPP's modified structure with rigid and flexible PSt and PCL is investigated by theoretical methods. These investigatons are performed by using Material Studio 4.1 First of all, to represent the general structure, a macromonomer is formed and propagated.

First investigation method was Quantitive Structure-Property Relationship (QSPR). The macromonomers that are formed as linear extended elongation of the monomers to the backbone without optimization is performed with Synthia Module in MS 4.1 . The obtained results was exposed that the structural and physicomechanical properties are directly related with the amount and the characteristic properties of type of side chains. So, the required properties could be obtained in nanocomposites by the different variations of side chains.

Second step was Molecular Dynamics, in this part purpose was the observation of final structures of propagated macromonomers at the end of simulation term. Due to Discover MD results, the final nanocomposites are showed PCL side chains are paralel or twisting to each other and moving far from backbone, PSt molecules are approaching to PPP and are folded on its neighbour PSt side chain in the single PPP backbone. In two chains of PPP backbones with substutition of PCL and PSt side chains, despite the parallel position of the PPP backbones to each other, side chain

orientation is dominant. The movement of backbones are completely under the effect of side chains' movement.

Last investigation step was Dissipative Particul Dynamics. In a cell, dynamics of PCL (with number of monomers 10, 20, 30, 40) and PSt (with number of monomers 10, 20, 30, 40) side chains on a single PPP backbone is applicated. And the phase seperated morphology results are showed that the final structure after required simulation gave an idea to identify the nanocomposite in mezoscale.

1. INTRODUCTION

1.1 Conjugated Polymers

Conjugated polymers have gained a great deal of attention after 1976 when it was discovered that they became highly conducting upon a redox chemical treatment. This discovery led to the 2000 Nobel Prize in Chemistry awarded to Alan Heeger, Alan MacDiarmid, and Hideki Shirakawa. By the mid-eighties, many research teams in both academia and industry were investigating π-conjugated oligomers and polymers for their nonlinear optical properties or their semiconducting properties, paving the way to the emergence of the fields of plastic electronics and photonics.

In the mid-1980s, with the increased importance attached to nonlinear optical properties conducting polymers, the goal of many calculations was to determine the nature of the excited states playing a role in the second-order and third-order molecular polarizabilities. Relaxation effects in the excited states and impact of intermolecular interactions became the focus of numerous quantum-chemical studies in the 1990s due to the advent of electroluminescent conjugated polymers.[1]

In the last decade, the studies in this field were concentrated on the synthesis of 'tailor-made' conducting materials (copolymers, grafted polymers, polymer nanocomposites, etc.) which are soluble, proccessable and having improved optical or mechanical properties for various industrial applications without loosing much from conductivity.[2]

Not only the properties but also the topology of the polymers (comb, star, dendritic, etc.) or the functional groups at various sites of the polymer (end, center, side) can be varied to create many new materials.[3]

The carbon nanotubes incorporated into a suitable supporting polymer matrix are good examples to conductive nanocomposites. These materials, compared to

conductive metal-filled systems, offer substantial weight savings, flexibility, durability, low-temperature processability, and tailored reproducible conductivity. They are mostly used to produce conductive paints, coatings, caulks, sealants, adhesives, fibers, thin films, thick sheets, and tubes as well as electromagnetic interference shielding for large structural components, electrostatic painting, electrostatic discharge and opto-electronic device applications.

How conducting polymers conduct electricity can be explained by the band theory.

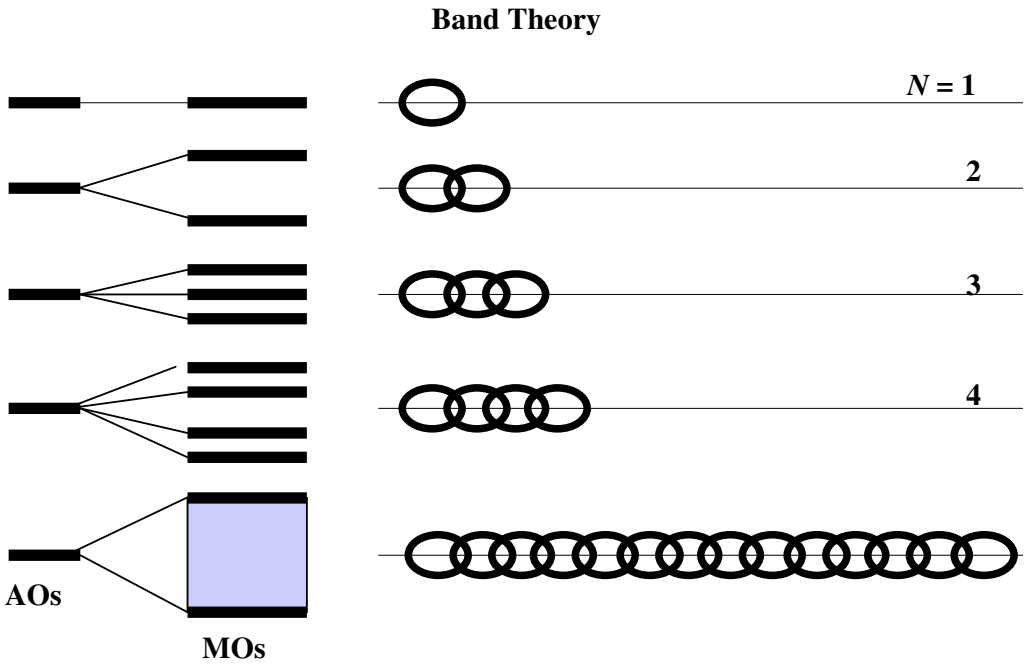

Band Theory : Metal, Semiconductor, Insulator

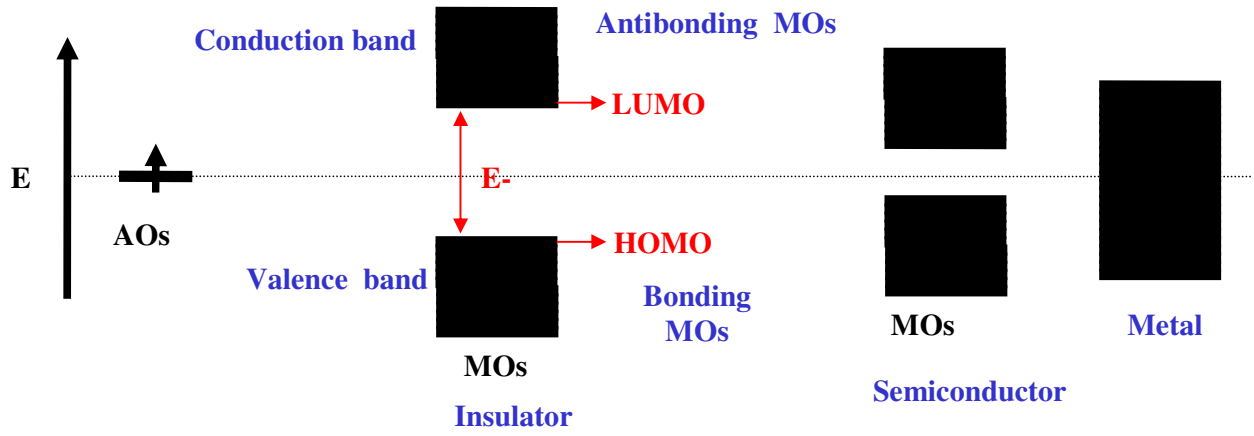

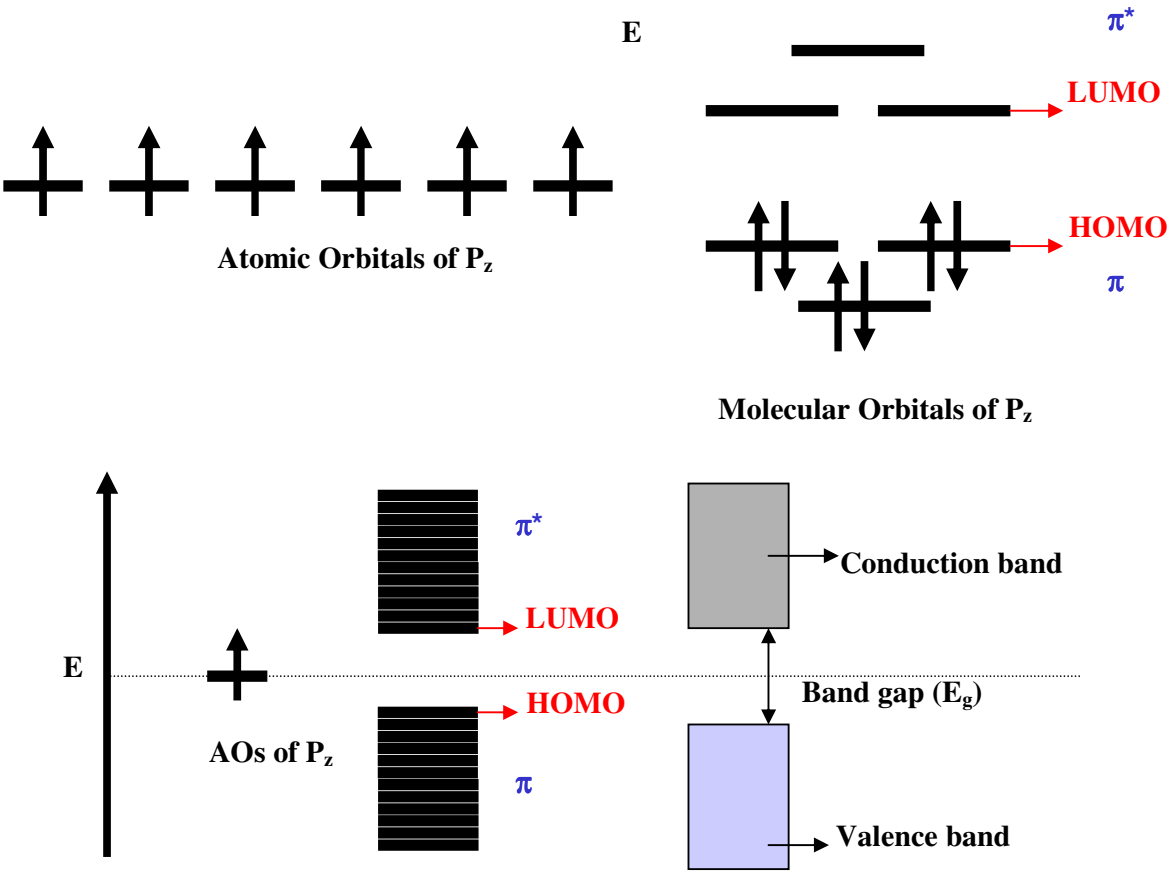

Figure 1.1: Conductivity of The Molecules.[3]

Conjugated polymers derive their semiconducting properties by having delocalized π-electron bonding along the polymer chain. The π (bonding) and π*(antibonding) orbitals form delocalized valence and conduction wavefunctions, which support mobile charge carriers.[4]

Table 1.1: Conductivities (in $S.cm^{-1}$) of Several Materials

		Polymers	**Molecular Crystals**	**Materials**
Insulator ($S.cm^{-1}$)	$10^{-20} – 10^{-15}$	PTFE (Teflon), Polyimide (Kapton), Polystyrene, PVC, Polyphenylene Sulphide (undoped), Poly(p-pheylene) (undoped)	Diamond	SiO_2
	$10^{-15} – 10^{-10}$	Polydiacetylene, Polythiophene, Polypyrrole (undoped), Nylon	Cu-phthalocyanine, Anthracene	-
	$10^{-10} – 10^{-5}$	Polyphthalocyanine, Polyacetylene (undoped)	Ag-TCNQ	ZnO, Iodine, H_2O, Boron
Semi – Conductor ($S.cm^{-1}$)	$10^{-5} – 10^{0}$	Poythiophene	Cu-TCNQ	Si
Conductor ($S.cm^{-1}$)	$10^{0} – 10^{5}$	Graphite, Pyropolymers, Polyacetylene, Polypyrrole, Poly(phenylene sulphide), Poly(p-pheylene)	TTF-TCNQ	Ge(doped), ZnO, Si, Bi, Hg
	10^{5} - …	-	$TMTSF_2PF_6$	Cu

Table 1.2: Conductivities (in $S.cm^{-1}$) of Several Conducting Polymers

POLYMER	**TYPICAL METHODS OF DOPING**	**TYPICAL CONDUCTIVITY ($S.cm^{-1}$)**
POLYACETYLENE	ELECTROCHEMICAL, CHEMICAL (AsF_5, I_2, Li, K)	500 – 1.5 x 10^{-5}
POLYPHENYLENE	CHEMICAL (AsF_5, Li, K)	500
POLY(PHENYLENE SULPHIDE)	CHEMICAL (AsF_5)	1
POLYPYRROLE	ELECTROCHEMICAL	600
POLYTHIOPHENE	ELECTROCHEMICAL	100
POLY(PHENYL-QUINOLINE)	ELECTROCHEMICAL, CHEMICAL (Sodium Naphthalide)	50

Conducting polymers are materials that exhibit the electrical and optical properties of metals or semiconductors and retain some of the mechanical properties and processing advantages of polymers. These materials with conjugated π-electron backbones display unusual electronic properties such as low-energy optical transitions, low ionization potentials and high electron affinities; thus they can be oxidized or reduced more easily and more reversibly than conventional polymers. They could be p- or n-doped either electrochemically or chemically to the metallic state. They can be synthesized by chemical or electrochemical polymerization techniques.

1.2 Studies On Poly(p-phenylene)s

1.2.1 Experimental Studies

Conducting polymers can be synthesized by either chemical or electrochemical

polymerization methods. Electropolymerization has several advantages, such as simplicity, reproducibility, and thickness control. Electrochemical initiation of polymerization reactions has been applied to the synthesis of a wide range of polymer types. However, some difficulties may appear in processing and application stages if the materials have poor mechanical and physical properties. The polymers with good mechanical and desired physical properties and also good environmental stability must be synthesized.[5]

Poly(p-phenylene)s (PPP)s are one of potentially most useful polymers for organic conducting materials and organic polymeric ferromagnets due to their extended planar conjugated π system, along with high strength and high heat resistance. Electrochemical polymerizations, also a method for the PPP synthesis, do allow the fabrication of thin films, but the molecular weight of the polymer is limited by its insolubility. Even numerous PPP bearing different types of pendant side groups were synthesized to induce different properties in PPP (see table 1.3), grafted copolymers having π-conjugated backbones are quite limited.[6]

In Figure 1.2, the PPPs with alternating PSt / hexyl **6** or methyl side chains **11** and PTHF / hexyl **15** were obtained by Suzuki polycondensations of macromonomers **4**,**10** and **14** in combination with the appropriate reaction partners by Yagcı et al. Moreover, by reacting two macromonomers with different functional groups (**10** and **14**) a PPP with alternating PSt and PHF side chains was obtained (**17**). Due to expected shape of the macromolecules, with very long polystyrene side chains, the obtained molecular weights do not give sufficient information about the polymerization degrees.[7]

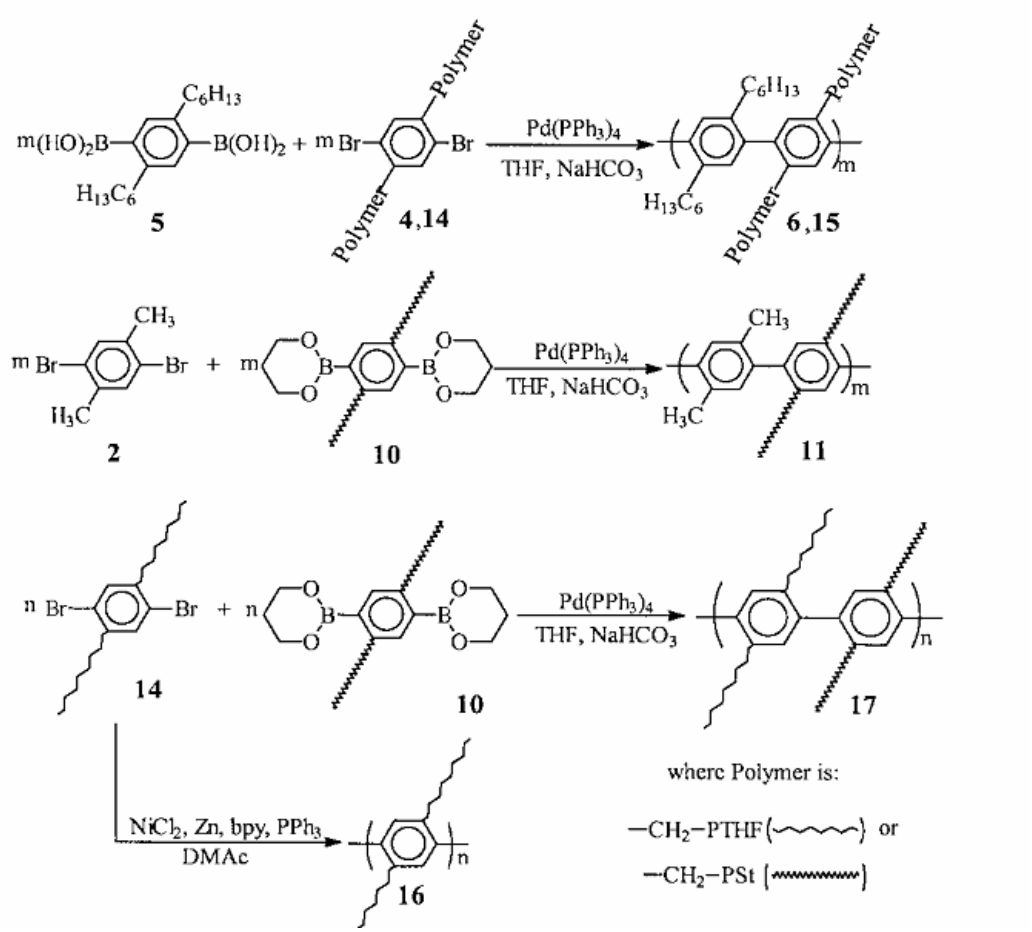

Figure 1.2: Mechanisms of PPP with Alternating Side Chains [7]

Table 1.3: PPP Properties with Different Types of Pendant Side Groups.[6]

Type of PPP		Method of Synthesis	Properties
PPPs with alkyl, alkoxy or hidroxy side group	$(CH_2)_nCH_3$, n=5-7	Yamamoto	Soluble in common organic solvents, DP<15
	$(CH_2)_nCH_3$, n=0-15	Suzuki	Soluble in common organic solvents, DP>100, Exhibits thermotropic liquid crystalline behaviour (R=dodecyl)
	$-CH_2-O-R$; R=butyl,hexyl,C_6H_4CN	Suzuki	Soluble in common organic solvents, DP=30-65
	$(CH_2)_x$OPh-R;x=1,6;R=H,CO_2CH_3	Suzuki	Applied in LED.
	$-O-CH_2-CH(CH)_3-CH_2-CH_3$	Suzuki	Optically activite
	-OH	Yamamoto	Soluble in DMF
PPPs with carboxyl or sulfonic ester groups	-COOH	Suzuki	Insoluble in organic solvents in free acid forms, Soluble in dilute aqueous base, Highly birefringence in film form.
	$-O(CH_2)_3SO_3Na$,$-SO_3R$;R=p-tolyl or 3,5-(di-t-butyl)benzene, $-O-CH_2-C_6H_4-SO_3Na$	Suzuki	Polyelectrolyte, Dopale (n-type or p-type) in lytropic solution in DMSO or thin film on ITO glass.
PPP with diketo or diethynyl side groups	-COR; R=C_6H_5, C_6H_{13}	Suzuki	Precursors for ladder polymers
	-C C-C_6H_4-OR; R=n-alkyl	Suzuki	Precursors for ladder polymers
	$-CO-CH_3$; -CHO; $-COC_6H_5$ (m-PPP)	Yamamoto	Soluble in DMF,DMAc, DMSO,THF,NMP
Dendronized PPPs	$-CH_2-O-C_6H_3(CH_2OC_6H_3)_2$... (Frechet-type dendritic fragments of low generations)	Suzuki	Exceptionally rigid and attain a cylindrical shape in solution and when adsorbed on surfaces.
PPPs with polymeric side chains	Oligo(etyhylene oxide)	Suzuki	Amphiphilic, Applied a separators in rechargeable solid state Li cells.
		Yamamoto	Exhibits liquid crystalline properties.

The conducting graft copolymers formed from the random copolymer are expected to exhibit the better mechanical properties than the corresponding graft copolymer formed from 3-methylthienyl methacrylate.[7]

Well-defined polystyrene- (PSt) or poly(e-caprolactone) (PCL)-based polymers containing mid- or end-chain 2,5 or 3,5- dibromobenzene moieties were prepared by controlled polymerization methods, such as atom transfer radical polymerization (ATRP) or ring opening polymerization (ROP). Yağcı and his research group have recently explored a new synthetic strategy to prepare soluble conjugated poly (p-phenylene) (PPP)-type graft copolymers by combining controlled polymerizations with metal catalyzed Suzuki or Yamamoto polycondensation.[8]

The poly(p-phenylenes) (PPP) obtained, with PCL side chains, have solubility properties similar to those of the starting macromonomer, ie soluble in common organic solvents at room temperature. Since the discovery that PPP conducts electricity when doped with oxidizing or reducing agents, a great deal of research has gone into the study of this material and its derivatives. Polyphenylene is used as a coating material in the packaging industry to protect integrated circuits from breakage, humidity and corrosion. Other interesting and important properties that PPPs exhibit include liquid crystallinity and photo- and electroluminescence. However, because of high crystallinity, insolubility and high melting temperature, the potential attractive properties are still under investigation. Several approaches to decrease the crystallinity of rigid conjugated polymers have been used. These approaches include introduction of bent or crank-shaped units into the main chain as well as lateral substitution and incorporation of flexible units as side chains. Substituted PPPs with flexible pendant moieties have received attention on account of their electrical and optical properties combined with solubility and fusibility.

Taking in account the considerable interest not only in the synthesis of new types of plastic materials but also in the modification of the commodity polymers to improve their properties to meet the requirements for high-tech applications, polystyrene (PS) or poly(methyl methacrylate) (PMMA) were used, in which nanostructured photoactive conjugated oligo(phenylene vinylene) segments are attached as side chains to the backbone.

Poly(p-phenylene)s containing oligo(oxyethylene) side chains, soluble in common organic solvents at room temperature were obtained by Wegner and coworkers. Graft copolymers of PPPs with macromolecular side chains prepared by using controlled radical polymerization methods. The purpose of this contribution is to report the synthesis of an ε-caprolactone (CL)-based macromonomer and its use in PPP formation. The new PPP type polymers with PCL side substituents have very good solubility in common organic solvents at room temperature.[9]

Polyphenylenes (PPs) with PSt chains as substitution groups were obtained. The same macromonomers were used in Yamamoto copolycondensation reactions, in combination with a poly(ε-caprolactone) (PCL) macromonomer, and this resulted in PPs with Pst / PCL side chains. The obtained PPs had good solubility properties in common organic solvents at room temperature similar to those of the starting macromonomers.

The characterization of polymers can be done with NMR, IR, chromatography and the optical properties are studied by UV and fluorescence spectroscopic techniques. The thermal behaviors are investigated with differential scanning calorimetry (DSC). The morphology of polymers are studied by atomic force microscopy (AFM).

The attachment of conformationally mobile alkyl side chains to the backbone has been important because it has allowed the controlled synthesis of soluble and processable PPs with high molecular weights. Because of the expected large persistence length of the main chain and the flexibility of the side chains, such molecules have been termed *hairy-rod polymers*. PPs with both PSt and PCL side chains were synthesized by combination in Yamamoto copolycondensation reactions of PSt and PCL containing macromonomers. These materials have interesting properties and they show phase separation due to crystalline (PCL) and amorphous (PSt) side groups proved by the AFM analysis.[10]

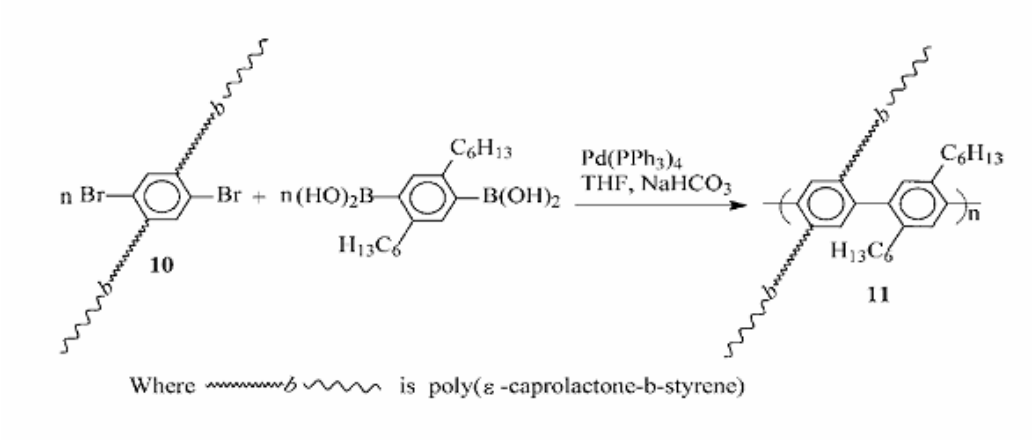

Figure 1.3: PPP with Both PSt and PCL Side Chains.[11]

During the last decade, controlled radical polymerization became an established method to prepare new polymers with complex architecture such as block, graft, star, and functional (co)polymers with controlled molecular weight and molecular weight distribution.[12]

The control of soft materials on the nanometer size scale is becoming an increasingly important aspect of polymer science. The preparation of well-defined nanostructures requires molecular building blocks of defined structure. New synthetic methods for introducing functional groups at specific location at either chain ends or along the backbone are emerging as powerful tools for the construction of these architectures. The field of electrically conductive polymers offers great opportunities for graft copolymers because of their unique nanoscopic morphologies and mechanical properties.

The rigid-rod polymers belonging to the PPP or PPV classes containing side chains with controlled size and shape can also be obtained by polycondensation methods. The graft copolymers of PPP with well-defined macromolecular side chains prepared by using controlled radical polymerization have been synthesized by this way and their glass transition temperature were reported to be between 82 and 100 °C.

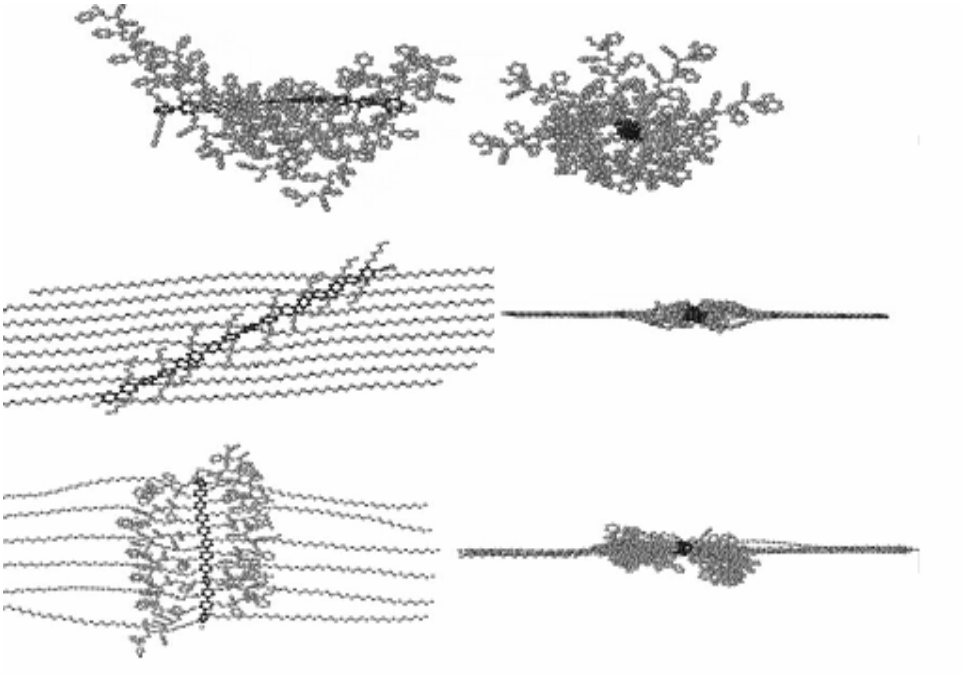

Figure 1.4: Three-dimensional Ball and Stick Models of PPPs.[13]

The properties of materials depend highly on the intra and intermolecular interactions between the polymeric side chains which can have hydrophobic or hydrophilic characters and can be combined appropriately to design new polymers in such a way that their applications in different areas become possible.[13]

In order to improve the solubility, a series of functionalized PPP with pendant alkyl groups has been synthesized by Wegner et al. Moreover, PPPs containing oligo(oxyethylene) side chains, soluble in common organic solvents at room temperature were also obtained. However, to general knowledge, grafted copolymers having π-conjugated backbones are quite limited. These new materials are more thermostable than the starting macromonomers.[14] The characteristics of the grafted polymers are very important in determining the property and the morphology of the thin films. It has shown that the type, lenght and the composition of the side groups grafted on to the PPP backbone are the dominant factors on the resulting material. If the side chains are opposite in structural behavior like PSt and PCL, a layered morphology is expected.[15]

The conducting polymer matrix host enzymes to obtain thermally stable and electrically conducting films. In terms of the immobilized enzyme activity, it has been showed that good results could be obtained with the conducting copolymer

matrices.[16]

The temperature dependence of conductivity and thermoelectric power of brittle polyparaphenylene films at temperatures between 150 and 450 K are studied by doping with ions. It is known that the doping process of conjugated polymers are efficient only at low temperatures and many studies are devoted to increase doping level around room temperature. [17]

Synthesis of poly(paraphenylene)s via Ni(0)-catalyzed coupling of bis(aryl halide)s is shown as to be a novel and flexible route and the resulting polymer can be readily modified to produce a fully substituted PPP using any nucleophile capable of nucleophilic aromatic substitution (SNAr). This methodology allows for selective control of polymer solubility and hydrophilicity, increase in the glass transition temperature, improvement in thermooxidative stability, creation of flexible, film-forming PPPs through grafting and production of thermoset PPPs through cross-linking. The substitution of small molecules along the PPP backbone serves as a model study to answer some fundamental structure / property questions, substitution of larger macromonomers can be used to significantly increase the molecular weight, solubility, and film forming ability of PPP derivatives.[18]

"Click Chemistry" is another powerful method to add pendant groups to a polymer backbone. If the resulting graft copolymers that studied are amphiphilic in nature it is expected to form micelles in aqueous media. As an example, in Figure 1.5, the structure formed by linking of PEG chains to a hydrophopic backbone is seen.[19]

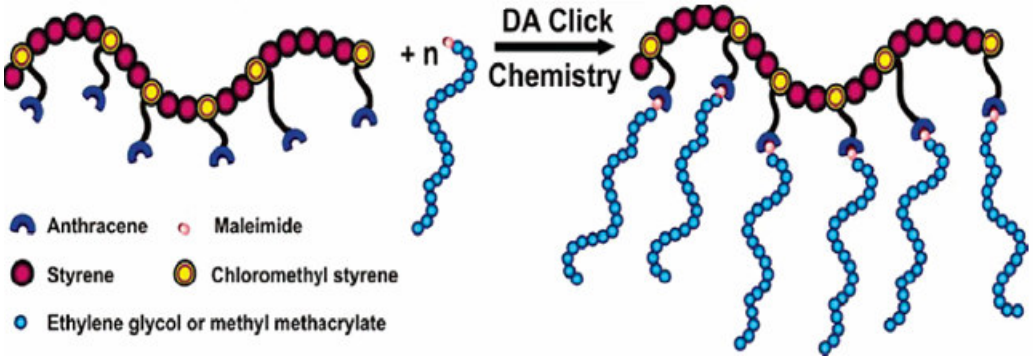

Figure 1.5: General Presentation of Grafting Process by Diels-Alder "Click Chemistry"[19]

Recently, bismaleimide (BMI) resin found some application areas such as in

aerospace and electronics applications because of their excellent low coefficient of thermal expansion, low dielectricity, and excellent mechanical performance at elevated temperatures. However, BMI resins in general are inherently brittle and they are softened by incorporation of poly(ethylene glycol) (PEG) segment as a side chain along the BMI polymer backbone. The presence of the side chains resulted in a phase-separated BMI polymer. The morphology was dependent on the concentration and molecular weight of the PEG side chains.[20] In such systems where the rigid backbone is functionalized by long and preferably soft side chains, a phase separation is highly expected.

1.2.2 Theoretical Studies

Although the number of experimental studies on poly(paraphenylene) based polymers has enormously increased in recent years, theoretical studies especially quantum mechanical calculations are not so many due to the large size of the systems. Simulations has gained a lot of importance since they provide realistic description for the atomic and molecular potential interactions so that the bulk properties are estimated. Besides, these statistical methods are successful reproducing the experimental data if available. Some of the theoretical calculations done on PPPs are given below.

The motion of PPP chains are modelled using the parametrization obtained from DFT calculations on dimeric model molecules. In the simulations, the phenylene rings treated as semi-rigid rotors that can change their geometry from aromatic A-phase to quinoidal B-phase structure. By the generated Hamiltonian, all possible structures like bipolaron formation are simulated.[21]

The DFT B3LYP/6-31g* calculations on the neutral, polaronic and bipolaronic oligo-para-phenylenes showed that the electrical and optical properties of the poly-paraphenylene chains are related to intramolecular delocalization of π-electrons. The degree of planarity directly determines the effective conjugation length. From the oscillator strength values, it was observed that the transition probability increases with the chain length.[22] Usually, the accurate calculations on these systems are carried out by using the DFT or post Hartree-Fock methods at oligomer level. The band gap and the ground and excited state electronic energies are calculated

successfully.[23]

The structural features and segment orientation of four poly-(phenylene vinylene) (PPV) derivatives with long, flexible side chains at room temperature are investigated by the Molecular Dynamics Simulations. The main chains of the polymers were found to be semirigid and to exhibit a tendency to coil into ellipsoidal helices or form zigzag conformations of limited regularity. The continuous quasi-coplanar segments along the backbone contained 2-4 repeat units. The ordered orientation and coupling distance of interchain aromatic rings were correlated with the optical properties of materials. A simplified quantum-mechanical method was developed to investigate optical properties based on MD trajectories. The method was tested to simulate the absorption spectra of four PPV derivatives. The absorption maxima of the calculated spectra were seen in reasonable agreement with experimental data. The conclusion was that the long-range electron transfer along the backbones of these polymers would not occur, but could be mediated by interchain interactions.[24]

The optical properties of conjugated polymers are highly relevant to the distribution of the length of coplanar segments between flips.[25] The presence of so-called "tetrahedral chemical defects" divides the polymer chains into structurally identifiable quasi-straight segments that allow the molecule to adopt a cylindrical conformation.[26] Photoluminescence is one of the important features of PPV thin films and it was found that the conjugation length has significant impacts on the absorption and photoluminescence spectra.[27,28,29] The emission spectra of poly(2-methoxy-5-(2-ethylhexyloxy)-p-phenylene vinylene) (MEH-PPV) solution was studied by using the exciton theory. The close correlation between interchain interactions and optical properties have been demonstrated by quantum-chemical computations of charge transfer between interchain segments.[30] Monte Carlo Simulation method can also be employed to find the time-independent properties like minimum energy structure of polymeric systems. Lowest energy configurations of amorphous CN-PPV and MEH-PPV systems with chain-chain distances of 3.3 and 4.1 Å, respectively were studied by the MC method.[31] Inter chain distances play an important role in packing and ordering of the polymer chains which determine many properties of materials. The formation of PPV aggregates in different chain packings

with variable interchain distances from 3 to 10 Å were analyzed.[32] Actually, the study of the relationship between molecular packing based on the crystal structures of model oligomers and their optical properties was the subject of many theoretical studies. Related computations can be classified into two major categories. The first class involves high level quantum-chemical methods such as ab initio methods, density functional theory, or semiempirical molecularorbital methods such as INDO, ZINDO and AM1. The second class of computations are mostly about the estimation of the energy bands as a function of polymer chain length. The methods employed basically are the Valence Effective Hamiltonian (VEH), Local Density Approximation (LDA), Electronic Polaron Model, coupled time-dependent Hartree-Fock (TDHF) method and Tight Binding (TB) theories.

During the search of different products, phenylene or polyphenylene is the macromolecule modified a lot. PPV and its derivatives are the mostly studied molecules in this context due to their interesting structural features and optical properties.[24] The interchain interactions are very important in keeping the coplanarity of the backbone and have some influences on the absorption and luminescence of these materials.[33,34]When the chain are separated around 5-7 Å, it has found that the molecular orbitals of the dimer start to delocalize over the two chains.[35]And also interchain ordered regions significantly improve interchain charge transport of a material, and eventually lead to high quantum efficiency.[24,36-40]

2. METHOD

2.1 Quantum Mechanical Methods

In quantum mechanics, the energy and the wavefunction are obtained by solving the electronic Schrödinger equation:

$$H\Psi = E\Psi \qquad \textbf{(2.1.1)}$$

Where Ψ is the wavefunction or mathematical function which depends on the cartesian coordinates of all the electrons in the system. E is the electronic energy and H is the Hamiltonian operator or total energy operator containing kinetic and potential energy operators for the system under consideration. Exact solution of Shrödinger equation only exists for hydrogen atom (one electron system). For larger systems, it is solved approximately. Various mathematical ways and electronic structure methods are developed to solve the equation at different level of accuracy depending on the size of the system. These methods are simply categorized as[41]:

1. Molecular Mechanics[42]
2. Semi – Emprical Methods[43]
3. Ab – Initio Methods[44]
4. DFT (Density Functional Theory)[45]

2.1.1 Molecular Mechanics

The term molecular mechanics refers to the use of Newtonian mechanics to model molecular systems. The potential energy of all systems in molecular mechanics is calculated using force fields. Molecular mechanics can be used to study small

molecules as well as large biological systems or material assemblies with many thousands to millions of atoms.[46]

2.1.2 Semi Empirical Methods

Semiempirical Methods depends on the Hartree-Fock (HF) theory using empirical (derived from experimental data) corrections in order to improve the speed and the performance of solving the equations. These methods are usually referred to through acronyms encoding some of the underlying theoretical assumptions. The most frequently used methods (MNDO, AM1, PM3) are all based on the Neglect of Differential Diatomic Overlap (NDDO) integral approximation, while older methods use simpler integral schemes such as CNDO and INDO. All three approaches belong to the class of Zero Differential Overlap (ZDO) methods, in which all two-electron integrals involving two-center charge distributions are neglected. A number of parameterized corrections are made in order to correct for the approximate quantum mechanical model. How the parameterization is performed characterizes the particular semiempirical method. For MNDO, AM1, and PM3 the parameterization is performed such that the calculated energies are expressed as heats of formations instead of total energies. Semi empirical methods are less accurate but can be preferred when the system is large. The methods so called AM1, MINDO/3 and PM3 implented in programs like MOPAC, AMPAC, HyperChem and Gaussian use parameters derived from experimental data to simplify the computation. They solve approximate Schrödinger Equation that depends on appropriate parameters available for the type of the chemical system under investigation. Different semi-emprical methods are largely characterized by their differing parameter sets.[41]

2.1.3 Ab – Initio Methods

Ab-initio (meaning “from the beginning” in Latin) methods, unlike either molecular mechanics or semi – empirical methods, do not use any experimental parameters in solving the equations. Instead, their computations are based on the laws of quantum mechanics and values of a small number of physical constants like the speed of light, the masses and charges of electrons and nuclei, Planck’s constant. Ab-inito methods also depend on Hartree-Fock theory which exchanges many electron problem by

only one electron problem. Ab–initio methods use a series of rigorous mathematical approximations without neglecting or parametrizing the two electron integrals. Because of that, they are expensive calculations as far as the computing time is concerned.[41]

2.1.4 Density Functional Theory

DFT (Density Functional Theory) presented firstly by Hohenberg and Kohn in 1964 states that all the ground state properties of a system are functionals of the electron density. In this method, the total electronic energy is divided into several terms which are computed separately:

$$E = E_T + E_V + E_J + E_{XC} \qquad \textbf{(2.1.4.1)}$$

where E_T is the total kinetic energy, E_V is the total potential energy including all interactions, E_J is the inter electronic repulsion energy and E_{XC} is called as exchange correlation energy that includes the remaining part of the electron-electron interactions.

Recently, DFT methods became very popular since they include the effects of electron correlations in a beter way than the HF methods which consider this effect only in an average sense i.e., each electron sees and reacts to an averaged electron density. Electron correlation methods like DFT method, consider the instantaneous interactions of pairs of electrons with opposite spin. DFT methods are superior to HF methods where the electron correlations are very important and have to be taken into account. The another advantage of DFT method is that it can be used for large systems up to ~100 atoms and it requires reasonable computation time. [41]

2.2 Statistical Mechanical Methods

Statistical mechanical methods are developed rapidly in the last decade enabling simulation of systems containing a great number of atoms up to ~10^6 -10^7 atoms. Using Molecular Mechanics force fields to describe the interactions at the molecular level, Molecular Dynamics (MD) and Monte Carlo (MC) methods successfully predict dynamic (time-dependent) and static (time-independent) properties,

respectively. Thermodynamic properties based on the principles of equilibrium and non-equilibrium statistical mechanics can also be calculated. [47]

2.2.1 Molecular Dynamics Simulation

MD simulation is also called as computer experiment and serves as a bridge between microscopic interactions and macroscopic properties of the system under consideration. It is a powerful tool for investigating a variety of phenomena in many-body systems. In particular, properties of condensed phases, such as liquids and solids, have been extensively investigated at an atomistic level. MD simulations are based on classical mechanics. The first and the most important step of the simulation is to generate or find an appropriate force field (ff) under which the particles are allowed to move in a 3D box. Then, the time evolution of each particle (atom or molecule) is determined by solving the Newton or Hamilton equations. The simulation box called unit cell is said to be periodic if it duplicates itself in all directions to mimic the real system at gaseous, liquid or solid states. Under different conditions (like temperature (T), number of particles in the unit cell (N), density, simulation time (t) , time step (Δt), etc.) the different methods or algoritms are chosen to solve the numerical integration of motion (second order differential equation).[48]

In standard MD simulations on condensed phases, the internal energy E as well as the number of particles N and the volume V is conserved. (NVE) ensemble is called microcanonical ensemble. However, the conservation of E and V sometimes make the MD not comparable with experimental data since temperature (T) and pressure (P) are kept constant instead of total energy (E) and volume (V) in laboratory experiments. In order to overcome this difficulty, many extensions of MD calculations have been introduced. In 1980, Andersen [49] introduced a pioneering technique that enables the volume of a MD cell to vary while the pressure is maintained at a desired value. In this constant-pressure MD technique, the volume is regarded as one of dynamical variables and its value is determined by the balance between the internal pressure and the external pressure. This technique was further extended by Parrinello and Rahman to deal with polymorphic transitions by allowing the shape of a MD cell as well as the volume to vary. The variable volume (and shape) especially aids in simulating phenomena accompanying large volume changes

like phase transitions. Controlling temperature is also desirable because T is an experimentally controllable parameter. On the basis of Andersen's idea, Nose [50] proposed a Hamiltonian that produces MD trajectories following the canonical (NVT) distribution. He proved that averages over the MD trajectories from his Hamiltonian are equivalent to averages over the canonical ensemble. The temperature (i.e. an average of kinetic energy) is maintained at a desired value in Nose's technique. Hoover [51] reformulated the equations from Nose Hamiltonian and the resultant equations are called as Nose–Hoover thermostat and have now widely been used. In our constant temperature simulations, we used Nose termostat. Both Andersen and Nose's techniques are based on "extended" Hamiltonians in which dynamical variables other than particles's positions and momenta are newly introduced. Combination of these two techniques is straight forward and the NPT ensemble, where N, P, and T are fixed as thermodynamic variables, can be generated from the Nose–Andersen Hamiltonian.[52]

2.2.1.1 Minimization

Before the simulation, the simulation box is subjected to minimization procedure to speed up the equilibration step to be followed. The forces on the atoms and their positions are changed until the total interaction energy converges to a minimum value. Depending on the studied system, the method of minimization, the level of convergence, the number of iterations, and the cell constraints can be chosen accordingly. Among the minimization methods, the most popular ones are Steepest Descent, Conjugate Gradient, Newton-Raphson methods and they are explained briefly as follows.

Steepest Descent (SD) Method: SD is one of the oldest and simplest methods. It is actually more important as a theoretical, rather than practical, reference by which to test other methods. However, `steepest descent' steps are often incorporated into other methods (e.g.,Conjugate Gradient, Newton) when roundoff destroys some desirable theoretical properties, progress is slow, or regions of indefinite curvature are encountered.

Conjugate Gradient (CG) Method: The CG method was originally designed to minimize convex quadratic functions but, through several variations, has been

extended to the general case. The first iteration in CG is the same as in SD, but successive directions are constructed so that they form a set of mutually conjugate vectors with respect to the (positive-definite) Hessian A of a general convex quadratic function qA(x). Whereas the rate of convergence for SD depends on the ratio of the extremal eigenvalues of A, the convergence properties of CG depend on the entire matrix spectrum. Faster convergence is expected when the eigenvalues are clustered. In exact arithmetic, convergence is obtained in at most 'n' steps. In particular, if A has m distinct eigenvalues, convergence to a solution requires 'm' iterations.[53]

Newton-Raphson (NR) Method: Newton-Raphson algorithms are very efficient for finding minima, particularly when inexpensive gradients (first derivatives) are available. These methods employ a quadratic model of the potential energy surface to take a series of steps that converges to a minimum. The optimization is generally started with an approximate Hessian (second derivative matrix), which is updated at each step using the computed gradients. The stability and rate of convergence of quasi-Newton methods can be improved by controlling the step size, using methods such as rational function optimization (RFO) or the trust radius model(TRM). [54]

In our MD simulations, the *Discover* module implemented in Material Studio (v. 3.01 and v. 4.1) software package was used. In the minimization step all three methods, SD, CG and NR were employed. Convergence level was set to "fine" meaning that the allowed energy deviations between successive steps of iteration are 1000 kcal $mol^{-1}Å^{-1}$ in SD, 10,0 $kcal.mol^{-1}Å^{-1}$ in CG, 0,001 kcal $mol^{-1}Å^{-1}$ in NR. Maximum iteration number was set to 10000 although the total energy converged before the maximum iteration number has been reached.

2.2.1.2 Dynamics

After minimization comes dynamics where the particles are moved under the predefined force field in a 3D simulation box. Time evolution of the particles are followed by solving the classical equations of motion which are modified under the effects of temperature and pressure on the system.

Newton's equation of motion:

$$\frac{d^2\vec{r}_i}{dt^2} = \frac{\vec{F}_i(\vec{r}_i,....\vec{r}_N)}{m_i} \qquad \textbf{(2.2.1.2.1)}$$

where $F_i(t)$ is the total force on the ith particle at time t and equals to the product of particle's mass and its accelaration. For N particle system, the cartesian coordinates are given by r.

$$\vec{F}_i(t) = m_i\vec{a}_i(t) \qquad \textbf{(2.2.1.2.2)}$$

The total force is assumed to be conservative and can be calculated from the total potential energy V_N as

$$\vec{F}_i = -\vec{\nabla}_i V_N(\vec{r}_1,.....\vec{r}_N) \qquad \textbf{(2.2.1.2.3)}$$

If there is no external field. The total potential energy of N-particle system is written as:

$$V_N = \sum_{i=1}^{N}\sum_{j>1}^{N} V_{ij}(\vec{r}_{ij}) \qquad \textbf{(2.2.1.2.4)}$$

V_{ij} is defined as pair potential or two-body potential and depends on the magnitude of the distance between the ith and jth particles:

$$\vec{r}_{ij} = \vec{r}_i - \vec{r}_j \qquad \textbf{(2.2.1.2.5)}$$

and

$$r_{ij} = |\vec{r}_{ij}| \qquad \textbf{(2.2.1.2.6)}$$

In our simulations, the system was brought to equilibrium at room temperature (298 K) in canonical (NVT) ensemble. Nose termostat was used to keep the temperature constant. The allowed energy deviation between the successive steps was 5000 kcal/mol. The typical simulation time was 600 ps, in other words, 600000 MD steps with the time step of 1 fs (10^{-15} seconds) were employed. After the equilibration, the system was simulated for another 50000 MD steps to store the positions and the velocities of the particles for the analysis.

2.2.1.3 Forcefield

Force field is the brain of the simulations and it should describe all the interparticle interactions accurately in order to obtain a good insight into the behavior of system to be studied. In our simulations COMPASS (Condensed-phase Optimized Molecular Potential for Atomistic Simulation Studies) force field [55] was used. It is an ab-initio forcefield that enables an accurate and simultaneous prediction of various gas-phase and condensed-phase properties of organic and inorganic materials. It generates a set of system configurations which are statistically consistent with a fully quantum mechanical description.

In general, the potential energy of a system of interacting particles can be expressed as a sum of the valence (or bond), $E_{valence}$, cross term, $E_{cross\text{-}term}$, and non-bond, $E_{non\text{-}bond}$, interaction energies as:

$$E_{total} = E_{valance} + E_{cross-term} + E_{non-bond} \quad \textbf{(2.2.1.3.1)}$$

Valence energy contains the following terms:

$$E_{valance} = E_{bond} + E_{angle} + E_{torsion} + E_{oop} + E_{UB} \quad \textbf{(2.2.1.3.2)}$$

E_{bond} is the valence energy generally includes a bond stretching term. E_{angle} is the dihedral bond-torsion term. $E_{torsion}$ is defined as inversion term. E_{oop} is out-of-plane interaction term and the final term E_{UB} is the Urey-Bradlay term and it involves interactions between two atoms bonded to a common atom.

The second term in the total energy is $E_{cross\text{-}term}$ the sum of the interaction energies between bond-bond, angle-angle, bond-angle, bond-torsion angle and angle-torsion angle interactions.

$$E_{cross-term} = E_{bond-bond} + E_{angle-angle} + E_{bond-angle} + E_{endbond-torsion} + E_{middlebond-torsion} + E_{angle-torsion} + E_{angle-angle-torsion} \quad \textbf{(2.2.1.3.3)}$$

The last term in the total energy expression is called total non-bonded interaction energy and it includes the energies of the van der Waals, Coulomb and H-bond type interaction in the system.

$$E_{non-bond} = E_{vdW} + E_{Coulomb} + E_{H-bond} \quad \textbf{(2.2.1.3.4)}$$

The COMPASS forcefield uses the following expressions for the various components of the potential energy mentioned above.

$$\mathrm{E_{bond}} = \sum_{b} \left[K_2 (b - b_0)^2 + K_3 (b - b_0)^3 + K_4 (b - b_0)^4 \right] \quad \textbf{(2.2.1.3.5)}$$

$$\mathrm{E_{angle}} = \sum_{\theta} \left[H_2 (\theta - \theta_0)^2 + H_3 (\theta - \theta_0)^3 + H_4 (\theta - \theta_0)^4 \right] \quad \textbf{(2.2.1.3.6)}$$

$$\mathrm{E_{torsion}} = \sum_{\phi} \left[V_1 \left[1 - \cos\left(\phi - \phi_1^0\right) \right] + V_2 \left[1 - \cos\left(2\phi - \phi_2^0\right) \right] + V_3 \left[1 - \cos\left(3\phi - \phi_3^0\right) \right] \right] \quad \textbf{(2.2.1.3.7)}$$

$$\mathrm{E_{oop}} = \sum_{x} K_x \chi^2 \quad \textbf{(2.2.1.3.8)}$$

$$\mathrm{E_{bond\text{-}bond}} = \sum_{b} \sum_{b'} F_{bb'} (b - b_0)\left(b' - b_0'\right) \quad \textbf{(2.2.1.3.9)}$$

$$\mathrm{E_{angle\text{-}angle}} = \sum_{\theta} \sum_{\theta'} F_{\theta\theta'} (\theta - \theta_0)\left(\theta' - \theta_0'\right) \quad \textbf{(2.2.1.3.10)}$$

$$\mathrm{E_{bond\text{-}angle}} = \sum_{b} \sum_{\theta} F_{b\theta} (b - b_0)(\theta - \theta_0) \quad \textbf{(2.2.1.3.11)}$$

$$\mathrm{E_{end\ bond\text{-}torsion}} = \sum_{b} \sum_{\theta} F_{b\theta} (b - b_0)\left[V_1 \cos\phi + V_2 \cos 2\phi + V_3 \cos 3\phi \right] \quad \textbf{(2.2.1.3.12)}$$

$$\mathrm{E_{middle\ bond\text{-}torsion}} = \sum_{b'} \sum_{\theta} F_{b'\theta} \left(b' - b'_0\right)\left[F_1 \cos\phi + F_2 \cos 2\phi + F_3 \cos 3\phi \right] \quad \textbf{(2.2.1.3.13)}$$

$$E_{\text{angle-torsion}} = \sum_{\theta}\sum_{\phi} F_{\theta\phi}\left(\theta - \theta^{'}\right)\left[V_1 \cos\phi + V_2 \cos 2\phi + V_3 \cos 3\phi\right] \quad \textbf{(2.2.1.3.14)}$$

$$E_{\text{angle-angle-torsion}} = \sum_{\phi}\sum_{\theta}\sum_{\theta'} K_{\phi\theta\theta'}\left(\theta - \theta_0\right)\left(\theta^{'} - \theta_0^{'}\right) \quad \textbf{(2.2.1.3.15)}$$

$$E_{\text{coulomb}} = \sum_{i>j} \frac{q_i q_j}{\varepsilon r_{ij}} \quad \textbf{(2.2.1.3.16)}$$

$$E_{\text{vdW}} = \sum_{i>j}\left[\frac{A_{ij}}{r_{ij}^{9}} - \frac{B_{ij}}{r_{ij}^{6}}\right] \quad \textbf{(2.2.1.3.17)}$$

where b and b' are the bond lengths, θ is the two-bond angle, Φ is the dihedral torsion angle, χ is the out of plane angle, q is the atomic charge, ε is the dielectric constant, r_{ij} is the i–j atomic separation distance. b_0, K_i (i = 2–4), θ_0, H_i (i = 2–4), Φ_i^0 (i = 1–3), V_i (i = 1-3), $F_{bb'}$, b'_0, $F_{\theta\theta'}$, θ'_0, $F_{b\theta}$, $F_{b\Phi}$, $F_{b'\Phi}$, F_i(i = 1–3), $F_{\theta\Phi}$, $K_{\Phi\theta\theta'}$, A_{ij}, and B_{ij} are the system dependent parameters implemented into Discover.[56]

2.2.2 Dissipative Particle Dynamics

In the DPD methodology, the fundamental particles are "beads" that represent small regions of fluid material rather than the atoms and molecules familiar from MD simulations. There are three types of force between pairs of beads, each of which conserves both bead number and linear momentum: an harmonic conservative interaction, a dissipative force representing the viscous drag between moving beads (i.e., fluid elements), and a random force to maintain energy input into the system in opposition to the dissipation. Integration of the equations of motion for the beads generates a trajectory through the system's phase space from which all thermodynamic observables (e.g., density fields, order parameters, correlation functions, stress tensor, etc) may be constructed from suitable averages. An immense advantage over conventional Molecular Dynamics and Brownian Dynamics simulations is that all forces are "soft" allowing the use of a much larger time-step and correspondingly shorter simulation times.

Polymers may be constructed out of the beads in a DPD simulation allowing the investigation of the morphologies of, for example, surfactants and branched

polymers. Just as a bead represents a small fluid element whose interactions with other beads include dissipative and random (thermal) terms, so a DPD polymer represents a segment of a real polymer whose size is of the order of the persistence length.

There are several ways to determine how much of a molecule constitutes a statistically correlated segment. Many properties such as persistence length, characteristic ratio, etc. can be used. However, experience shows that the characteristic ratio gives reliable results so we recommend this parameter. A DPD chain should therefore be made up of 'n_{DPD}' beads, where:

$$n_{DPD} = \frac{M_p}{M_m C_n} \qquad \textbf{(2.2.2.1)}$$

M_p is the molar mass of the polymer, M_m is the molar mass of a repeat unit and C_n is the characteristic ratio of the polymer.

Groot and Warren performed a series of DPD calculations on binary mixtures with a variety of repulsion parameters. They then computed Flory-Huggins parameters and found a linear relationship between χ and a_{ij}. This relationship can be used to obtain input parameters for a pair of species with a known χ value.

The relationships that Groot and Warren obtained are for bead densities of 3 and 5. Lower values than three should not be used. Thus, this can cause problems and also using values higher than five leads to long simulation times, since the time taken to perform simulations increases with the square of the density.

As lower densities are more efficient, in this study ρ=3 is used, for which the relationship between the Flory-Huggins parameter and the repulsion parameter is [57]

$$a_{ij\,DPD} = \frac{\chi}{0{,}306} + 25 \qquad \textbf{(2.2.2.2)}$$

2.2.2.1 Calculation of χ Parameter

Blends provides a way to shorten the discovery process by estimating the miscibility behavior of binary mixtures. These include solvent-solvent, polymer-solvent, and polymer-polymer mixtures. Blends predicts the thermodynamics of mixing directly from the chemical structures of the two components and, therefore, requires only their molecular structures and a forcefield as input.

Blends combines a modified Flory-Huggins model and molecular simulation techniques to calculate the compatibility of binary mixtures. Two important extensions to the Flory-Huggins model are employed:

- Blends incorporates an explicit temperature dependence on the interaction parameter. This is accomplished by generating a large number of pair configurations and calculating the binding energies, followed by temperature averaging the results using the Boltzmann factor and calculating the temperature-dependent interaction parameter.

- Blends is an off-lattice calculation, meaning that molecules are not arranged on a regular lattice as in the original Flory-Huggins theory. The coordination number is explicitly calculated for each of the possible molecular pairs using molecular simulations.

Blends distinguishes the components by using the role property: one component has a base role and the other has a screen role. A given base-screen combination can give four potentially different clusters, each of which will have an associated coordination number:

- Base-base cluster (Z_{bb})

- Screen-screen cluster (Z_{ss})

- Base-screen cluster (Z_{bs})

- Screen-base cluster (Z_{sb})

The last two clusters generally have different coordination numbers.

$$E_{mix} = \frac{1}{2}\left(Z_{bs}\left\langle E_{bs}\right\rangle_T + Z_{sb}\left\langle E_{sb}\right\rangle_T - Z_{bb}\left\langle E_{bb}\right\rangle_T - Z_{ss}\left\langle E_{ss}\right\rangle_T\right) \quad \textbf{(2.2.2.3)}$$

The interaction parameter, χ, is simply the mixing energy divided by RT, following χ is the central quantity in Flory-Huggins theory. Its temperature dependence gives rise to various phase diagrams. The χ parameter is also routinely used in mesoscale models as a measure of the interaction between mesoscale particles, which form a coarse-grained representation of the molecular structures used in Blends.

$$\chi = \frac{E_{mix}}{RT} \quad \textbf{(2.2.2.4)}$$

Firstly, the structures minimized with Discover module are imported to Blends module. To calculate the coordination number and the energy between two polymers, the optimized structure, charges on the atoms and forcefield are given as input in Blends module. The initial structures are reoptimized by the charges and forcefield given. The charges can be computed by using different methods like Electrostatic Potential method (ESP) or DFT (BLYP-DNP) charges are calculated.

Secondly, χ parameter is calculated by using experimental solubility parameters or the values calculated in Synthia module. The average molar volume is used as reference molar volume.

$$\chi = \frac{V_{ref}\left(\delta_i - \delta_j\right)^2}{RT} \quad \textbf{(2.2.2.5)}$$

Table 2.1: χ Interaction Parameters That are Calculated by Different Methods.

	Force field assigned		**Gasteiger**		**Charge Eq. Method**		**ESP (ab initio-BLYP/DNP)**	**Experimental Data**	**Synthia**
χ	**Compass**	**PCFF**	**Compass**	**PCFF**	**Compass**	**PCFF**	**PCFF**		
PPP-PCL	0,289	1,226	0,553	0,881	1,910	2,811	**0,549**		0,251
PS-PCL	0,749	1,688	0,482	0,717	2,011	2,772	**0,375**	0,04-0,86	0,122
PPP-PS	0,111	0,105	0,078	0,071	0,116	0,089	**0,085**		0,031

The polymers whose interaction parameter between each other is zero refers there is no mixing. Many method can be used to calculate interaction parameter (see Table

2.1) but Forcefield assigned, Gasteiger and Charge Equilibrium Methods are mechanical methods. In this study, we used DFT method (BLYP/DNP) to compute the interaction parameter more accurately. The example to the DPD input is as follows:

Species → Bead Types: ppp, ps, pcl

→ Topology for 40 PSt and 40 PCL on 4 PPP: (ppp 1 [ps 4] ppp 1 [ps 4] ppp 1 [pcl 14] ppp 1 [pcl 14]) x 3

The values in 'Topology' is calculated by using Eq. 2.2.3.3 .

Interactions → Repulsion:

And then by using Eq. 2.2.3.5, the repulsion parameters are calculated as seen in Table 2.2 .

Table 2.2: Calculated Repulsion Parameters of the Structures for DPD.

$a_{ij_{DPD}}$	PPP	PS	PCL
PPP	25	25,278	26,794
PS	25,278	25	26,226
PCL	26,794	26,226	25

In DPD, all properties are reported in the reduced units m, r_c, and k_BT, or combinations thereof. To relate the results of a simulation to a physical system requires substitution of the values of m, r_c, and k_BT for the appropriate physical units. Having specified the reduced units, all derived properties can be calculated. For example, if t_r is the time in reduced units, the time in physical units is $t = t_r r_c\sqrt{(m/k_BT)}$. Typical orders of magnitude are m = 0.1 kg mol^{-1}, k_BT = 1000 J mol^{-1}, r_c = 1 nm, with a time unit of $r_c\sqrt{(m/k_BT)}$ = 0.01 ns.

Setup → Run:

Number of steps → 20000

Time step → 0.0005 ns.

Total Simulation time → 10 ns.

System → Grid: 400 Å x 400 Å x 100 Å

Density → 3,0

Temperature → 1,0

At ρ=3, a_{ii} and a_{ij} parameters have been calculated according to the relationship established by Groot and Warren where $a_{ii}=25k_BT$ and $a_{ij} \approx a_{ii} + 3.27\chi_{ij}$. Also temperature of the system in DPD shown as 1. This value is calculated by using k_BT equation.

3. ANALYSES

3.1 System Description

The polymers modelled as a backbone or as side chains are poly(p-phenylene)-PPP, polystyrene-PSt, poly(ε-caprolactone)-PCL. PPP $(—C_6H_4—)_n$ is electroactive and electroluminescent material. Its electrical properties can be tuned by choice of doping and preparation procedure. It is insoluble and infusible material and it sustains high temperature treatments.[58] PSt ($—CH(C_6H_5)–CH_2—)_n$ is crystal clear thermoplastic. It is hard, rigid, free of odor and taste. It can be processed easily. It has high thermal stability, low specific gravity, excellent thermal and electrical properties to be used for insulating purposes, and it is a low cost polymer.[58] PCL $(—CO–(CH_2)_5–O—)_n$ is mostly synthesized as semicrystalline thermoplastic. It is a clear and fexible polyester with elastomeric properties.[58]

In this study, the macromonomer (Figure 3.1) containing two units of PSt bearing phenylenes and two units of PCL bearing phenylenes was modelled. n is the number of macromonomers in the polymers whose structures are to be studied and is equal to 3 and kept constant throughout the calculations. The lenghts of the side chains (PST or PCL) were increased in the form of blocks of 4 monomer units. The number of blocks were changed between 0 and 5 which corresponds to 0 -20 monomers in the side chains. The macromonomer modelled is the minimum –sized macromonomer which represents all kinds of interchain interactions. n was chosen to be 3 which is the large enough to get reasonable polymer behavior and properties and small enough to be afforded computationally.

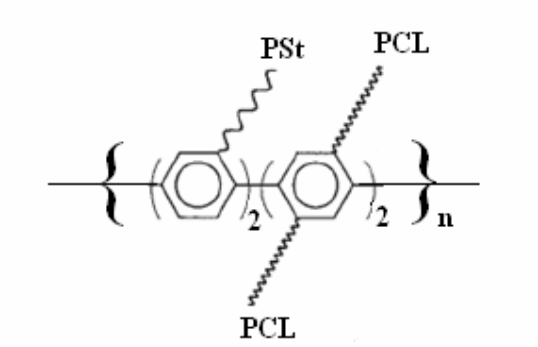

Figure 3.1: The Macromonomer Modelled In This Study. (n=3 in the polymer)

3.2 The Methods Used In Quantitative Structure–Property Relationship (QSPR) Calculations

One of the most successful approaches to the prediction of chemical properties starting only with molecular structural information is modeling of quantitative structure–activity/property relationships (QSAR/QSPR). The concept that there exists a close relationship between bulk properties of compounds and their molecular structure allows one to provide a clear connection between the macroscopic and the microscopic properties of matter. Quantitative structure–property relationships are mathematical equations relating chemical structure to a wide variety of physical, chemical, biological, and technological properties. QSPR models, once established, can be used to predict properties of compounds as yet unmeasured or even unknown. A major step in constructing the QSPR models is finding a set of molecular descriptors that represent variation in the structural properties of the molecules.[59]

The Synthia module in Materials Studio 4.1 allow to make rapid estimates of polymer properties using empirical and semiempirical methods.

Synthia can predict a wide range of thermodynamic, mechanical, and transport properties for bulk amorphous homopolymers and random copolymers. The key advantage of Synthia is that it uses connectivity indices, as opposed to group contributions, in its correlations; this means that no database of group contributions is required, and properties may be predicted for any polymer composed of any combination of the following nine elements: carbon, hydrogen, nitrogen, oxygen,

silicon, sulfur, fluorine, chlorine, bromine. This methodology is based on research conducted by Dr Jozef Bicerano.[57]

Equations that are used in Synthia as follows;

Molar Volume at 298 K ($V_{M,298K}$):

The molar volume is the volume occupied by one mole of ideal gas at STP.

$$V_{M,298K} = 3.642770\,\chi + 9.798697\,\chi^{v} - 8.542819\,\chi + 21.693912\,\chi^{v} + 0.978655N_{MV} \quad \textbf{(3.2.1)}$$

χ = Simple connectivity index.

χ^{v} = Valence connectivity index.

N_{MV} = Total values of number of elements, carbon-carbon double bonds, nonaromatic rings and number of rings in “fused” ring structures in the repeating unit.

Density at 298 K (ρ_{298K}):

Density defined in a qualitative manner as the measure of the relative "heaviness" of objects with a constant volume.

$$\rho_{298K} = \frac{M}{V_{M,298K}} \quad \textbf{(3.2.2)}$$

Glass Transition Temperature (Tg):

The temperature below which molecules have little relative mobility.

$$T_g = 351.00 + 5.63\delta + 31.68\frac{N_{T_g}}{N} - 23.94x_{13} \quad \textbf{(3.2.3)}$$

δ = Solubility parameter.

x_{13} = Total number of nonhydrogen side group atoms attached to the backbone silicon atoms flanked by ether (-O-) linkages on both sides along the chain backbone, divided by the number N_{BB} of atoms on the chain backbone.

N = Number of nonhydrogen atoms in the repeat unit.

Solubility Parameter by Fedors (δ_{Ecoh1}):

A parameter which is a characteristic of a polymer used in predicting the solubility of that polymer in a given solvent.

$$\delta_{Ecohl} = \sqrt{\frac{E_{coh1}}{V_{M,298K}}} \qquad \textbf{(3.2.4)}$$

E_{coh1} = Molar cohesive energy by Fedors Method.

$V_{M,298K}$ = Molar volume at 298 K.

Solubility Parameter by van Krevelen (δ_{Ecoh2}):

$$\delta_{Ecoh2} = \sqrt{\frac{E_{coh2}}{V_{M,298K}}} \qquad \textbf{(3.2.5)}$$

E_{coh2} = Molar cohesive energy by the Hoftyzer-Van Krevelen Method.

$V_{M,298K}$ = Molar volume at 298 K.

Cohesive Energy by Fedors (E_{coh1}):

The cohesive energy of a solid is the energy required to break the atoms of the solid into isolated atomic species.

$$E_{coh1} = 9882.5\chi + 358.7(6N_{atomic} + 5N_{group}) \qquad \textbf{(3.2.6)}$$

χ = Simple connectivity index.

N_{atomic} = Number of atomic units.

N_{group} = Number of different types of molecules.

Cohesive Energy by van Krevelen (E_{coh2}):

$$E_{coh2} = 10570.9(\chi^v - \chi) + 9072.8(2\chi - \chi^v) + 1018.2N_{VKH} \quad \textbf{(3.2.7)}$$

χ = Simple connectivity index.

χ^v = Valence connectivity index.

N_{VKH} = Total values of number of elements, carbon-oxygen double bonds, nonaromatic rings and number of caboxylic acid and anhydride in the repeating unit.

Thermal Conductivity at 298 K (λ_{298K}):

The thermal conductivity is the medium-dependent properties which relate the rate of heat loss per unit area to the rate of change of temperature.

$$\lambda_{298K} = 0.135614 + 0.126611\xi_{BB} + 0.108563\xi_{NOH} \quad \textbf{(3.2.8)}$$

ξ_{BB} = Specialized connectivity indices, used in calculating steric hindrance parameter on backbone.

Young's Modulus (σ):

The modulus of elasticity in tension.

$$\sigma = 0.028\ E_T \quad \textbf{(3.2.9)}$$

E_T = Young's modulus of rubbery or glassy polymer at temperature ,T.

Bulk Modulus:

The bulk elastic properties of a material determine how much it will compress under a given amount of external pressure. The ratio of the change in pressure to the fractional volume compression is called the bulk modulus of the material.

$$B = \frac{\frac{205V_{M,T}}{V_W}}{\left[\frac{V_{M,T}}{V_W} - 1.27\right]^2} - 2329\left[\frac{V_W}{V_{M,T}}\right]^2 \quad \textbf{(3.2.10)}$$

$V_{M,T}$ = Molar volume at temperature,T.

V_W = Van der Waals volume.

Dielectric Constant at 298 K (ε_{298K}):

Molecular quantities like dipole moment or polarizability is related to a macroscopic observable polarization or dielectric constant. Most often, the relationship may be assumed to be based on the separation of chains, the bending and streching of chemical bonds, and the orientation of (groups) of chemical bonds. Polarization is a material's response to an electric field, and the dielectric constant is an intrinsic measure of polarization.[60] The two quantities necessary to define electrical properties of materials are capacitance and conductance. The dielectric constant(e′) is the ratio of capacitance with the test specimen in the cell (C) to the capacitance without the specimen in place(C_0).

$$e' = C/C_0 \quad \textbf{(3.2.11)}$$

The dielectric loss (e″) is defined as $e'' = g/(2\pi f C_0)$ where g is the conductance(reciprocal of resistance, r) and f is frequency of the electric field. The quantities e′ and e″ make up the components of a complex dielectric constant (e^*) and given by

$$e^* = e' - ie'' \quad \textbf{(3.2.12)}$$

Materials employed as electrical insulators like undoped polyphenylenes are characterized by their low dielectric constants, usually below 5.[61] In polymers, it has shown that the dielectric constant at room temperature can be increases to very values $\geq 10^4$ with increasing percent crystallinity, the size of crystalline regions, and polymer chain alignment in the disordered regions, supporting the establishment of mesoscopic metallic regions.[62]

Here, the dielectric constant is calculated by the empirical formula given in the Equation (3.2.13). It depends on E_{cohl}, N_{dc}, V_w

$$\varepsilon_{298K} = 1.412014 + \frac{0.001887E_{coh1} + N_{dc}}{V_W} \quad \textbf{(3.2.13)}$$

E_{coh1} = Molar cohesive energy by Fedors Method.

V_W = Van der Waals volume.

Permeability of Oxygen (P_{O_2}):

The relative permeability is arrived at by taking the ratio of the material's permeability to the permeability in a type of gas phase.

$$P_{O_2} = 4991.6 \exp(-0.017622\nu) \quad \textbf{(3.2.14)}$$

ν = Newchor.

Volume Resistivity:

Volume resistivity is defined as the ratio of the DC voltage drop per unit thickness to the amount of current per unit area passing through the material. A basic material property, volume resistivity indicates how readily a material conducts electricity through the bulk of the material. Volume resistivity is expressed in ohm-centimeters (Ω-cm).[63]

The founded literature values to compare the results that is analysed the properties above with Synthia (see Table 3.1).

With Synthia in Materials Studio 4.1; the model structures are performed according the temperatures at 298 °K and molecular weight of 50000.

Table 3.1: Experimental Data [58,64]

Property	Poly(p-phenyl) PPP	Polystyrene PSt	Polycaprolactone PCL
Repeat unit molecular weight (g/cm)	76	104	114
Glass transition temperature T_g (K)		373	201
Molar volume at 298K (cm^3/mol)	68.46	100	104.20
Density at 298K (g/cm^3)	1.11 ± 0.02	1.04 - 1.06	1.09
Cohesive energy at 298K(kJ/mol)		29.60 - 35.40	
Solubility parameter at 298K $(J/cm^3)^{1/2}$		15.60 - 21.10	20.07
Thermal conductivity (J/Kms)		0.10 - 0.11	
Dielectric constant at 298K		2.49 - 2.55	
Volume resistivity at 298K (ohm.cm)		10^{20} - 10^{22}	
Bulk modulus (MPa)		3000	
Young's modulus (MPa)		3000	
Poisson's ratio at 298K		0.32 - 0.33	
Permeability of oxygen at 298K (Dow unit)		$2x10^{-4}$	

4. RESULTS AND DISCUSSIONS

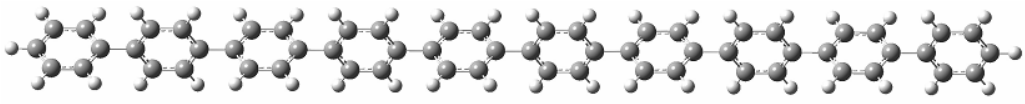

Figure 4.1: The Poly(p-phenylene) Chain

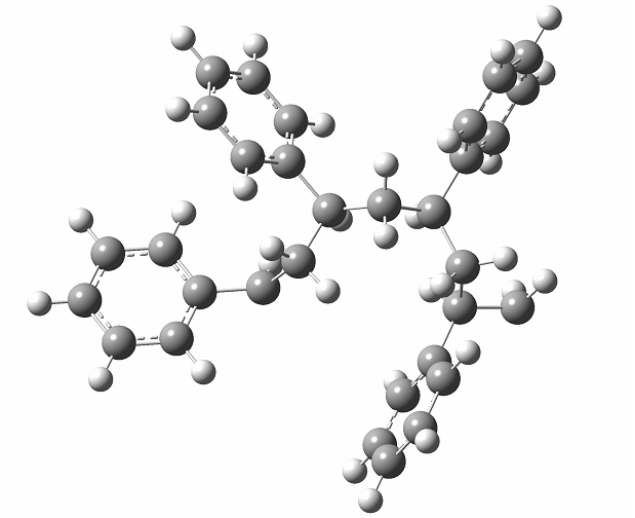

Figure 4.2: The Polystyrene Chain

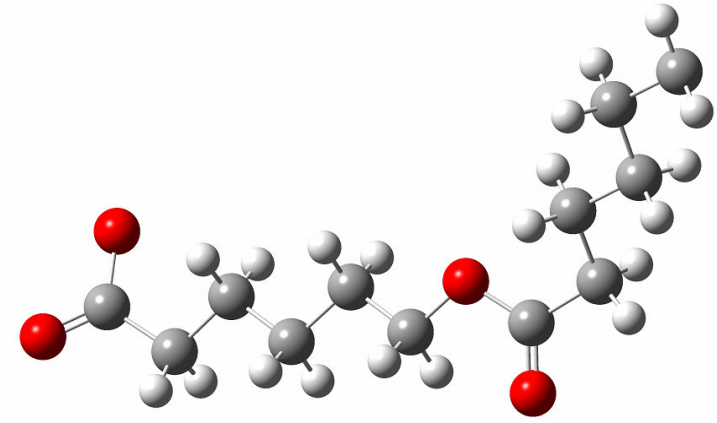

Figure 4.3: The Poly(ε-caprolactone) Chain

4.1 QSPR Results

In this study, some properties are investigated by using QSPR Method. And the results are shown as a table and figures.

Table 4.1: The QSPR Results

T=298 K MW=50 000	Repeat unit molecular weight (g/mol)	Glass transition temperature Tg (°K)	Molar volume at 298K (cm^3/mol)	Density at 298K (g/cm^3)	Cohesive energy (Fedors) at 298K (kJ/mol)	Cohesive energy (van Krevelen) at 298K (kJ/mol)	Solubility parameter (Fedors) at 298K (J/cm^3)$^{1/2}$
Poly(p-phenylene)	76	625	67	1,143768	29	28	20,990620
Polystyrene	104	382	97	1,074008	39	37	20,104694
Polycaprolactone	114	229	104	1,101634	42	33	20,149588
PSt – PCL							
0-0	76	625	67	1,143768	29	28	20,990620
0-4	2252	320	1980	1,137434	913	797	21,477472
0-8	4077	285	3603	1,131655	1587	1320	20,987968
0-12	5903	272	5229	1,128915	2260	1844	20,789404
0-16	7730	265	6856	1,127478	2933	2368	20,684319
0-20	9556	261	8482	1,126587	3606	2892	20,619261
4-0	1138	453	1044	1,089906	431	408	20,316772
4-4	3084	339	2754	1,119864	1228	1093	21,112307
4-8	4910	304	4380	1,120971	1901	1617	20,829836
4-12	6737	287	6007	1,121480	2574	2141	20,699078
4-16	8563	278	7633	1,121772	3247	2665	20,623671
4-20	10389	272	9260	1,121956	3920	3189	20,574604
8-0	1971	428	1820	1,083130	744	703	20,226639
8-4	3917	351	3530	1,109787	1541	1388	20,895014
8-8	5744	318	5156	1,113906	2214	1912	20,722368
8-12	7570	300	6783	1,116053	2887	2436	20,631981
8-16	9396	289	8409	1,117364	3560	2960	20,576355
8-20	11222	281	10036	1,118248	4233	3484	20,538673

12-0	2804	418	2595	1,080405	1058	999	20,190275
12-4	4750	359	4306	1,103339	1855	1684	20,754839
12-8	6577	328	5932	1,108690	2528	2208	20,642662
12-12	8403	310	7559	1,111738	3201	2732	20,578497
12-16	10229	298	9185	1,113700	3874	3255	20,536945
12-20	12056	290	10812	1,115071	4547	3779	20,507843
16-0	3637	412	3371	1,078934	1372	1294	20,170616
16-4	5584	364	5081	1,098861	2168	1979	20,656914
16-8	7410	335	6708	1,104680	2841	2503	20,581182
16-12	9236	318	8334	1,108223	3514	3027	20,534868
16-16	11063	306	9961	1,110606	4188	3551	20,503616

Table 4.2: The QSPR Results (Continued)

T=298 K MW=50 000	**Solubility parameter (van Krevelen) at 298K $(J/cm^3)^{1/2}$**	**Thermal conductivity (J/Kmol)**	**Dielectric constant at 298K**	**Volume resistivity at 298K (ohm.cm) (10^{-17})**	**Bulk modulus (Mpa)**	**Young's modulus (Mpa)**	**Poisson's ratio at 298K**	**Permeability of oxygen at 298K (Dow unit)**
poly(p-phenyl)	20,48181	0,189162	2,651925	4,97	5036,441	2566,074	0,415083	264,789368
polystyrene	19,515451	0,134966	2,567054	7,34	3598,705	3025,375	0,359886	363,687103
polycaprolactone	17,777895	0,19828	2,911814	1,50	2445,652	3,155	0,426696	28,864779
PSt – PCL								
0-0	20,48181	0,189162	2,651925	4,97	5036,441	2566,074	0,415083	264,789368
0-4	20,061216	0,153212	3,08359	0,68	3602,927	5464,799	0,247206	30,247561
0-8	19,143858	0,149961	3,042147	0,82	3083,545	6437,668	0,152042	57,707317
0-12	18,780178	0,148678	3,025383	0,89	3160,071	8028,177	0,076583	74,486702
0-16	18,586197	0,147999	3,016551	0,93	3206,351	0,019	0,008722	85,210114
0-20	18,465574	0,147579	3,011097	0,95	3183,814	0,013	-0,039889	92,590347
4-0	19,768066	0,139869	2,587895	6,67	4074,267	4534,051	0,314525	343,488403
4-4	19,9189	0,144179	2,937966	1,33	3645,245	6776,77	0,190155	25,646778
4-8	19,210777	0,144765	2,956401	1,22	3187,06	7303,947	0,118042	46,696812
4-12	18,87731	0,145039	2,964917	1,18	3055,695	8565,608	0,032806	61,649113
4-16	18,683226	0,145197	2,969821	1,15	3091,551	11047,78	-0,09559	72,36676
4-20	18,556231	0,145301	2,973009	1,13	3165,55	10756,73	-0,066343	80,325081
8-0	19,660769	0,132364	2,579026	6,95	3911,216	5763,62	0,254398	352,156097
8-4	19,830931	0,13926	2,855827	1,94	3666,467	7858,385	0,142781	23,625917
8-8	19,256969	0,14127	2,897091	1,61	3331,805	8746,715	0,062464	40,21344
8-12	18,951399	0,142334	2,918726	1,45	3100,507	8955,421	0,018604	53,221874
8-16	18,761551	0,142992	2,932045	1,37	3042,873	10014,92	-0,048545	63,278172
8-20	18,632141	0,14344	2,94107	1,31	3062,196	11114,38	-0,104924	71,167748
12-0	19,617441	0,129306	2,575452	7,06	3842,201	6818,736	0,204217	355,618225
12-4	19,774458	0,13613	2,803472	2,47	3675,104	8562,107	0,111707	22,434988
12-8	19,290989	0,138706	2,853462	1,96	3393,788	9231,136	0,046665	36,051495
12-12	19,010063	0,140198	2,882144	1,72	3196,383	9806,311	-0,011323	47,401749
12-16	18,826391	0,141171	2,900747	1,58	3063,531	10232,91	-0,056706	56,646229
12-20	18,696922	0,141855	2,913791	1,49	3035,253	11446,48	-0,128529	64,202393
16-0	19,594006	0,127646	2,573521	7,13	3804,056	7711,152	0,162152	357,481201
16-4	19,735161	0,133962	2,767189	2,92	3678,972	9167,037	0,08471	21,650894
16-8	19,317076	0,136746	2,82002	2,29	3436,495	10718,02	-0,019813	33,168972
16-12	19,057669	0,138469	2,852455	1,97	3273,291	10710,08	-0,045327	43,166203
16-16	18,880962	0,139641	2,874393	1,78	3133,971	11070,56	-0,08874	51,620998

The change of the different properties of the PPP based polymers with increasing either one of the polymeric side chains are plotted and shown in Figures 4.4 - 4.16. The calculations with structure 16-20 couldn't be carried out since the number of atoms in the polymer exceeded the maximum number of atoms allowed by the software.

4.1.1 Glass Transition Temperature (°K)

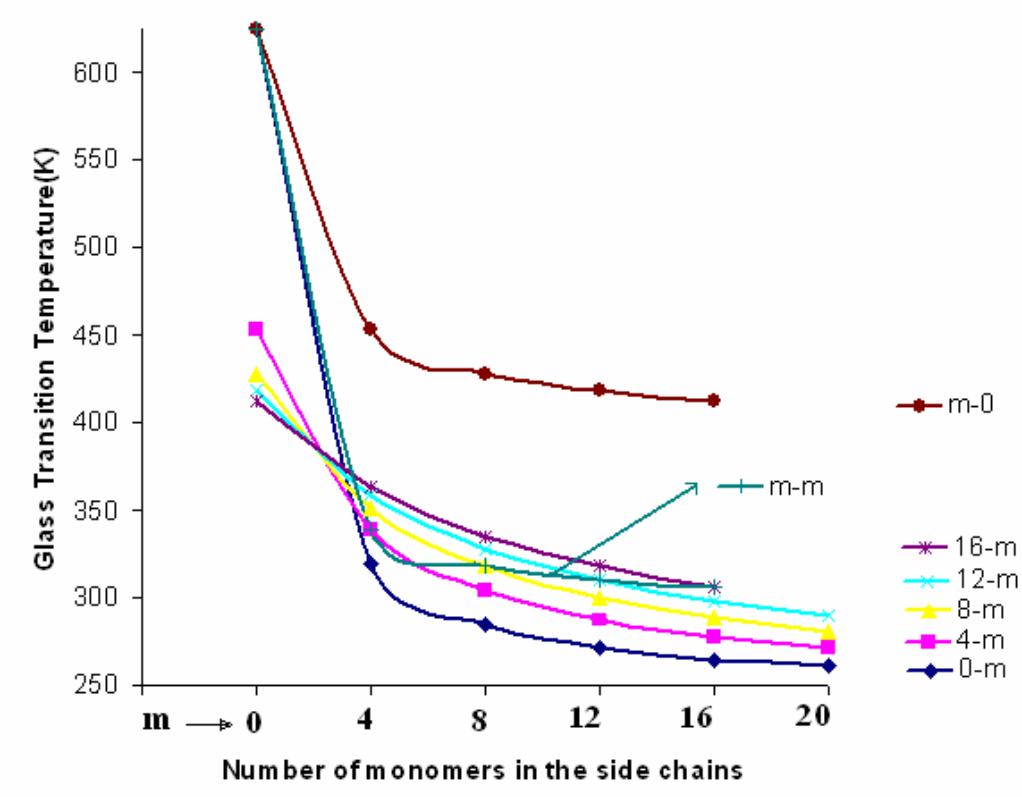

Figure 4.4: The Effect of Side Chains on T_g

The T_g values of PPP, PSt, and PCL are 625 K, 382 K, and 229 K, respectively. Because of the fact that the T_g of PSt is much closer to T_g of PPP than that of PCL, a drastic decrease is observed when the first PCL segment is added to naked PPP backbone. When the side chain length of PCL is increased, T_g of the material keeps falling and approaches a value which is closer to the T_g of the PCL homopolymer, indicating that the chain mobility was improved by incorporating side groups. With the improved chain mobility, molecular ordering was slightly improved, showing a bundle-like ordering without regular packing.

The decrease in T_g is less drastic when the substituted polymer is PSt. On the other

hand, the T_g of PSt bearing PPP decreases upon increase of PCL side chains where as the T_g of the PCL bearing PPP slightly increases upon increase of PSt side chains, as expected. The change in the initial and final T_g values are related to the initial concentration or %wt of the side chain kept constant while the other side chain length increases. For example, if one starts with high PCL concentration and increases PSt chain length (indigo curve in the Figure 4.4), the change in T_g is smaller compared to the other curves in the same plot where the initial concentration of PCL is lower. Same argument is valid for the curves in the plot 4.4. The smallest change in the T_g is observed again for the indigo curve where the PCL concentration is the highest. The T_g of the materials studied here have a very wide range between 625 K and 261 K. We show that it is possible to control the T_g of the material by changing the length of the side chains on the PPP backbone. The presence of two different side chains incorporated in various weight percentages helps to prepare conducting material with improved elasticity and processibility and controllable glass transition temperature as well as many other properties as it will be discussed later.

4.1.2 Molar Volume (cm^3 / mol)

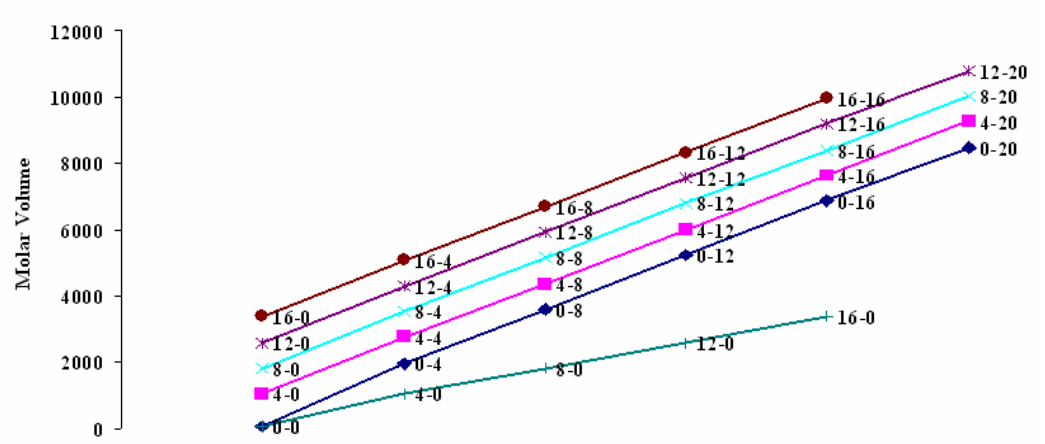

Figure 4.5: The Effect of Side Chains on Molar Volume

Incorporation of the side chains increases the molar volume of PPP and it increases linearly as the same segment of the side chain is added to the backbone. Addition of the first PCL segment increases molar volume than the addition of the first PSt segment although they have comparable monomer volumes ($V_{styrene}$ =173 $Å^3$ and $V_{caprolactone}$ =202 $Å^3$, approximately). It should be kept in mind that the PCL side chains are added from both sides of PPP skeleton but PSt side chains are added only

from one side of the PPP skeleton, i.e., the number of the PCL segment is twice of the number of the PSt segments. Because of that the molar volume of 0-4 structure is almost twice of the molar volume of 4-0 structure.

4.1.3 Cohesive Energy (KJ / mol)

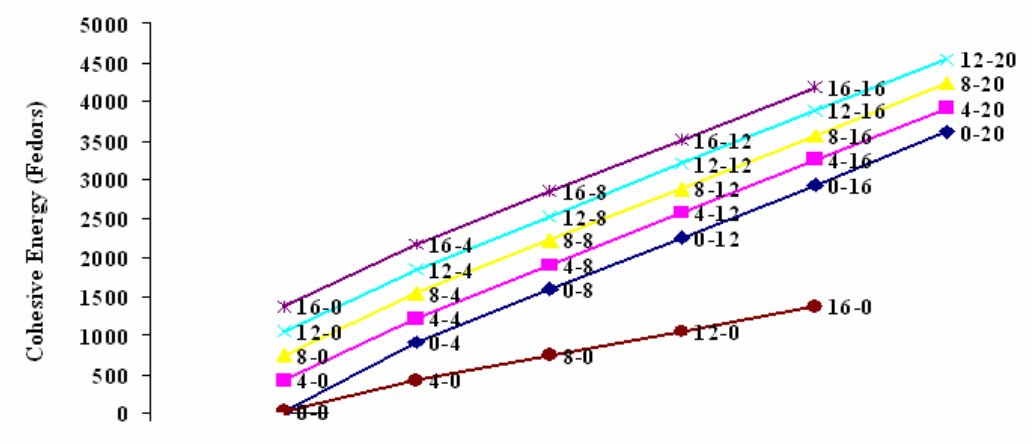

Figure 4.6: The Effect of Side Chains on Cohesive Energy(Fedors)

Cohesive energy is calculated by two different methods as described above. Both methods predict that the energy increases upon increase in the side chain lengths. The slopes of the curves may vary but the increase in cohesive energy is linear meaning that there is no critical side chain length at which the energy changes drastically. This fact is very understandable. When the polymer gets bigger, the non-bonded interactions like van der Waals, Coulomb and H-bond interactions between the polymer chains become more pronounced and it becomes harder to break the intermolecular interactions. As it can be seen later, this can be reflected in many properties of the materials.

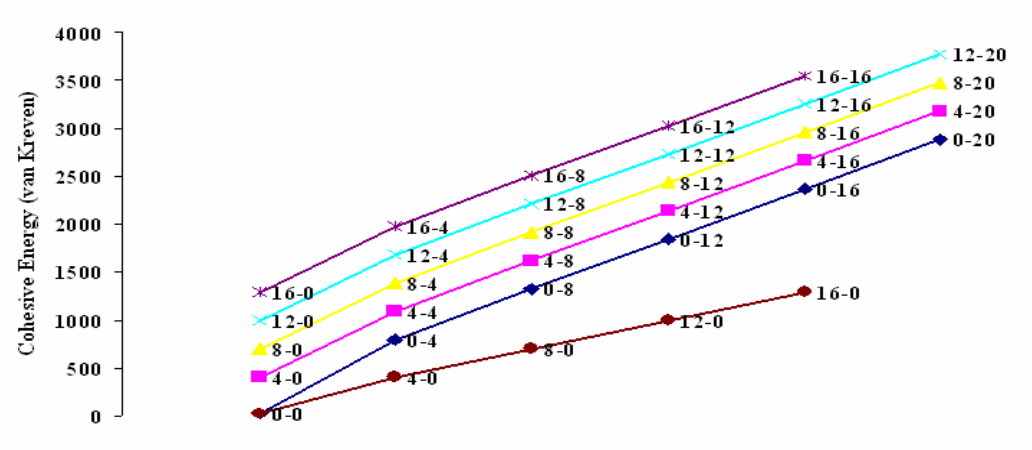

Figure 4.7: The Effect of Side Chains on Cohesive Energy(van Kreven)

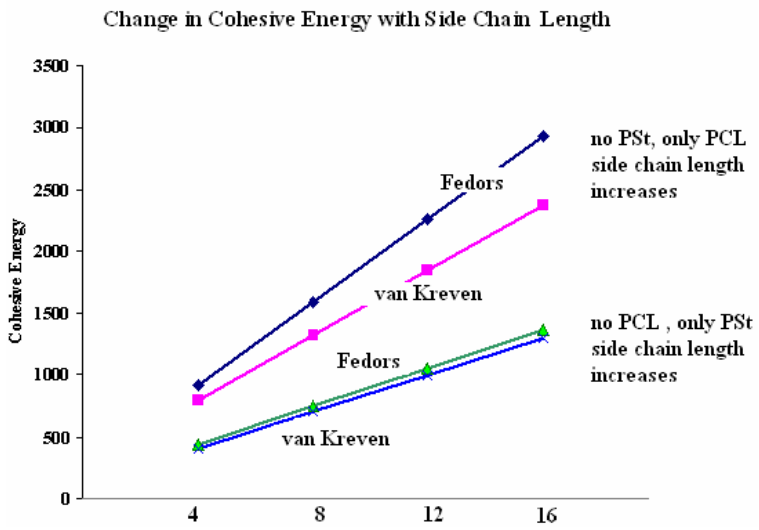

Figure 4.8: Comparison of the Cohesive energy of PPPs Containing One-type of Side Group In Terms of Two Different Methods.

The linear relationship between the cohesive energy and the length of the side chains is preserved by the both methods and the values estimated by Fedors and van Kreven differ slightly in the high energy region. It is not surprising that the PCL containing structures have higher cohesive energy than the PSt containing structures. PCL chains have higher molar volumes and many rotatable single bonds between the C-C atoms and sp^3 oxygen atoms which have H-bond making capacities with the hydrogen atoms of the interacting chains. The total non-bonded interaction energies between PCL chains are obviously higher than that of PSt chains regardless whether these polymers are substituted to the PPP backbone as side chains or they interact as single chains.

4.1.4. Solubility Parameter $(J / cm^3)^{1/2}$

Solubility parameter, δ calculated by the Fedors method varies within the narrow range between 20.1 and 21.5. It can be thought that the solubility parameter does not depend heavily on the side chain length. Hovewer, the solubility parameter versus increasing side chain length of PCL plot shows an interesting behavior. The δ is increased up to 0.8 points upon incorporation of short side chains but it reduces when the side chain is lenghtened.

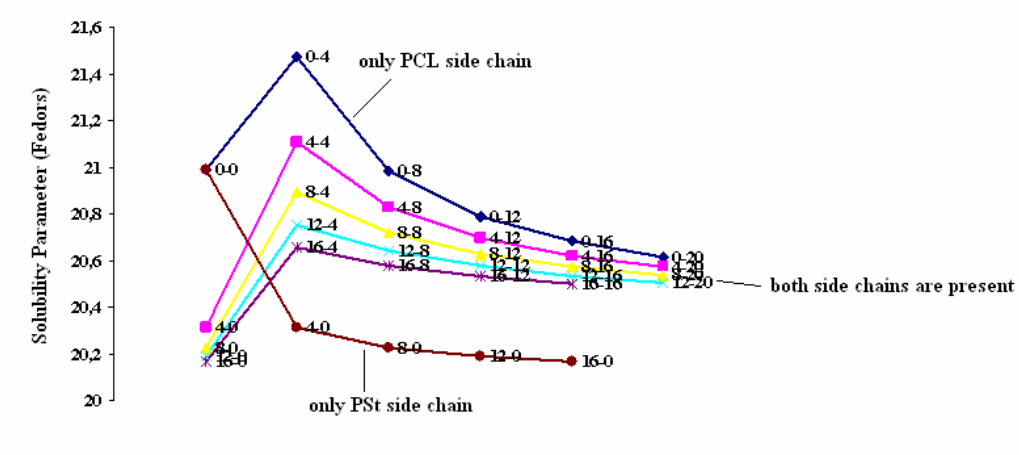

Figure 4.9: The Effect of Side Chains on Solubility Parameter(Fedors)

The sudden increase observed following the substitution of the first PCL block into the structure can not be seen in the change of the solubility parameter versus increasing side chain length of PSt plot and the δ of the structures with constant chain length of PCL and variable chain length of PSt reduces hyperbolically. The decrease in the solubility is maximum when there is no PCL side chains on the PPP backbone.

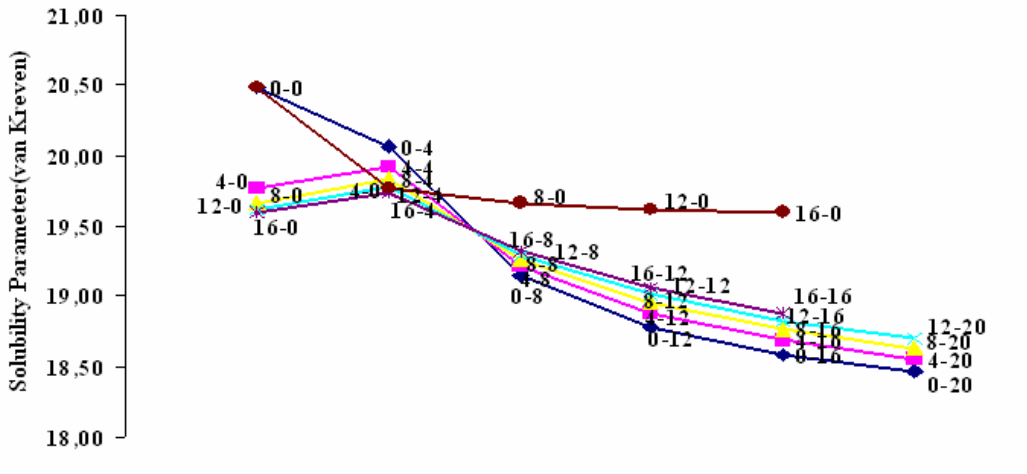

Figure 4.10: The Effect of Side Chains on Solubility Parameter (van Kreven)

Solubility parameter,δ, calculated by the second method (Van Kreven) are lower than the values obtained by the first method but again within the narrow range between 18.5 and 20.5. It reduces with increasing PCL side chain length and almost stays constant with increasing PSt side chain length. Almost in all of the solubity parameter plots, the drastic decrease occurs during the passage from the pure to impure or substituted (0-4 or 4-0) structure. Once the PPP backbone is impured, the decrease in δ is mostly linear. It would be too ambitious to say that the solubility character of the material could be controlled by the side chain lengths. Hovewer, δ can be changed up to 2 units depending on the type and the length of the side chains wherever 2 units make difference in these systems.

4.1.5 Thermal Conductivity (J / Kms)

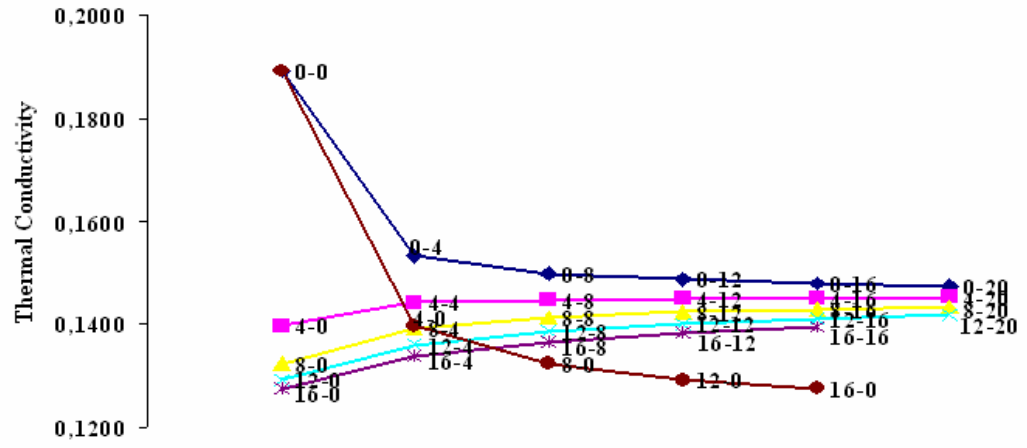

Figure 4.11: The Effect of Side Chains on Thermal Conductivity

Thermal conductivity of the unsubstituted PPP is much higher than the substituted PPPs. It drops from 0.189 to 0.153 then slowly reduces and stays constant. If the initially the PPP contains PSt, upon substitution of the PCL side chains increases slowly the thermal conductivity and after a while it reaches a plateau where it stays constant.

When there is no PCL side chains, lowest thermal conductivities are obtained. In case of its presence, the thermal conductivity values can be increased from 0.130 to 0.145.

4.1.6 Dielectric Constant

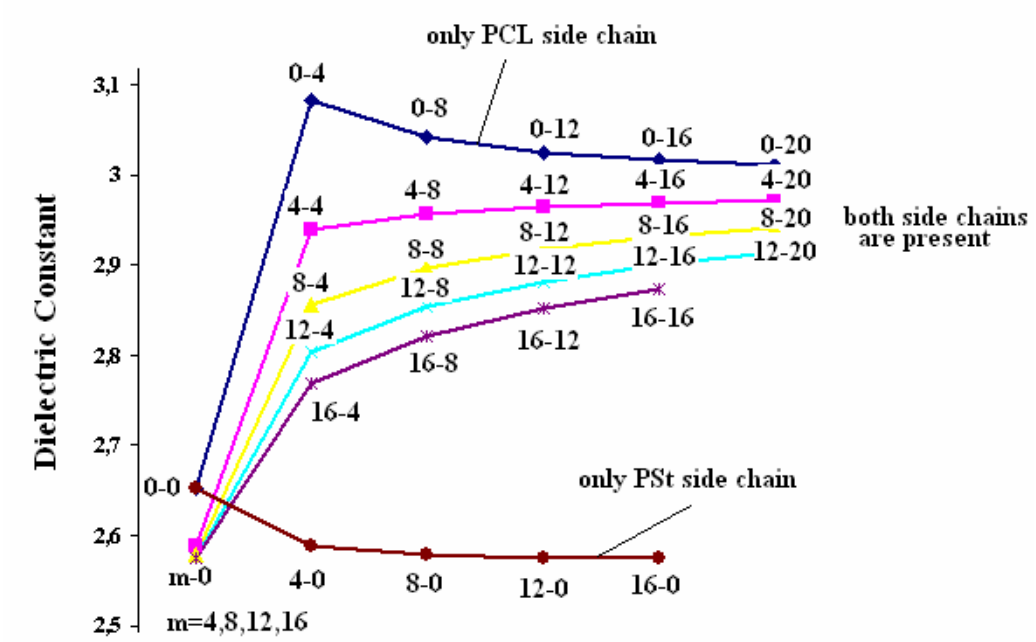

Figure 4.12: The Effect of Side Chains on Dielectric Constant

Dielectric constant of PPP slightly reduces by incorporation of PSt side chains and stays constant with increasing PSt chain length whereas it rapidly increases by incorporation of the first PCL segment then reduces slowly. When PPP contain PSt side chains, by increasing PCL side chain length, all the curves converge to the average value of 2.95. If the PCL side chain length is long enough (larger than 20), the reducing affect of the PSt side chains diminish.

4.1.7 Volume Resistivity (ohm.cm)

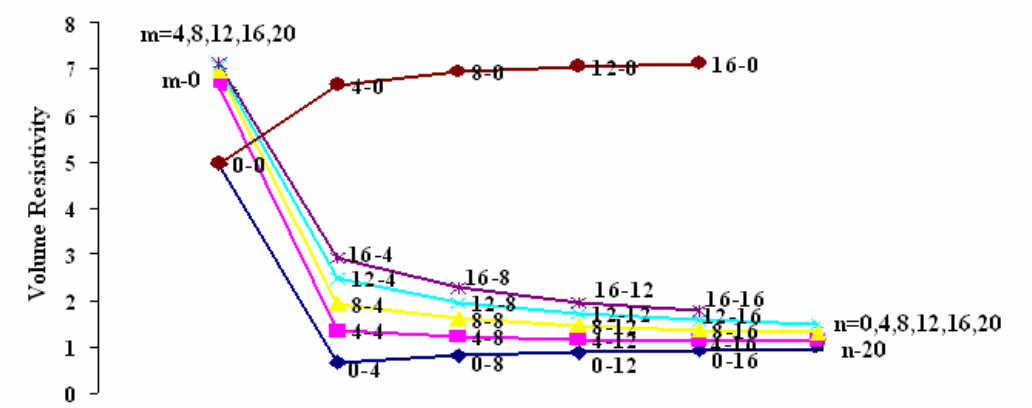

Figure 4.13: The Effect of Side Chains on Volume Resistivity

Volume resistivity is related to the material's electrical conductivity. As expected, this quantity is increased by the presence of the rigid PSt side chains and decreased by the presence of flexible, semi-crystalline PCL side chains. The reason can be that the incorporation of PSt side groups increases the rigidity of the backbone by restoring the planarity of the phenylene units.

4.1.8 Bulk Modulus (MPa)

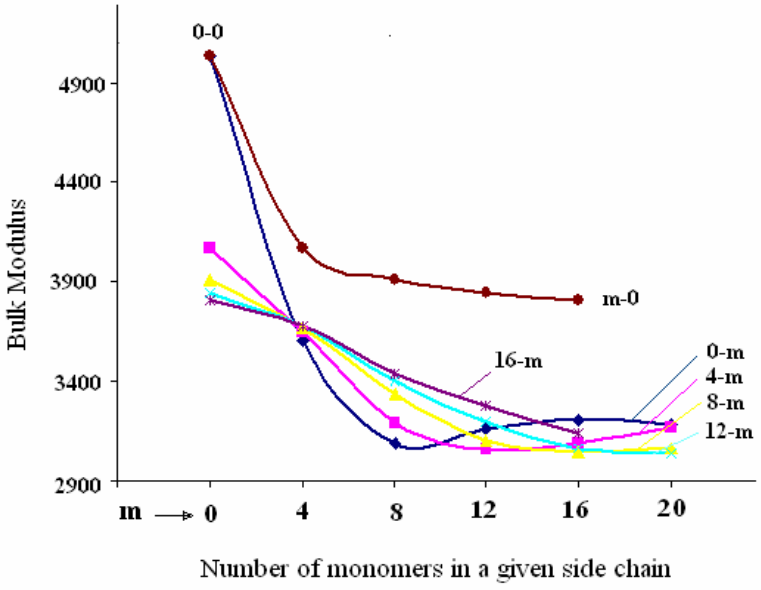

Figure 4.14: The Effect of Side Chains on Bulk Modulus

Bulk Modulus is inversily proportional to compressibility of a material. Molar

volumes of both styrene and caprolactone monomers are larger than that of the phenylene monomer. As it has been shown before molar volume of the PPPs with rigid (PSt) and flexible(PCL) side groups increases steadily as the length of the side chains increases. Compressibility of structures increases (bulk modulus decreases) as the material contains more flexible PCL chains. The structures which are rich in PSt have relatively less compressibility (higher bulk modulus) as expected. When there is no or very short PSt side chains, the maximum compressibility or minimum bulk modulus is obtained at a specific chain length of PCL group. After this point, adding more flexible chains do not help to reduce the compressibility any more. For the structures $(\text{-(PP)}_4(\text{St})_0(\text{CL})_8\text{-})_n$, $(\text{-(PP)}_4(\text{St})_4(\text{CL})_{12}\text{-})_n$ and $(\text{-(PP)}_4(\text{St})_8(\text{CL})_{16}\text{-})_n$ maximum compressibility so; minimum bulk modulus can be seen.

4.1.9 Young's Modulus (MPa)

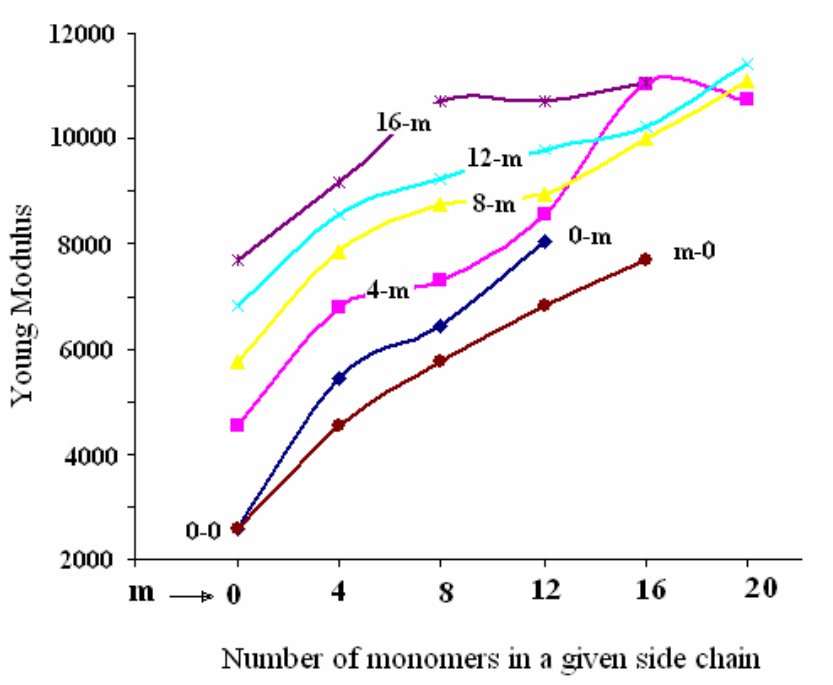

Figure 4.15: The Effect of Side Chains on Young Modulus

Young Modulus is a measure of the change in the length under applied force per unit area and it depends on the direction of the force applied. In this case, the plot here shows the changes of the length of the rigid backbone. Young modulus increases due to the effects of the side groups which add extra rigidity to the PPP backbone by forcing the phenylene ring to be planar to minimize the repulsive interactions.

4.1.10 Permeability of Oxygen (Dow)

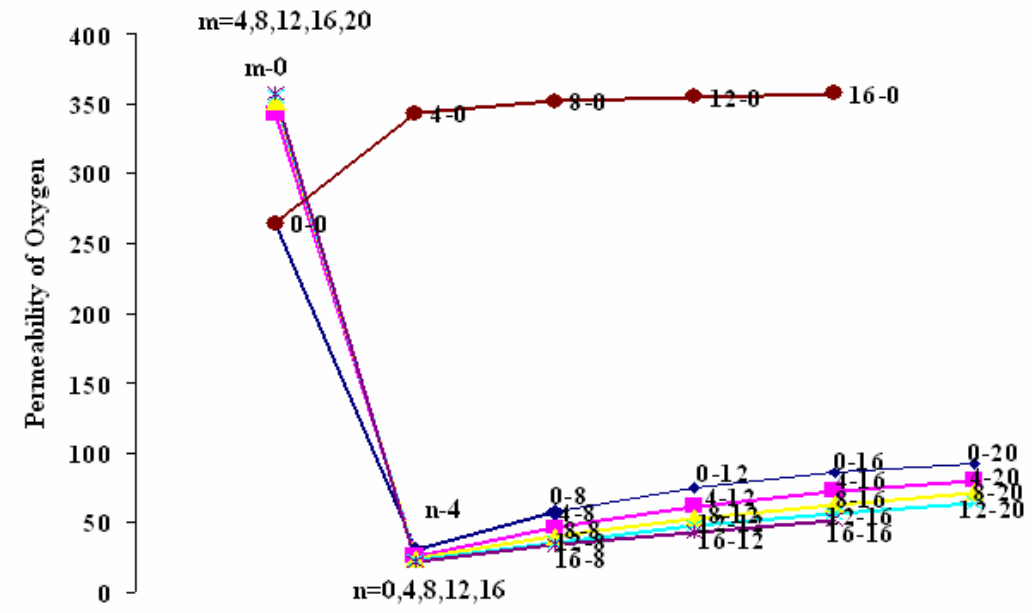

Figure 4.16: The Effect of Side Chains on Permeability of Oxygen

Oxygen permeability of PCL containing polymers reduces drastically whereas only PSt side chains containing polymers have oxygen permeability very close or almost identical to that of naked PPP.

4.2 MD Results

In the second part of the study, the single and double PPP backbones with PCL and PSt side chains of different %wt are exposed to Molecular Dynamics (MD) Simulations in canonical ensemble in which number of molecules, volume of the simulation box and the temperature (NVT) is constant. Simulations were carried out by using Material Studio 4.1 software at room temperature. In the first part, the QSPR calculations are carried out for the single chain PPPs with linearly increasing non-interacting side chains. The interactions of the side chains of the same types (PCL-PCL,PSt-PSt) and different types (PCL-PSt) with each other and also with the PPP backbone are not considered. In reality, at any temperature, these interactions exist and play an important role in the behavior and the properties of these materials. Because of the sterically not-hindered free rotations around the single bonds and the chain vibrations, the bonded and non-bonded interactions within the molecule

increase and result in the change of the microstructure. MD simulations are used to find the optimized microstructures of the polymers under investigation at a given temperature otherwise, it would not be possible to obtain by using quantum mechanical methods. For the single chain MD calculations, the three repeating units of the "macromonomers" having 4 phenylene rings, all substituted by the side groups with different chain lengths. n_{St} is the number of styrene repeating units in PSt side groups and similarly n_{CL} is the number of caprolactone repeating units in the PCL side groups. The so called PPP, PSt and PCL are not the long chains but the oligomers of the corresponding polymers. Two adjacent phenylene ring have the same substitution in the macromonomers. An example to macromonomers is given in Figure 4.18.

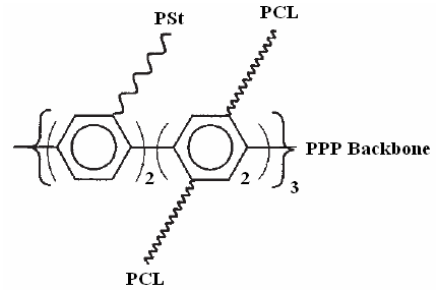

Figure 4.17: Single Chain of PPP Backbone.

A snapshots of the structures with one or two PPP backbones optimized by MD simulations by equilibrating at room temperature for 600 ps are given in the appendix part, in the Tables A.1 and A.2.

Single chain PPPs exhibit an interesting behavior of the PCL chains in the absence of PSt groups. If the PCL chains are not long enough, they lie almost paralel to each other interacting mostly with the nearest neighboring chains. The long chains start folding immediately and their interactions are not limited to next neighbor, many chains interact because of the length and folding. When the PSt chains are introduced, they are called as soft coils, they tend to aggregate by pushing the PCL chains paralel to rigid PPP backbone, they prevent folding of the PCL chains. Folding only occurs towards the end of the PCL chains and separated PCL chains are forced to make group of two. In the Figure 4.19, grouping of PCL chains on one side of the backbone and the phase formed by the PSt chains on the opposite side of the backbone can be seen. From the single chain PPP simulations, it is possible to get

some signals that PCL, a semi-crystalline polymer has a capacity of forming crystalline regions within the structure by ordering the chains which also induces liquid-crystalline behavior. In literature, the improved processibility of the rigid-rod polymer PPP is explained by this liquid crystalline behavior. However, in order to come to this conclusion, the ordering of the PCL chains must be better understood by studying the dynamics of the more than one chain. For this reason, two identical PPP chains having exactly the same side chains initially placed paralel to each other are subjected to minimization followed by the equilibration under the same simulation conditions as explained before. The inter and intra chain interactions of the side chains as well as the interactions of backbones are studied.

When simulations with two PPP backbones are investigated, it can be seen that substituted PPP chains lie almost parallel to each other but they can not form ideal π-stacks as observed for the unsubstituted PPP backbones. Long PCL side chains prefer to stay parallel to each other. Although, PPPs are rigid rod-like crystal polymers, the structure and stability of the systems are governed by the chain dynamics here. Dominating interactions are the interactions between the same kind of chains due to the significant discrepancy between their solubility parameters. Another important factor to be mentioned is that the side groups are much more bulkier than the backbone and they can be longer as well depending upon the preparation conditions. The interactions of the side chains with the PPP backbones are supressed and the strength of the interactions between the side chains, if they are long enough, gain too much importance to become a control parameter to favor or unfavor the microphase separation.

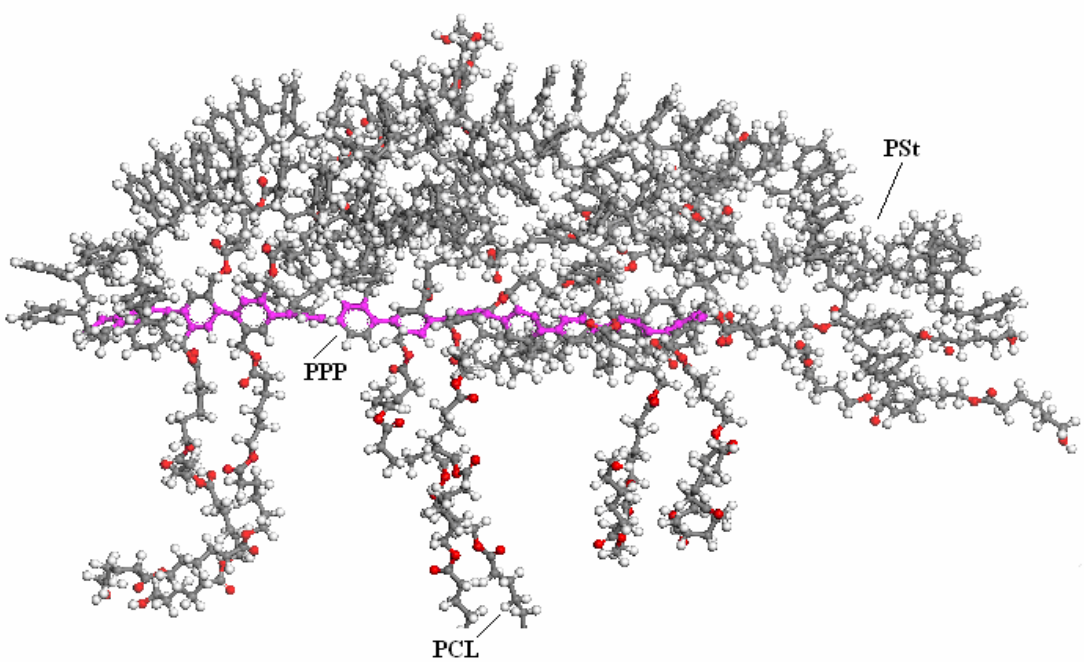

Figure 4.18: Single PPP Chain Substituted With PSt (n_{St}=16) and PCL (n_{CL})=4 Side Groups.

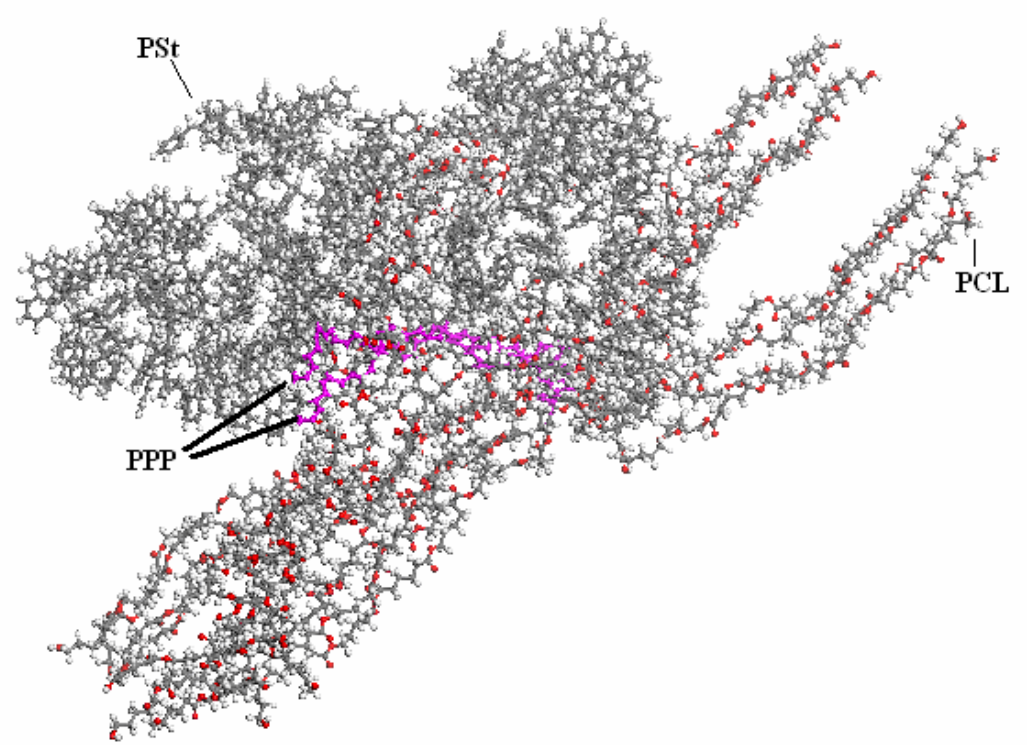

Figure 4.19: Two PPP Chains Substituted With PSt (n_{St}=16) and PCL (n_{CL})=4 Side Chains.

4.3 DPD Results

The morphology of the substituted PPP chains modelled as beads and put into the cell with dimensions of 40 x 40 x 10 Å are studied by the Dissipative Particle Dynamics method as explained above. The two-dimensional pictures from the cell containing PPP chains with different PSt and PCL side groups can be seen in the Figure 4.20. In the figures, blue color represents PPP side chains, green color represents PSt side chains and orange color represents PCL chains. It can be seen that the same colors form heteregeneous islands and the blue colors are covered by the green ones implying that rigid PSt side groups are alligned paralel to the PPP backbone whereas flexible PCL side groups come together, shown by the orange islands. PSt and PCL chains are not miscible as expected, they prefer to interact with each other. This is the reason for the microphase separation observed experimentally from AFM picture given in the Figure 4.21.[65]

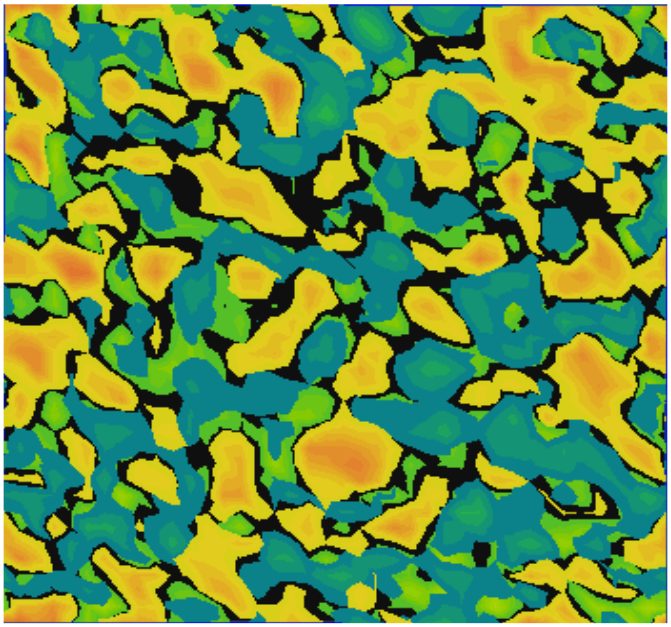

(a)

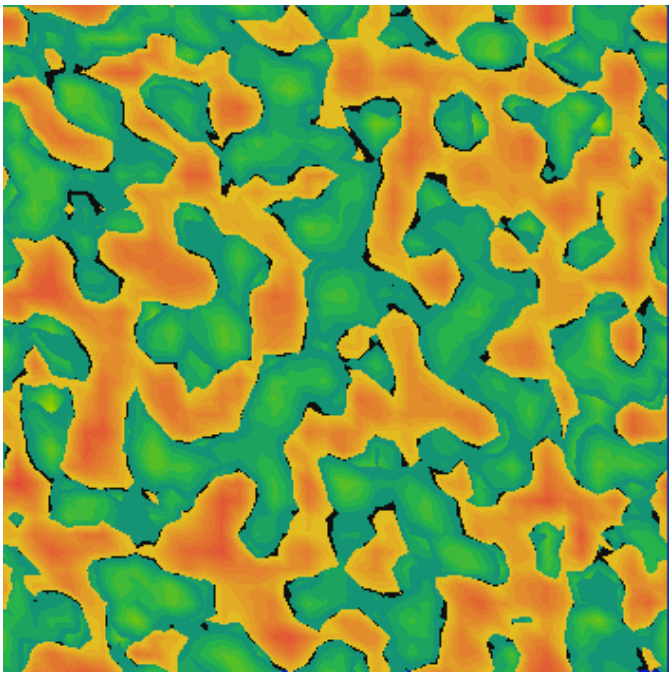

(b)

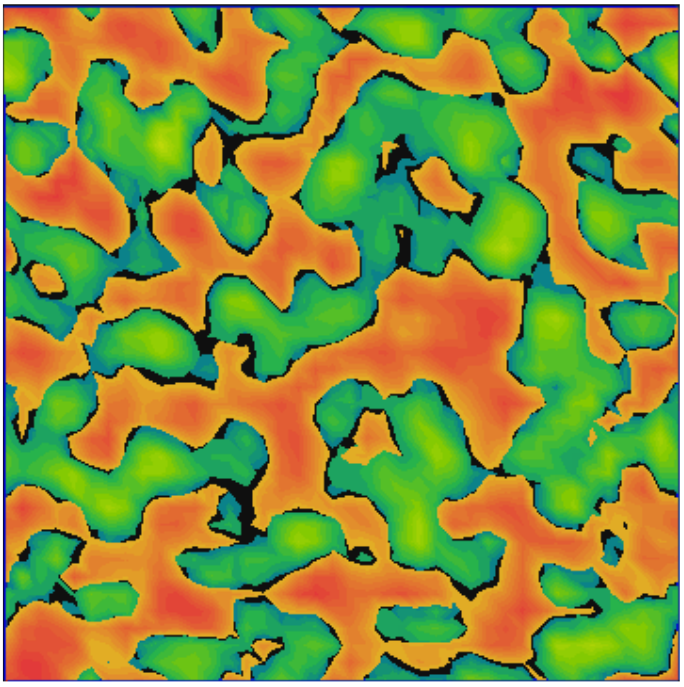

(c)

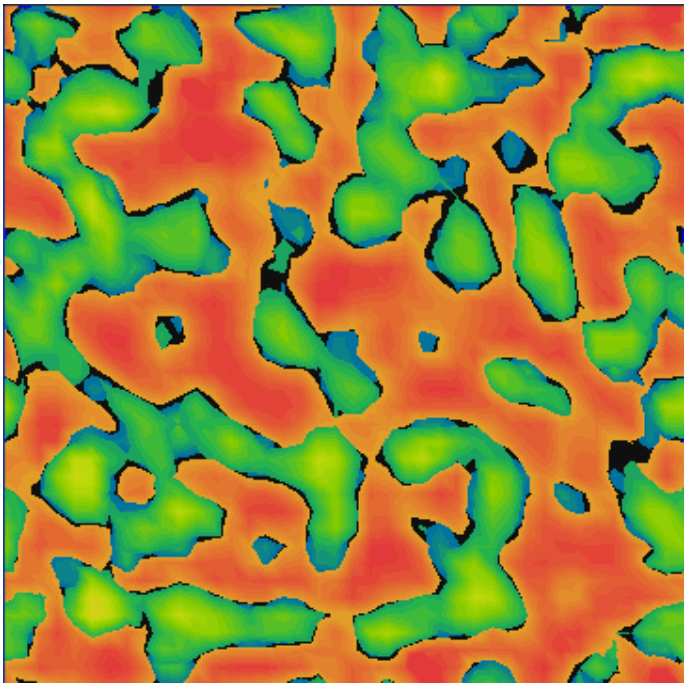

(d)

Figure 4.20: The Top Views From the Cell. Morphology of the Materials Formed By Varied Side-Chain Lenghts (a) (n_{St}=10; n_{CL}=10), (b) (n_{St}=20; n_{CL}=20), (c) (n_{St}=30; n_{CL}=30), (d) (n_{St}=40; n_{CL}=40)

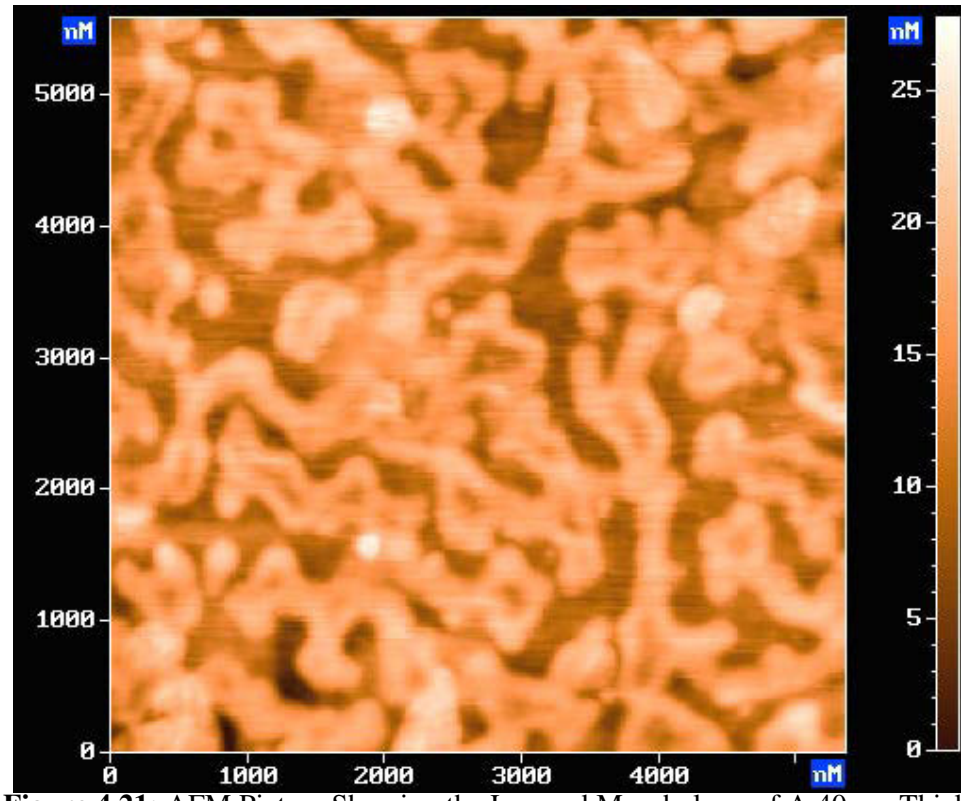

Figure 4.21: AFM Picture Showing the Layered Morphology of A 40 nm Thick Film of The PSt and PCL Substituted PPP Oligomers On The Glass Surface.[65]

5. CONCLUSION

The effect of immiscible polymeric (oligomeric) side chains of the PPP backbone on the physical, mechanical, thermal and morphological behavior of the resulting material are investigated with quantum mechanical and statistical mechanical tools. How the structure and molecular properties governed by the side chains are studied at the microscopic level. The mechanical properties of the PPPs having linearly extended side groups are succesfully estimated from the monomer properties by using empirical methods. The microphase separation observed experimentally are reproduced by the DPD morphology calculations and attributed to the immiscibility of the polymeric side chains and their lessened interactions with the rigid PPP backbones. The layered morphology is not observed due to the absence of a substrate which may induce a sort of alignments of the chains depending on the strength of the molecular interactions between the substrate and the side groups.

REFERENCES

[1] Bredas, J. L., Beljonne, D., Coropceanu, V., Cornil, J., 2004**.** Charge-Transfer and Energy-Transfer Processes in ∏-Conjugated Oligomers and Polymers: A Molecular Picture, *Chem. Rev.,* 104, 4971-5003.

[2] Unur, E., Toppare, L., Yagci, Y., Yilmaz, F., 2005. Conducting Copolymers of Polytetrahydrofuran and Their Electrochromic Properties, *Journal of Applied Polymer Science*, Vol. 95, 1014–1023.

[3] Tarkuc, S., Sahin, E., Toppare, L., Colak, D., Cianga, I., Yagci, Y., 2006**.** Synthesis, characterization and electrochromic properties of a conducting copolymer of pyrrole functionalized polystyrene with pyrrole, *Polymer*, 47, 2001–2009.

[4] Friend, R. H., **Gymer, R. W., Holmes, A. B., Burroughes, J. H., Marks, R. N., Taliani, C., Bradley, D. C., Dos Santos, D. A., Bredas, J. L.,** 1999. Electroluminescence in conjugated polymers, *Nature* ,Vol 397, 121-128.

[5] Papila, Ö., Toppare, L., Yağcı, Y., Cianga, L., 2004. Conducting Copolymers of Thiophene-Functionalized Polystyrene International, *Journal of Polymer Anal. Charact.*, 9, 13–28.

[6] Cianga, L., **Hepüzer, Y., Yağcı, Y.,** 2002**.** Poly(p-phenylenes) with Well-defined Side Chain Polymers**,** *Macromol. Symp*. 183, 145–157.

[7] Guner, Y., Toppare, L., Hepüzer, Y., Yağcı, Y., 2004. Conducting graft copolymers of pyrrole and thiophene with random copolymers of methyl methacrylate and 3-methylthienyl methacrylate, *European Polymer Journal* 40 1799–1806.

[8] Çolak, D., Cianga, I., Müftüoğlu, A. E., Yağcı, Y., 2006. Synthesis and Characterization of Mid- and End-Chain Functional Telechelics by Controlled Polymerization Methods and Coupling Processes, *Journal of Polymer Scence Part A*: *Polymer Chemistry,* 44, 727–743.

[9] Yurteri, S., Cianga, I., Degirmenci, M., Yağcı, Y., 2004. Synthesis and characterization of poly(p-phenylene)-graft-poly(ε-caprolactone) copolymers by combined ring-opening polymerization and cross-coupling processes, *Polym. Int.*, 53, 1219–1225.

[10] Yurteri, S., Cianga, I., Demirel, A. L., Yağcı, Y., 2005. New Polyphenylene-g-Polystyrene and Polyphenylene-g-Polystyrene/Poly(ε-caprolactone) Copolymers by Combined Controlled Polymerization and Cross-Coupling Processes, *J.Polym Sci Part A: Polym Chem*, 43, 879–896.

[11] Yurteri, S., Cianga, I., Yağcı, Y., 2005 Synthesis and characterization of poly(ε-caprolactone)-b-polystyrene macromonomer by combined ring-opening and atom transfer radical polymerizations and its use for the preparation of grafted polyphenylenes by Suzuki polycondensation, *Designed Monomers and Polymers*, Vol. 8, No.1,. 61–74.

[12] Yilmaz, F., Sel, O., Guner, Y., Toppare, L., Hepuzer, Y., Yagci, Y., 2004. Controlled Synthesis of Block Copolymers Containing Side Chain Thiophene Units and Their Use in Electrocopolymerization with Thiophene and Pyrrole, *Journal of Macromolecule Science Part A—Pure and Applied Chemistry* Vol. A41, No.4, 401–418.

[13] Cianga, I., Yağci, Y., 2004 New polyphenylene-based macromolecular architectures by using well defined macromonomers synthesized via controlled polymerization methods, *Prog. Polym. Sci*., 29, 387–399.

[14] Cianga, I., Yağci, Y., Hepuzer, Y., 2002. Poly(p-phenylene)graft copolymers with polytetrahydrofuran/polystrene side chains, *Polymer*, 43, 2141-2149.

[15] Demirel, A. L., Yurteri, S., Cianga, I., Yağci, Y., 2005. Layered Morphology of Poly(phenylene)s in Thin Films Induced by Substitution of Well-Defined Poly(ε-caprolactone) Side Chains, *Macromolecules* 38, 6402-6410.

[16] Böyükbayram, A. E., Kıralp, S., Toppare, L., Yağci, Y., 2006. Preparation of biosensors by immobilization of polyphenol oxidase in conducting copolymers and their use in determination of phenolic compounds in red wine, *Bioelectrochemistry*, 69, 164–171.

[17] Moreau, C., Antony, R., Moliton, A., Francois, B., 1997. Sensitive Thermoelectric Power and Conductivity Measurements on Implanted Polyparaphenylene Thin Films, *Adv. Mater. Opt. Electron*. Vol 7, 281–293.

[18] Bloom, P. D., Sheares, V. V., 2001. Novel Poly(paraphenylene)s via Nucleophilic Aromatic Substitution of Poly(4'-fluoro-2,5-diphenyl sulfone), *Macromolecules*, 34, 1627-1633.

[19] Gacal, B., Durmaz, H., Tasdelen, M. A., Hizal, G., Tunca, U., Yagci, Y., Demirel, A. L. , 2006**.** Anthracene-Maleimide-Based Diels-Alder "Click Chemistry" as a Novel Route to Graft Copolymers, *Macromolecule*s 39, 5330-5336.

[20] Chian, K. S., Du, X. Y., Goy, H. A., Feng, J. L., Yi, S., Yue, C. Y., 2002. Mechanical Properties and Morphology of Poly(ethylene glycol)-Side-Chain-Modified Bismaleimide Polymer, *Journal of Applied Polymer Science*, Vol. 86, 715–724.

[21] Förner, W., 2004. Theoretical study of bipolaron dynamics in polyparaphenylene: I. Derivation of the formalism and density functional (DFT) calculations on neutral and charged model systems, *Journal of Molecular Structure (Theochem)*, 682, 115–136.

[22] Bouzakraoui, S., Bouzzine, S. M., Bouachrine, M., Hamidi, M., 2005**.** Density functional theory study of conformational and opto-electronic properties of oligo-para-phenylenes, *Journal of Molecular Structure:Theochem*, 725, 39–44.

[23] Salzner, U., Lagowski, J.B., Pickup, P.G., Poirier, R.A., 1998. Comparison of Geometries and Electronic Structures of Polyacetylene, Polyborole, Polycylopentadiene, Polypyrrole, Polyfuran, Polysilole, Polyphosphole, Polythiophene, Polyselenophene and Polytellurophene, *Synth. Met.,* 96, 177.

[24] Yang, H. C., Yu, H. C., Yu, K. M., Huang, Q., Chen, C. L., 2004. Computer Simulation of Long Side Chain Substituted Poly(phenylene vinylene) Polymers, *ChemPhysChem*, 5, 373-381.

[25] Yaliraki, S. N., Silbey, R. J., 1996. Conformational Disorder of Conjugated Polymers:Implications for Optical Properties,*J.Chem.Phys.*,104, 1245.

[26] Hu, D., Yu, J., Wong, K., Bagchi, B., Rossky, P. J., Barbara, P. F., 2000. Collapse of Stiff Conjugated Polymers with Chemical Defects into Ordered, Cylindrical Conformations, *Nature*, 405, 1030.

[27] Yu, J., Fann, W. S., Kao, F. J., Yang, D. Y., Lin, S. H., 1994. Molecular Orbital Calculations of Electronic Excited States in Poly(p-phenylene vinylene), *Synth. Met.*, 66, 143.

[28] Yu, J., Hsu, J. H., Chuang, K. R., Chao, C. L., Chen, S. A., Kao, F. J., Fann, W. S., Lin, S. H., 1995. Experimental and Theoretical Studies of Absorption and Photoluminescence Excitation Spectra of Poly(p-phenylene vinylene), *Synth. Met*., 74, 7.

[29] Cornil, J., Beljonne, D., Friend, R. H., Bredas, J. L., 1994. Optical Absorptions in Poly(paraphenylene vinylene) and Poly(2,5-dimethoxy-1,4-paraphenylene vinylene) Oligomers, *Chem. Phys. Lett.*, 223, 82.

[30] Chang, R., Hsui, J. H., Fann, W. S., Liang, K. K., Chang, C. H., Hayashi, M., Yu, J., Lin, S. H., Chang, E. C., Chuang, K. R., Chen, S. A., 2000. Experimental and Theoretical Investigations of Absorption and Emission Spectra of the Light-emitting Polymer MEH-PPV in Solution, *Chem. Phys. Lett.*, 317, 142.

[31] Conwell, E. M., Perlstein, J., Shaik, S., 1996. Interchain Photoluminescence in Poly(phenylene vinylene) Derivatives, *Phys. Rev. B*, 54, R2308.

[32] Tretiak, S., Saxena, A., Martain, R. L., Bishop, A. R., 2000. Interchain Electronic Excitations in Poly(phenylenevinylene) (PPV) Aggregates, *J. Phys. Chem. B.*, 104, 7029.

[33] Johansson, A., Stafstrom, S., 2002**.** Interchain charge transport in disordered pi-conjugated chain systems, *S. Phys. Rev. B*, 66, 085208.

[34] Beljonne, D., Pourtois, G., Silva, C., Hennebicq, E., M. Herz, L., Friend, R. H., Scholes, G. D., Setayesh, S., Mllen, K., Bredas, J. L., 2002**.** Interchain vs. intrachain energy transfer in acceptor-capped conjugated, *Proc. Natl. Acad. Sci. USA*, 99, 10982- 10987.

[35] Cornil, J., Dos Santos, D. A., Crispin, X., Silbey, R., Bredas, J. L., 1998. Influence of interchain interactions on the absorption and

luminescence of conjugated oligomers and polymers: A quantum-chemical characterization, *J. Am. Chem. Soc.* 120, 1289-1299.

[36] Hoofman, R. J. O. M., de Hass, M. P., Siebbeles, L. D. A., Demandt, R., Warman, J. M., 1998. Highly mobile electrons and holes on isolated chains of the semiconducting polymer poly(phenylenevinylene), *Nature*, 392, 54-56.

[37] Crone, B. K., Campbell, I. H., Davids, P. S., Smith, D. L., 1998. Charge injection and transport in single-layer organic light-emitting diotes, *Appl. Phys. Lett.* 73, 3162-3164.

[38] Bozano, L., Carter, S. A., Scott, J. C., Malliaras, G. G., Brock, P. J., 1999. Temperature- and field-dependent electron and hole mobilities in polymer light-emitting diyotes, *Appl. Phys. Lett.*, 74, 1132-1134.

[39] Tretiak, S., Saxena, A., Martain, R. L., Bishop, A. R., 2000. Interchain electronic excitations in poly(phenylenevinylene) (PPV) aggregates, *J. Phys. Chem.*, B104,7029-7037.

[40] Bredas, J. L., Calbert, J. P., da Silva, F. D. A., Cornil, J., 2002 Organic semiconductors: A theoretical characterization of the basic parameters governing charge transport, *J Proc. Natl. Acad. Sci. USA*, 99, 5804-5809.

[41] Foresman, B., 1996. Exploring Chemistry with Electronic Structure Methods – Second Edition, pp 4-7, Eleen Frisch Gaussian Inc., Pittsburg, USA

[42] Kanaan, N., Marti, S., Moliner, V., 2002. A quantum mechanics/molecular mechanics study of the catalytic mechanism of the thymidylate synthase, *Biochemistry*, 46 (12), 3704-3713.

[43] Dewar, S., Zoebisch, G., Healy, F., Stewart, J., 1985.The development and use of Quantum Mechanical Molecular Models.76. AM1 – A new general- purpose Quantum- Mechanical Molecular Models, *Journal Of The American Chemical Society,* 107 (13), 3902-3909.

[44] Pople, J., 1998. Theoretical models for chemistry: Ab initio and empirical, *Abstracts Of Papers Of The American Chemical Society,* 215, U209-U209 233-PHYS Part 2.

[45]Lill, S., Kohn, U., Anders, E., 2004. Carbon dioxide fixation by lithium amides: DFT studies on the reaction mechanism of the formation of lithium carbamates, *European Journal Of Organic Cemistry,* 13, 2868-2880.

[46] http://en.wikipedia.org/wiki/Molecular_mechanics

[47] Fermeglia, M., Pricl, S., 2007.Multiscale modeling for polymer systems of industrial interest, *Progress in Organic Coatings*, 58, 187–199.

[48] Allen, M., Tildesly, D., 1987. Computer Simulation Of Liquids, pp 1-28, Clarendon Press, Oxford, UK.

[49] Allen, T., Andersen, O., Roux, B., 2006. Molecular dynamics - potential of mean force calculations as a tool for understanding ion permeation and selectivity in narrow channels, *Biophysical Chemistry,* 124 (3), 251-267.

[50] Mima, T., Yasuoka, K., Nose, S., 2007**.** Molecular dynamics simulation of time-irreversibility of stationary heat flux, *Molecular Simulation,* 33 (1-2), 109-113.

[51] Hoover, W., Pierce, T., Hoover, C., Shuart, J., Stein, C., Edwards, A., 1994. Molecular Dynamics, Smooted-Particle, Applied Mechanics and Irreversibility, *Computers and Mathematics with Applications,* 28 (10-12), 155-174.

[52] Morishita, T., 2007. Isothermal–isobaric first-principles molecular-dynamics: application to polymorphism in liquids and amorphous materials, *Molecular Simulation*, Vol. 33, 5–12.

[53]www.ipp.mpg.de/de/for/bereiche/stellarator/Comp_sci/CompScience/csep/csep1. phy.ornl.gov/mo/node17.html - 8k -

[54] http://organ.chem.elte.hu/farkas/teach/opt_bev.html

[55] Sun, H., 1998. COMPASS: An ab initio force-field optimized for condensed-phase applications - Overview with details on alkane and benzene compounds, *Journal of Physical Chemistry B*, 102 (38), 7338-7364.

[56] Grujicic, M., Sun, Y.P., Koudela, K.L., 2007. The effect of covalent functionalization of carbon nanotube reinforcements the atomic-level mechanical properties of poly-vinyl-ester-epoxy, *Applied Surface*

Science, 253, 3009–3021.

[57] Accelrys Materials Studio 4.1 Version Tutorial

[58] Mark, J. E., 1999. Polymer Data Handbook, Oxford University Press, Inc., UK

[59] Ghasemi, J., Saaidpour, S., Steven, D. 2007. QSPR study for estimation of acidity constants of some aromatic acids derivatives using multiple linear regression (MLR) analysis, *Brown Journal of Molecular Structure: Theochem*, 805, 27–32.

[60]Havriliak, S. Jr., 1997. Dielectric and Mechanical Relaxation in Materials, Hanser Publishers, NewYork, USA.

[61] http://www.freepatentsonline.com/20060180922.html

[62] Joo, J., Long, S. M., Pouget, J. P., Oh, J. P., MacDiarmid, A. G., Epstein, A. J. 1998. Charge transport of the mesoscopic metallic state in partially crystalline polyanilines, *Physical Review B(Condanset Materials and Materials Physics)*, Vol.57, Issue 16, 9567 – 9580.

[63] Polymer Design Tools Users' Guide Version 1.0, DTW Associates, Inc.1998

[64] Brandrup, J., Immergut, E. H., Grulke, E. A. 1999. Polymer Handbook Fourth Edition. John Wiley & Sons, Inc., USA.

[65] Yurteri, S., Cianga, I., Demirel, A. L., Yağcı, Y. 2007 The Effect of Polymeric Side Chains on the Morphology of Phenyl Rings and Phenylene Oligomers in Thin Films. *Journal of Polymer Science Part A: Polymer Chemistry*, 45, 2091–2104.

APPENDIX

Table A.1: The Optimized Structures of Single Chain PPPs With Alternating PSt and PCL Side Blocks After MD Simulations of 600 ps at 298K.

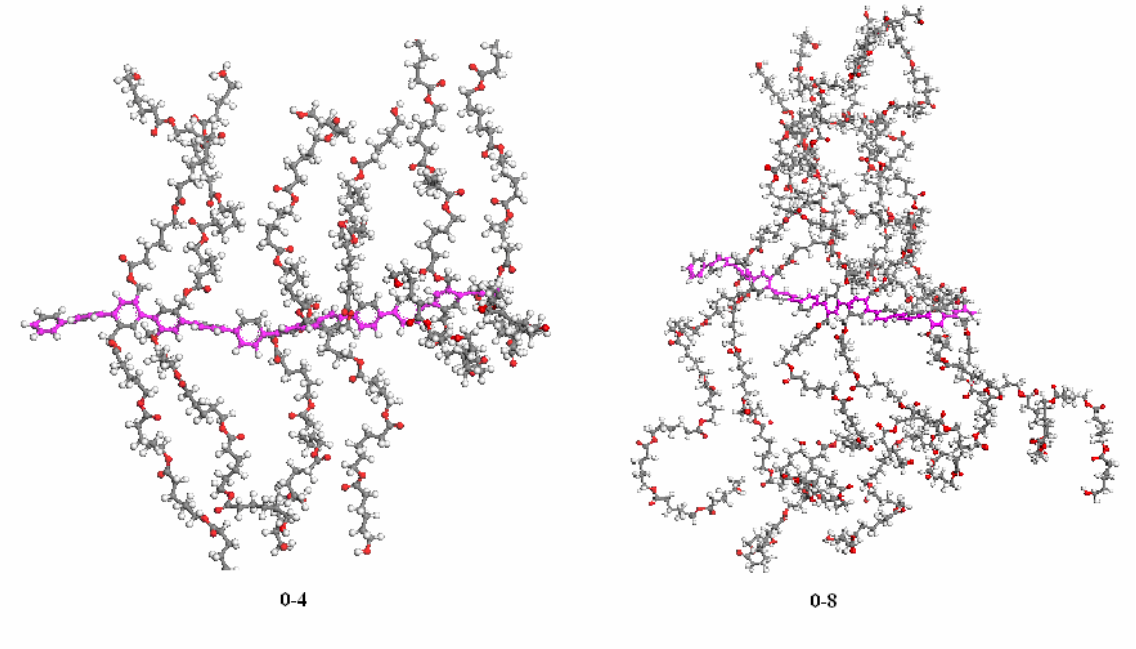

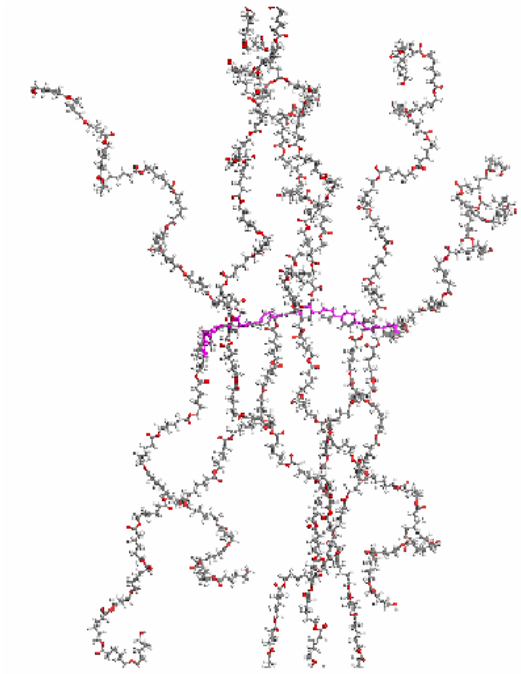

0-12

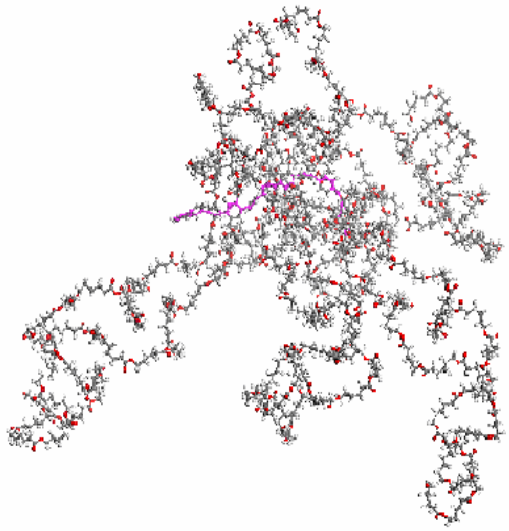

0-16

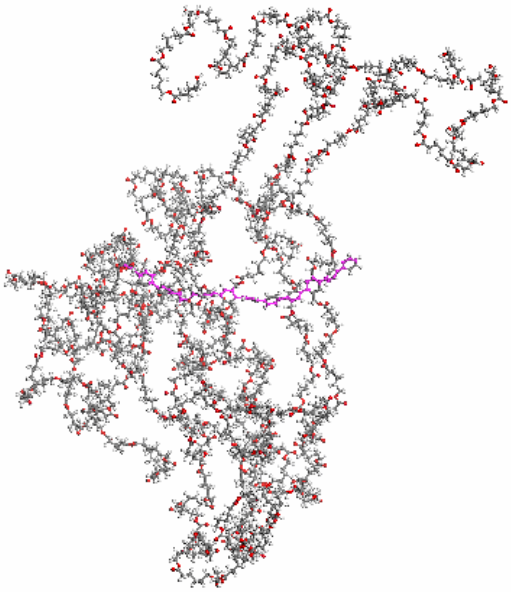

0-20

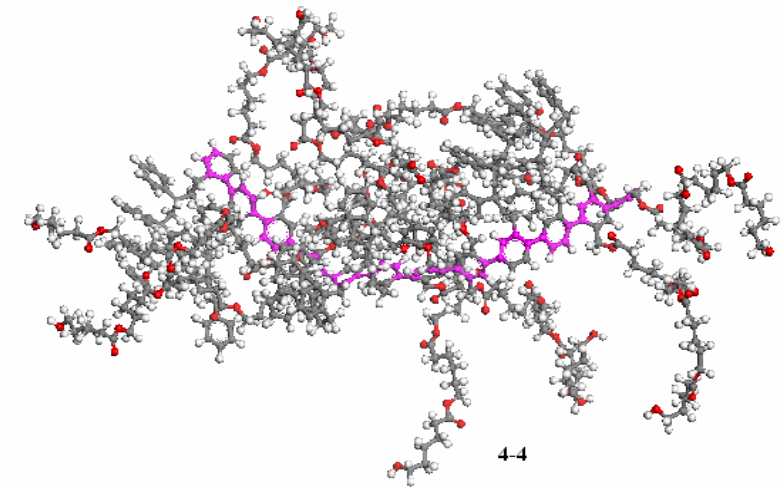

4-4

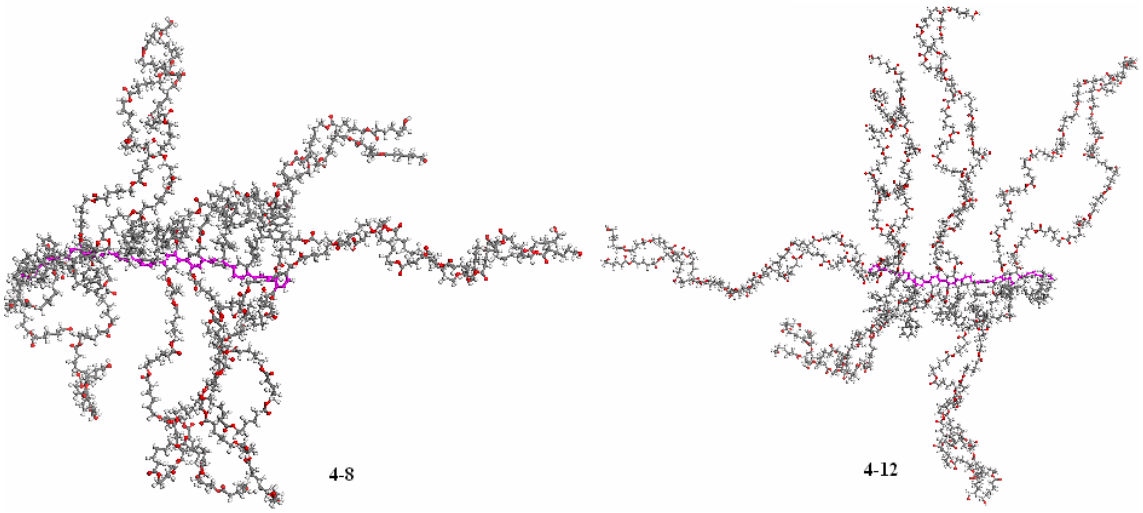

4-8

4-12

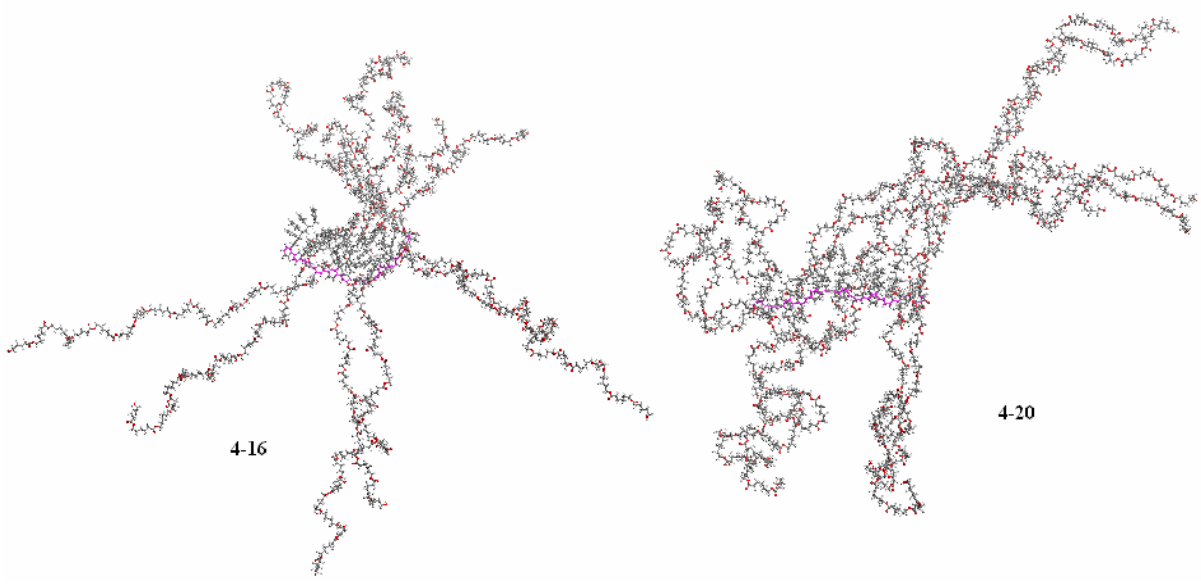

4-16

4-20

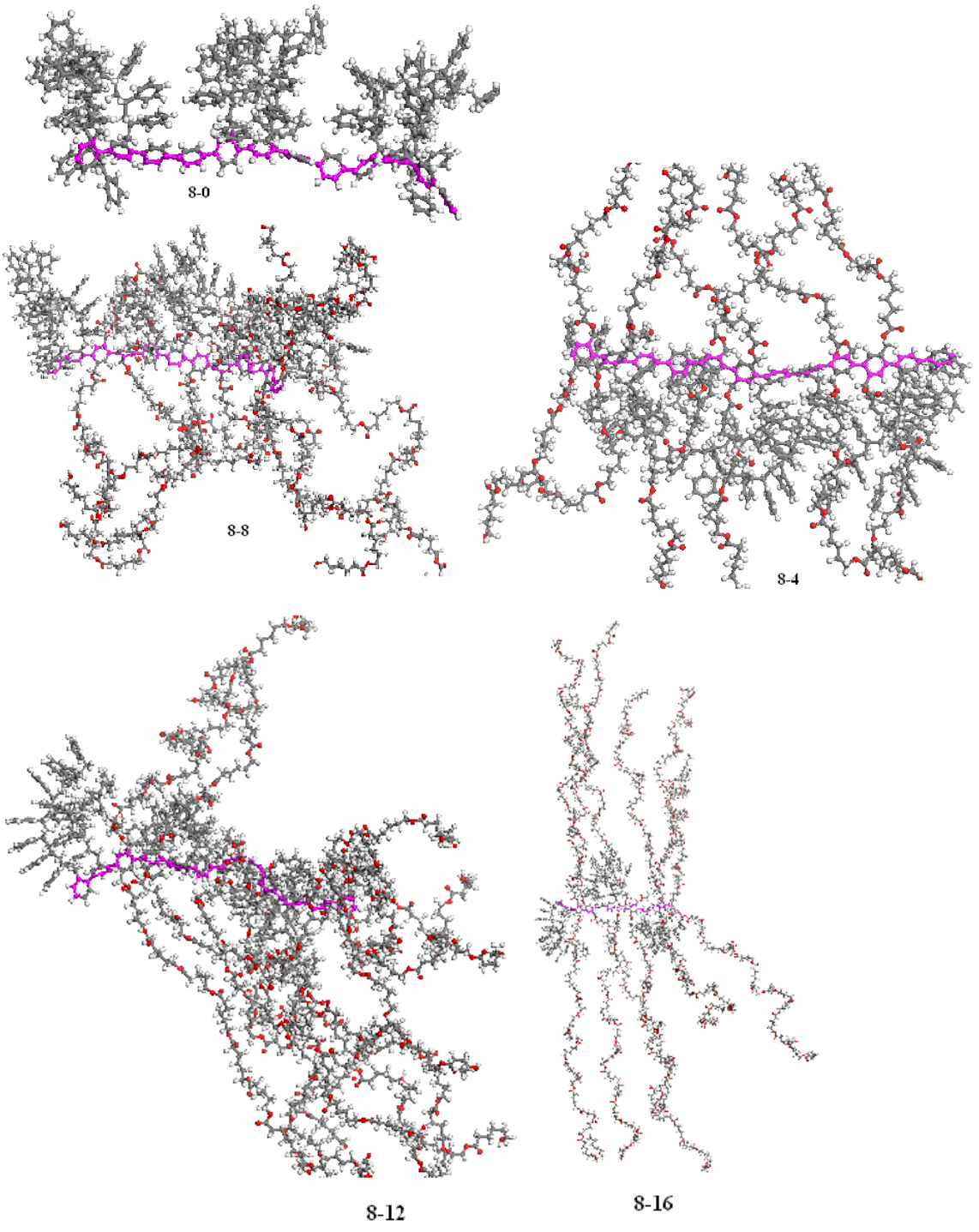
8-0
8-8
8-4
8-12
8-16

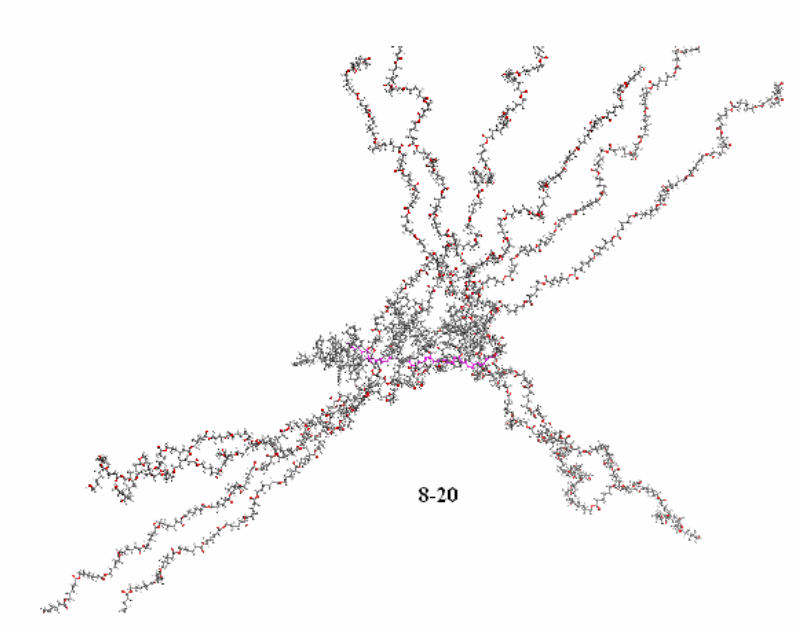

8-20

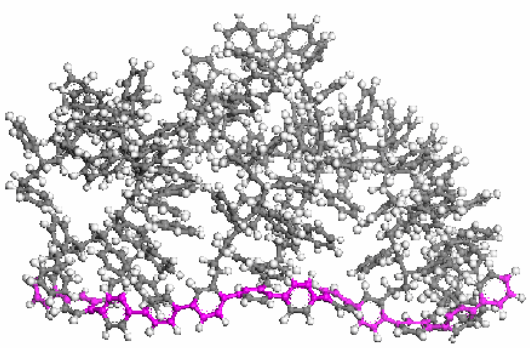

12-0

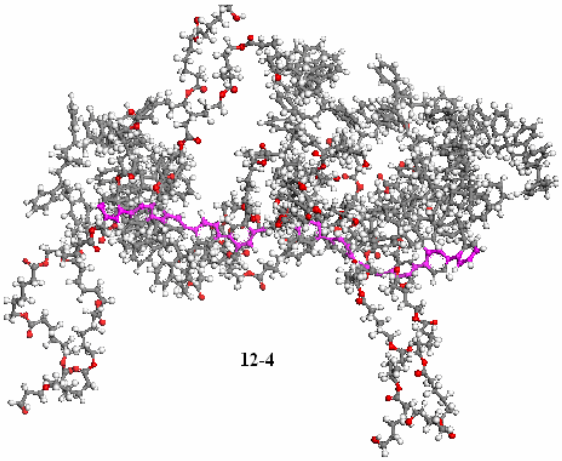

12-4

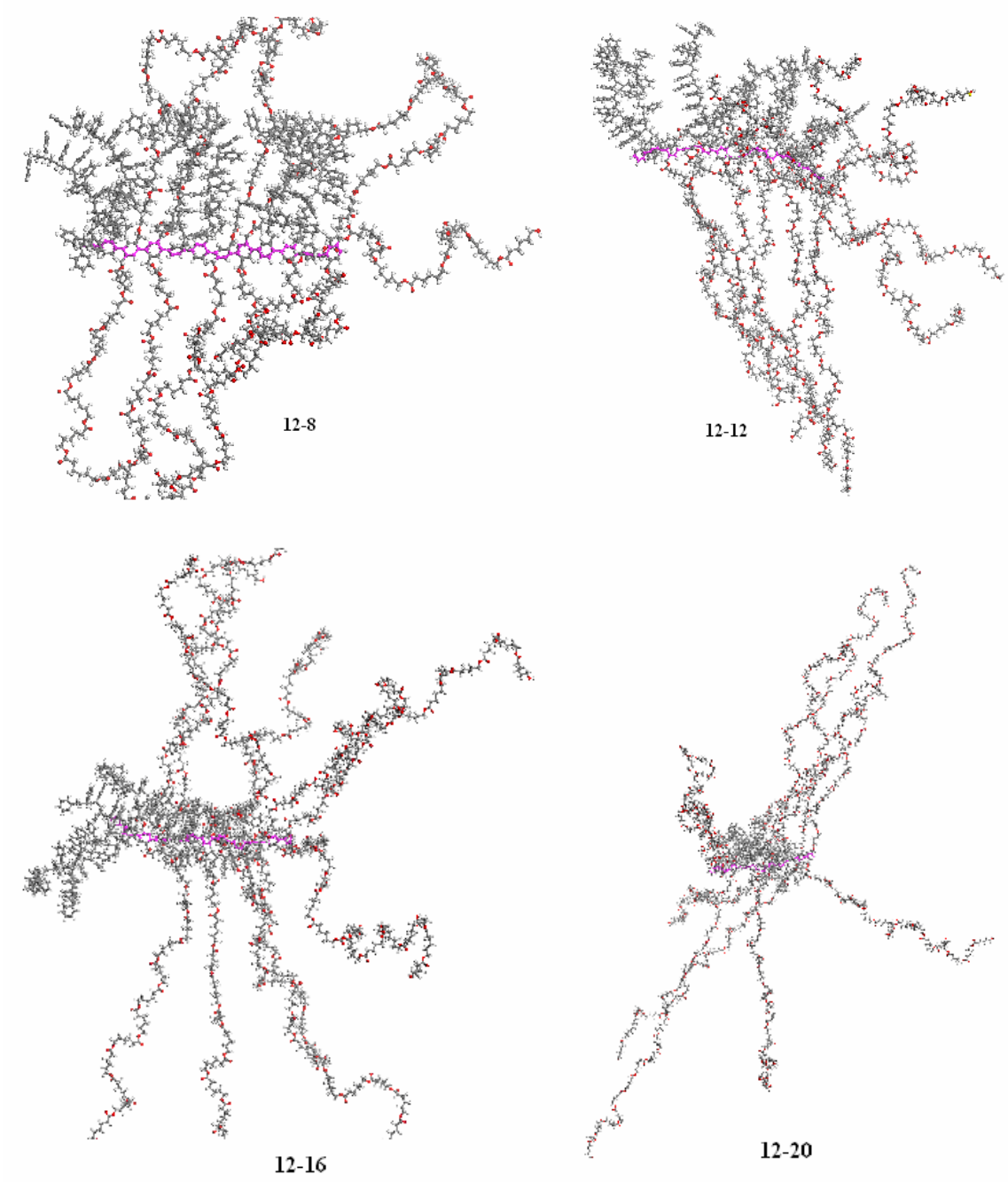
12-8
12-12
12-16
12-20

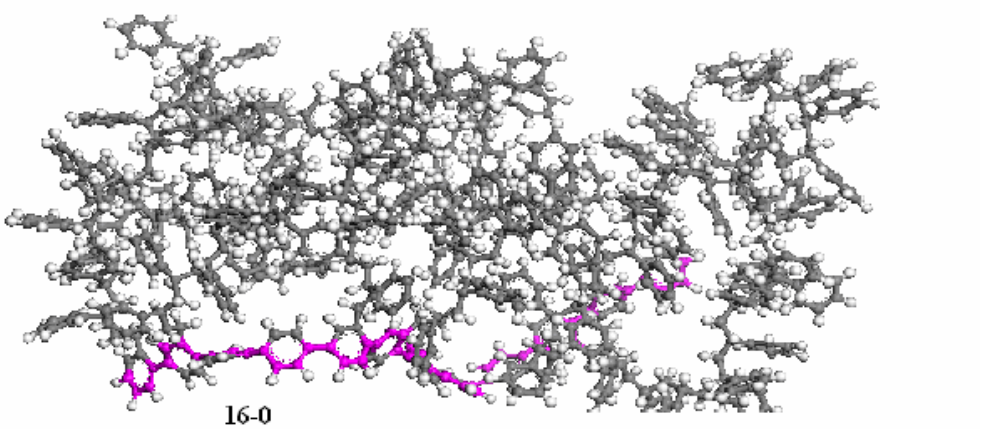

16-0

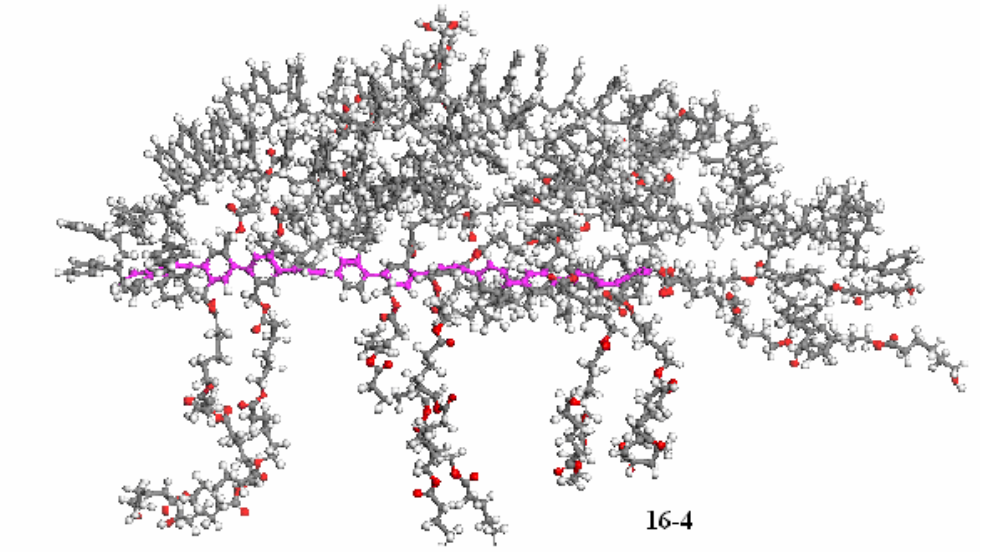

16-4

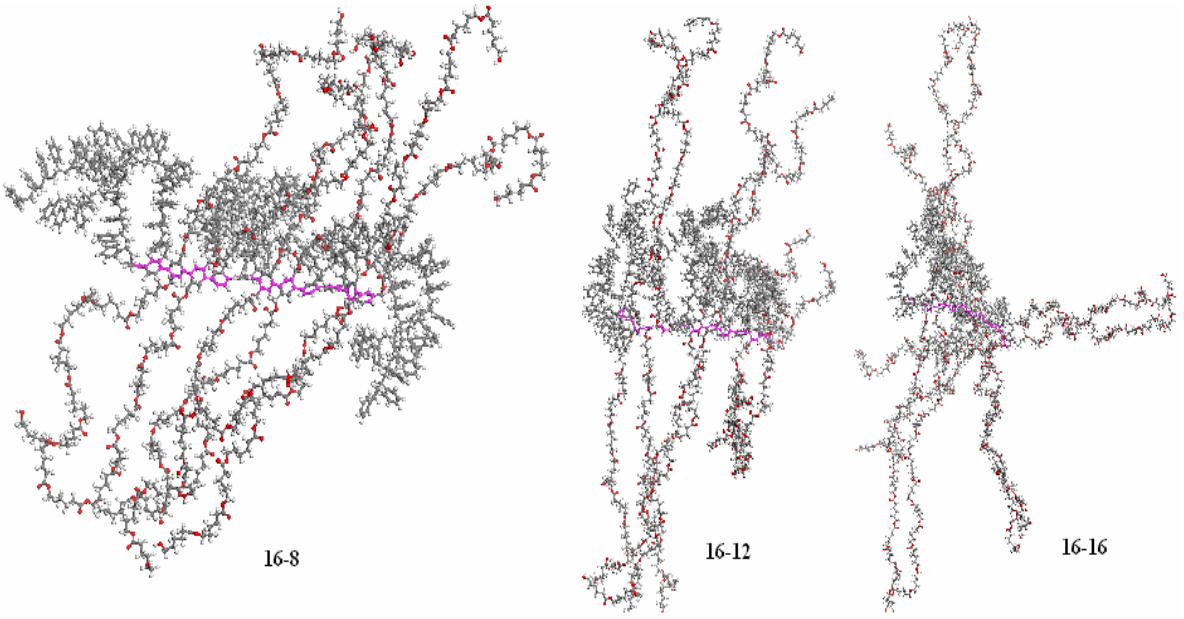

16-8

16-12

16-16

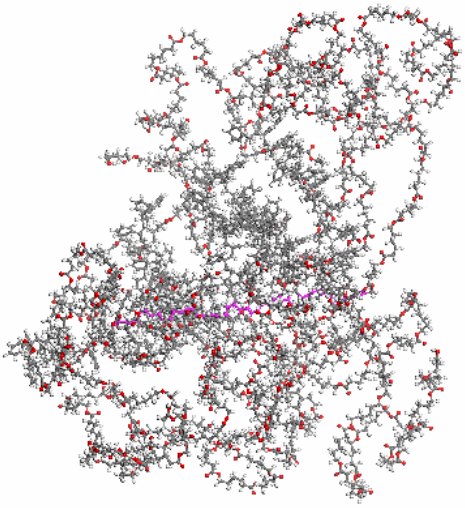

16-20

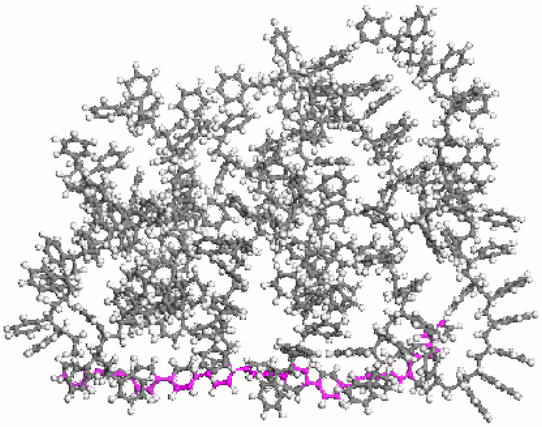

20-0

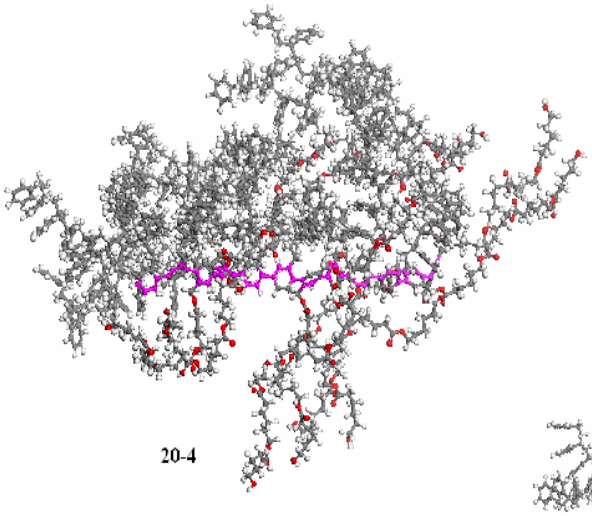

20-4

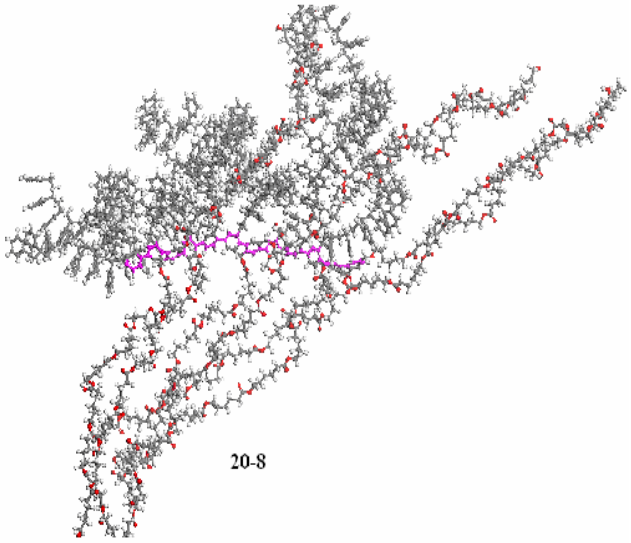

20-8

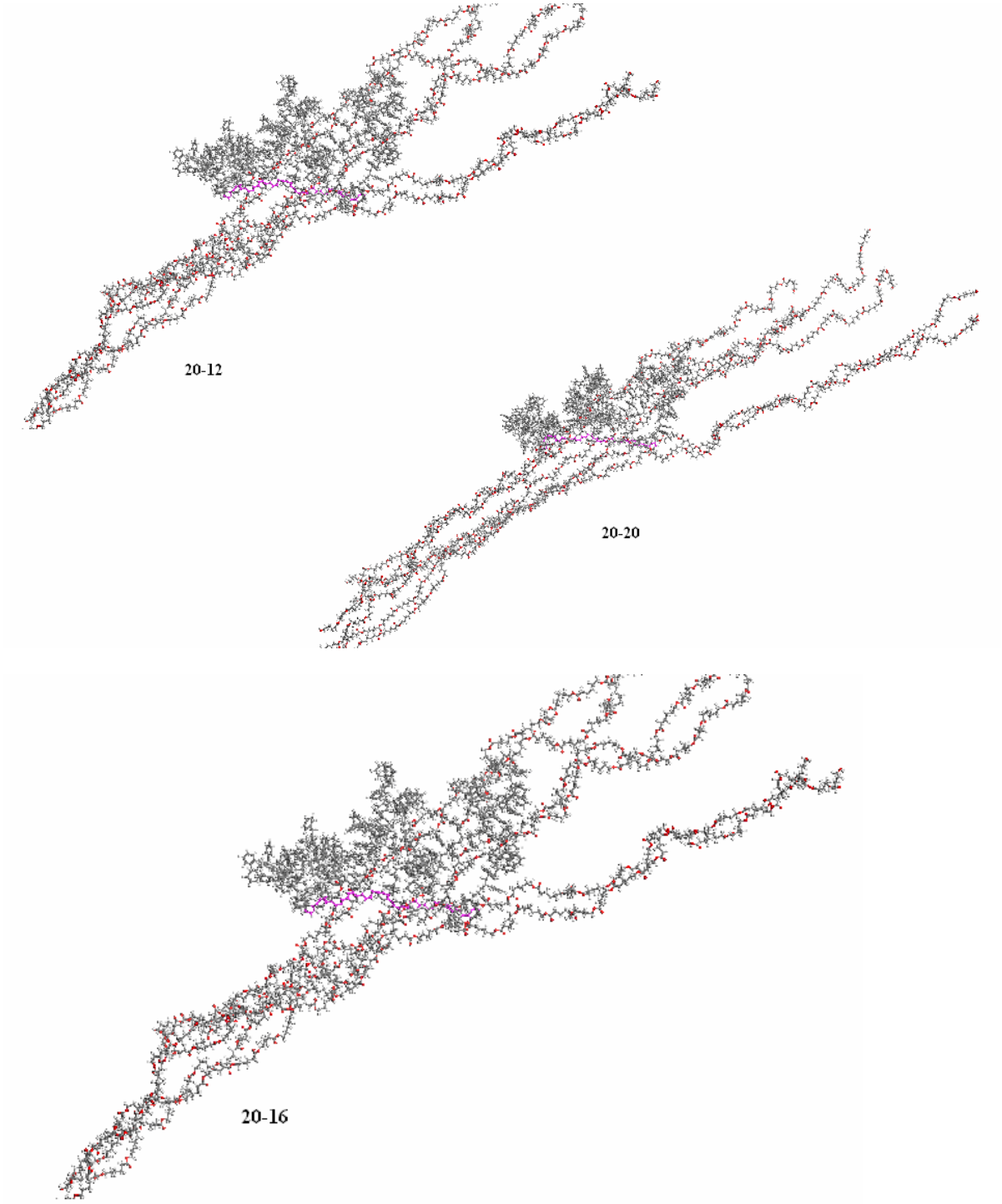
20-12
20-20
20-16

Table A.2: The Optimized Structures of Two PPP Chains With Alternating PSt and PCL Side Blocks After MD Simulations of 600 ps at 298K.

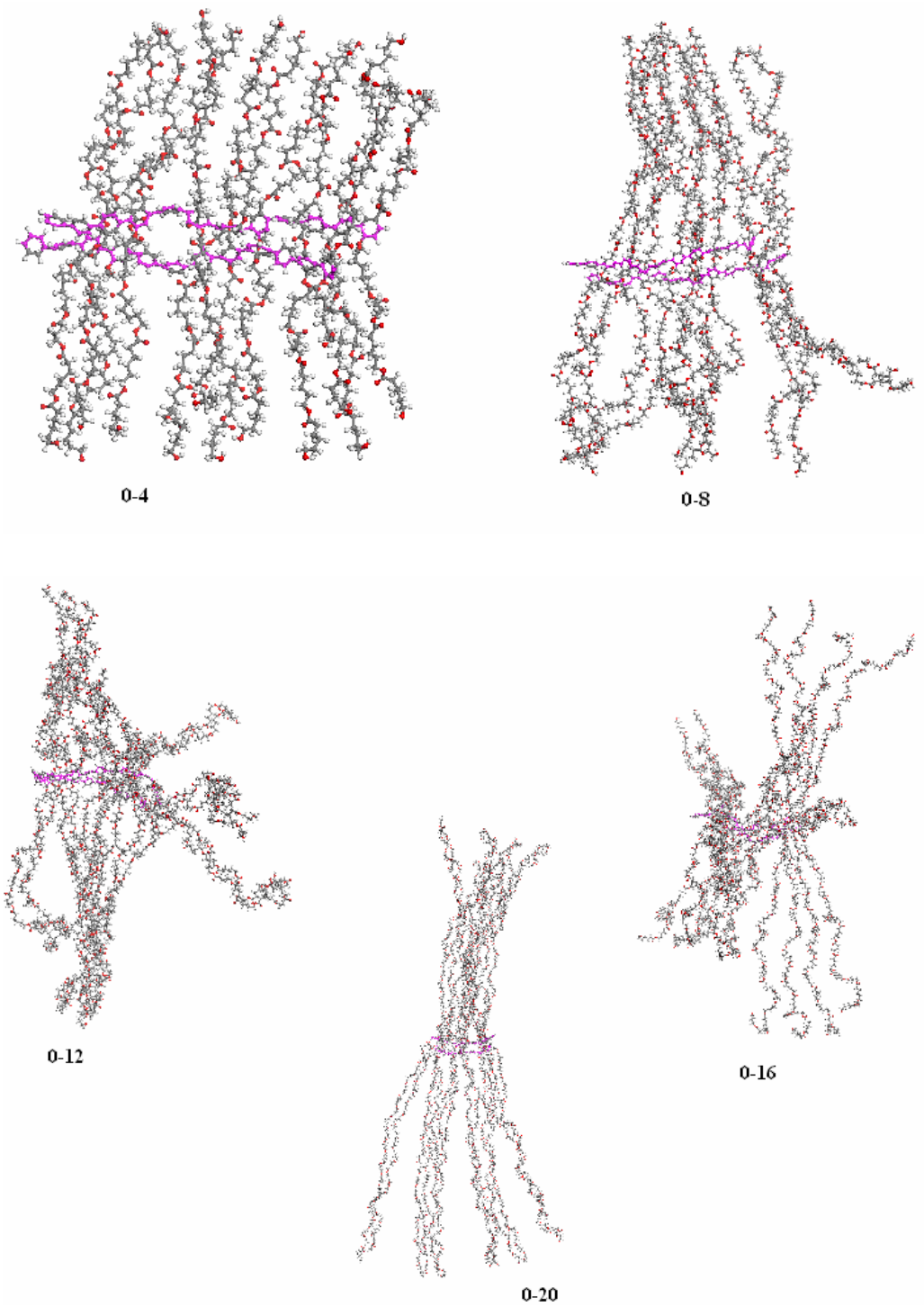

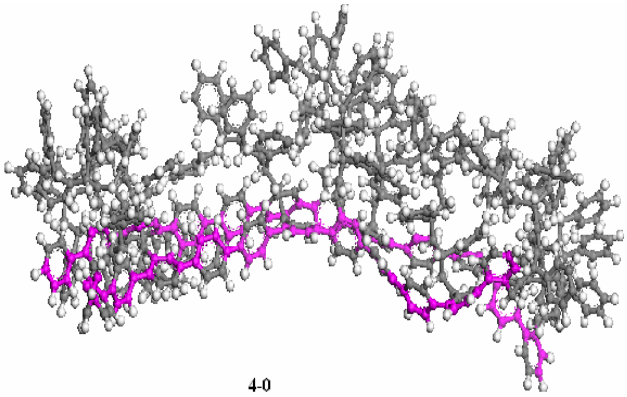

4-0

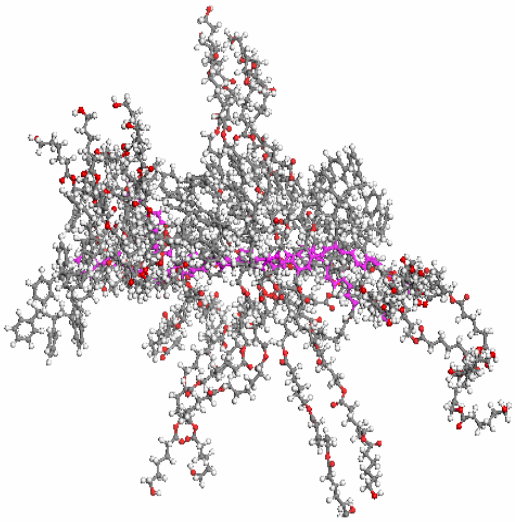

4-4

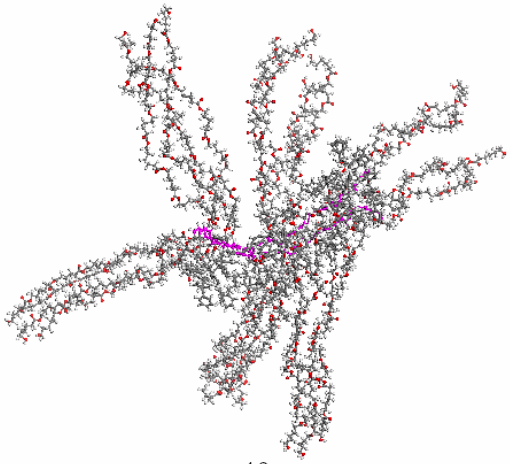

4-8

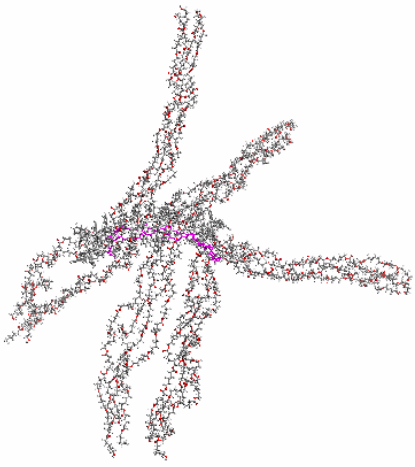

4-12

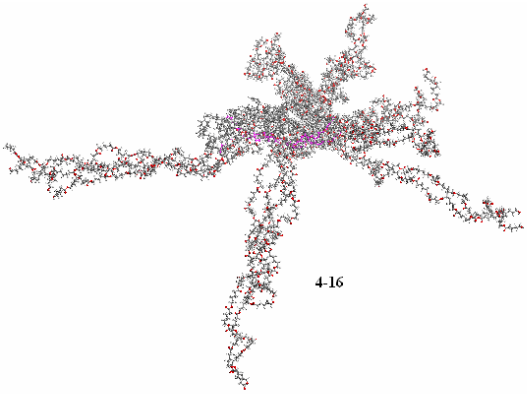

4-16

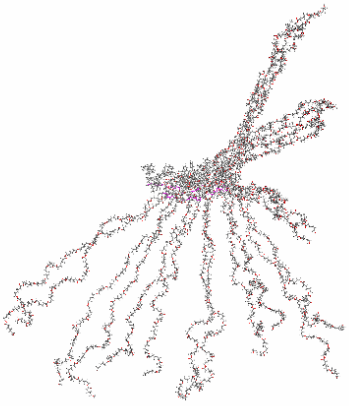

4-20

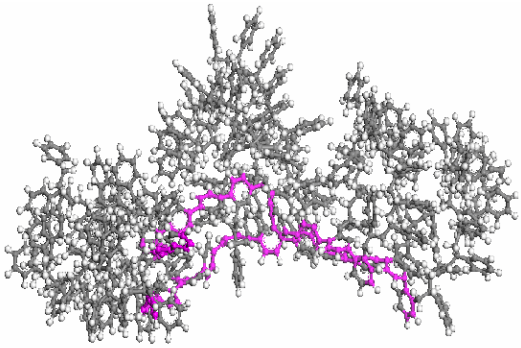

8-0

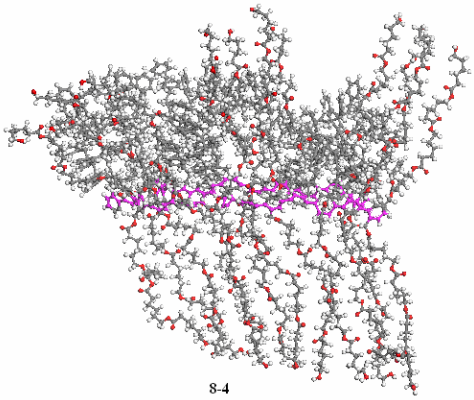

8-4

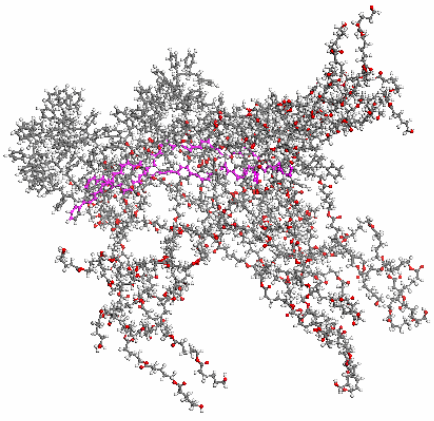

8-8

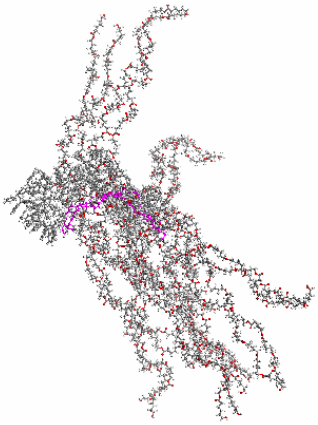

8-12

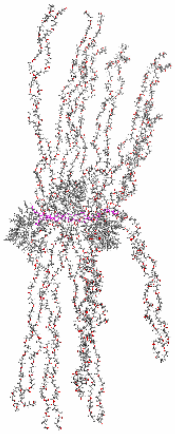

8-16

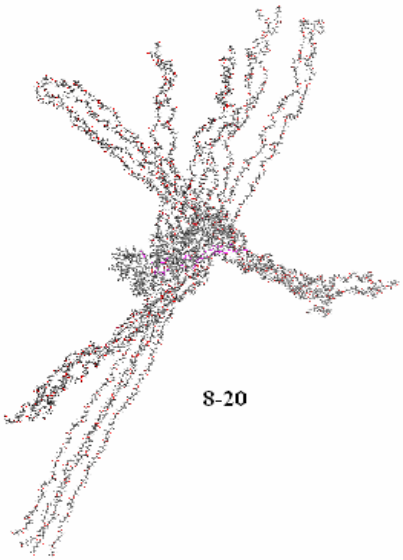

8-20

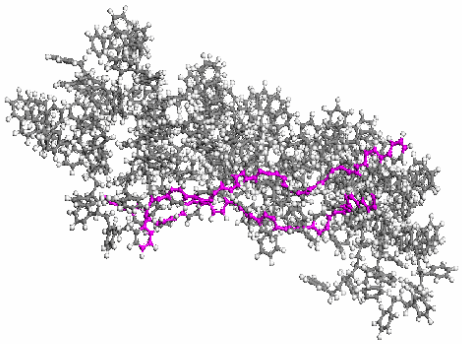

12-0

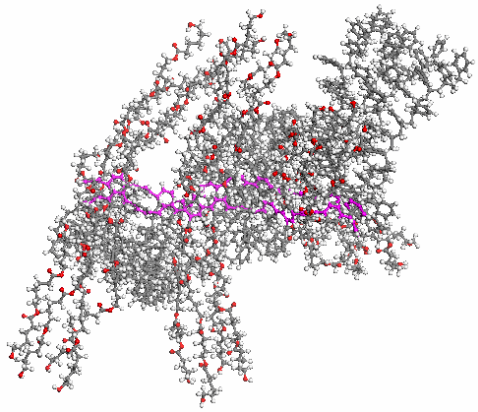

12-4

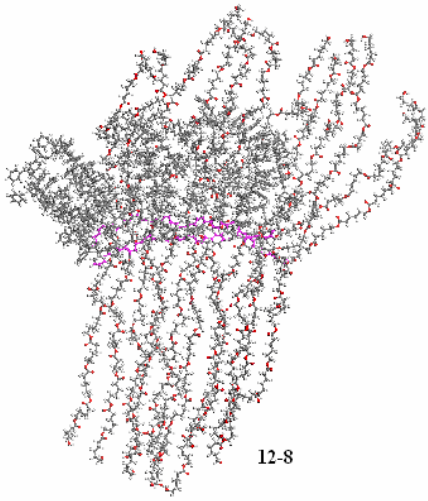

12-8

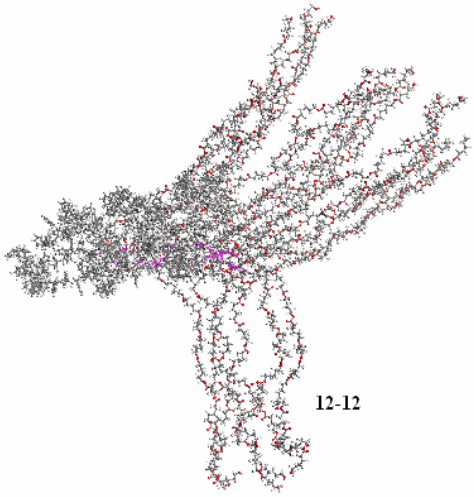

12-12

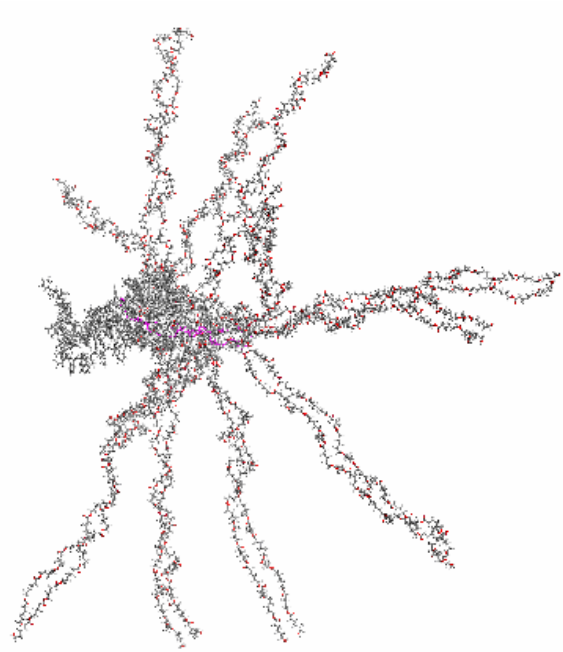

12-16

12-20

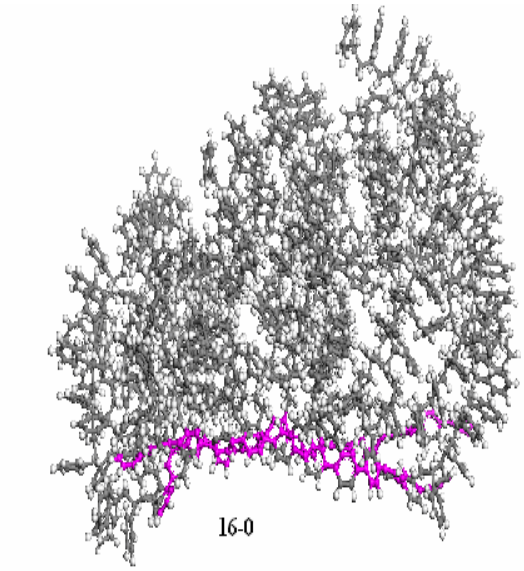

16-0

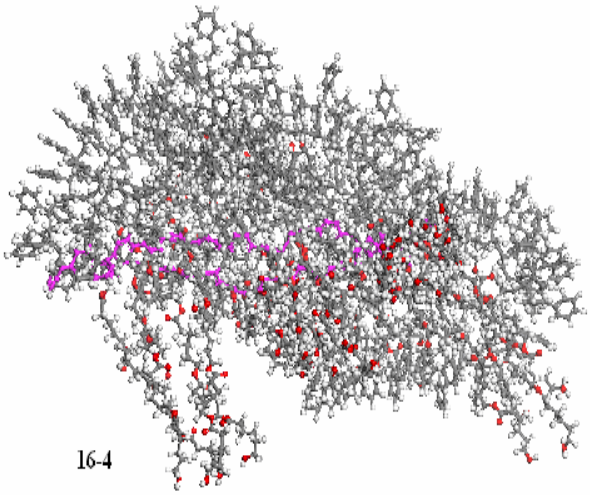

16-4

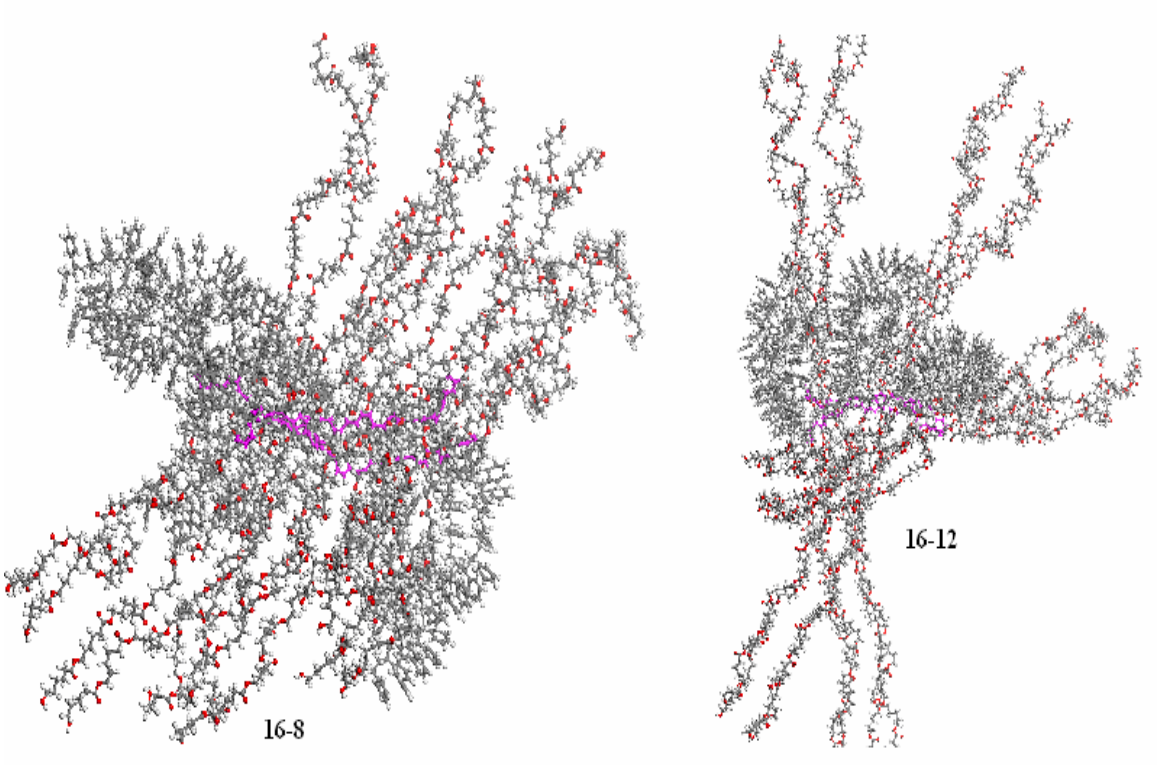
16-8
16-12

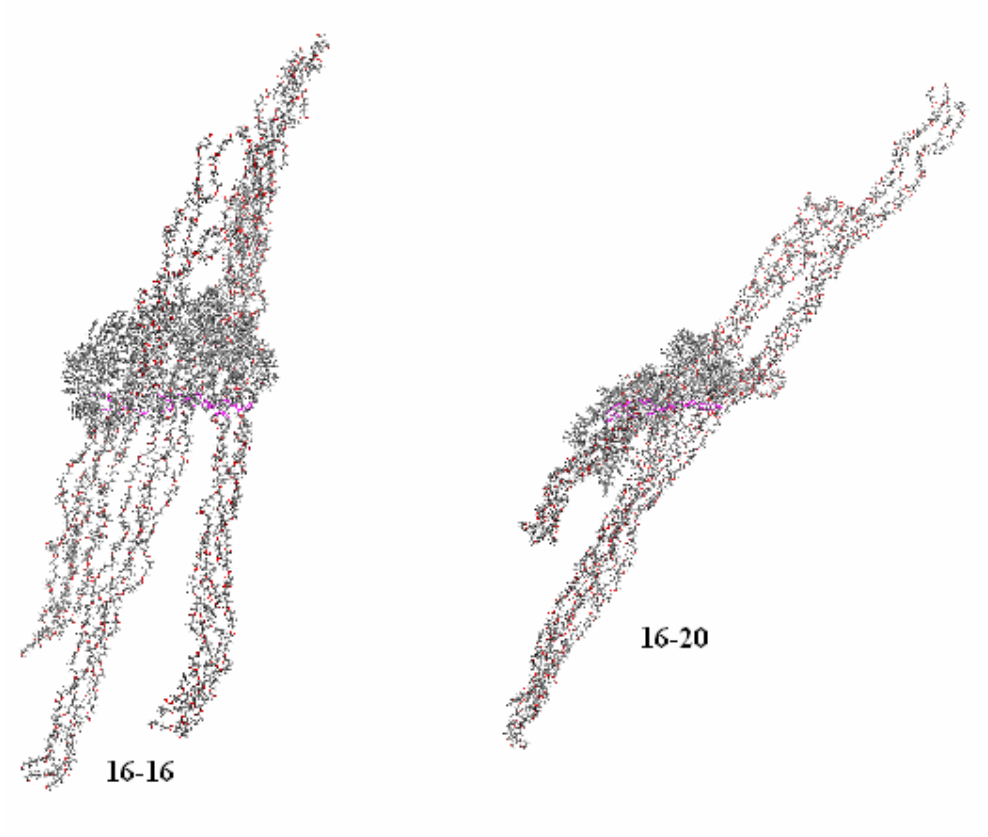
16-16
16-20

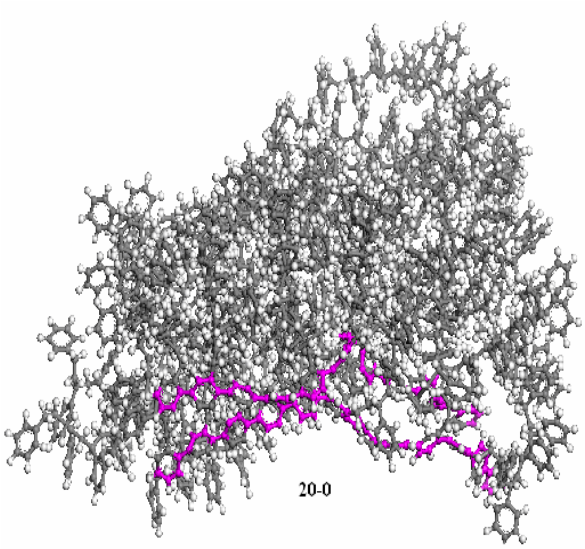
20-0

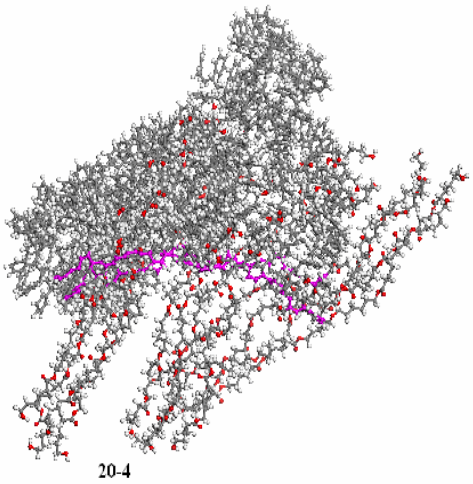
20-4

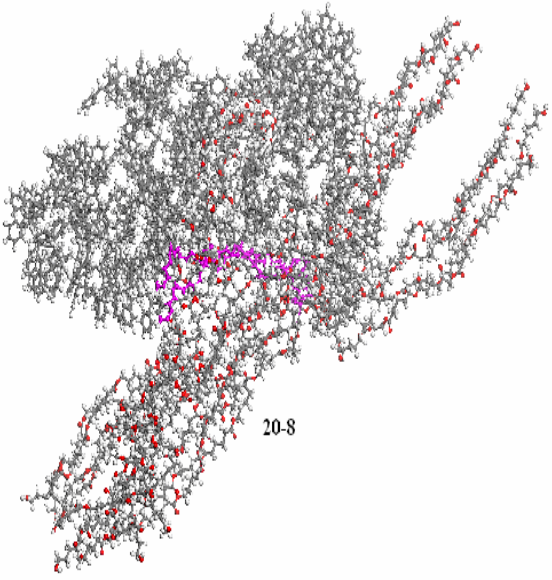
20-8

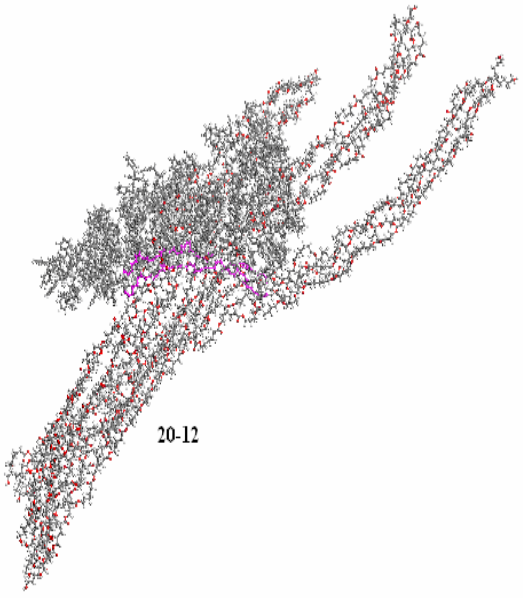
20-12

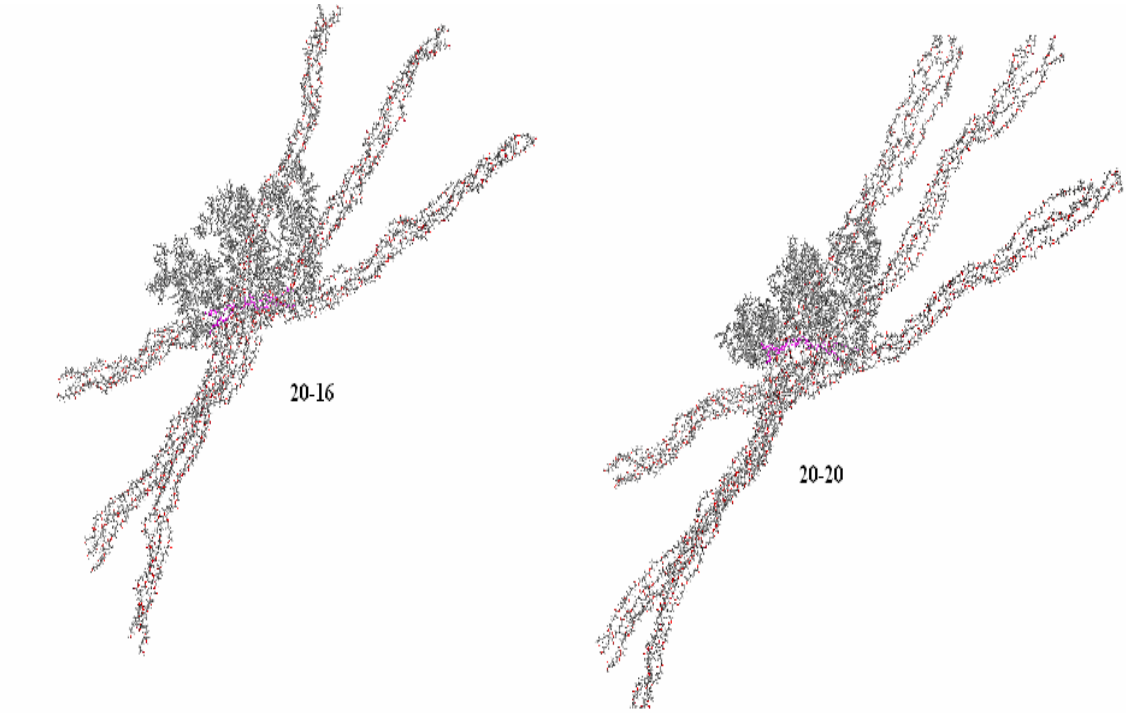
20-16
20-20

BIOGRAPHY

Barış GÜNDOĞDU was born in 1981, Balıkesir. He graduated from Antalya Anatolian High School in 1999. He started his undergraduate education in Sakarya University, Enginnering Faculty, and obtained BSc. Degree Metallurgical and Materials Enginnering Department in June, 2004. After he has worked for special companies for one year, in 2005, he attended in Istanbul Technical University, Polymer Science and Technology, where he prepared hereby master thesis.